Vadose Zone Journal

Soil Moisture Measurement for Ecological and Hydrological Watershed-Scale Observatories: A Review

D. A. Robinson,* C. S. Campbell, J. W. Hopmans, B. K. Hornbuckle, S. B. Jones, R. Knight, F. Ogden, J. Selker, and O. Wendroth

At the watershed scale, soil moisture is the major control for rainfall–runoff response, especially where saturation excess runoff processes dominate. From the ecological point of view, the pools of soil moisture are fundamental ecosystem resources providing the transpirable water for plants. In drylands particularly, soil moisture is one of the major controls on the structure, function, and diversity in ecosystems. In terms of the global hydrological cycle, the overall quantity of soil moisture is small, ~0.05%; however, its importance to the global energy balance and the distribution of precipitation far outweighs its physical amount. In soils it governs microbial activity that affects important biogeochemical processes such as nitrification and CO_2 production via respiration. During the past 20 years, technology has advanced considerably, with the development of different electrical sensors for determining soil moisture at a point. However, modeling of watersheds requires areal averages. As a result, point measurements and modeling grid cell data requirements are generally incommensurate. We review advances in sensor technology, particularly emerging geophysical methods and distributed sensors, aimed at bridging this gap. We consider some of the data analysis methods for upscaling from a point to give an areal average. Finally, we conclude by offering a vision for future research, listing many of the current scientific and technical challenges.

Abbreviations: ATV, all-terrain vehicle; CASMM, catchment average soil moisture monitoring; DC, direct current; DPHP, dual-probe heat pulse method; EM, electromagnetic; EMI, electromagnetic induction; GPR, ground penetrating radar; H, horizontally polarized; HPP, heat pulse probe; LIDAR, light detection and ranging; MFHPP, multifunctional heat pulse probe; NMR, nuclear magnetic resonance; SCAN, soil analysis climate network; T_1, spin-lattice relaxation time in NMR; T_2, spin-spin relaxation time in NMR; TDR, time domain reflectometry; TDT, time domain transmission; V, vertically polarized.

Despite its importance, our understanding of soil moisture and related hydrological processes in small watersheds (catchments [0.1–1 km^2] and subwatersheds [1–80 km^2]) is reaching an impasse. Watershed modeling has developed significantly with the advent of computers; however, measurement capability has not kept pace. Measurements at a point, with a scale (~1 dm^3), have advanced with a range of in situ sensors, while measurements at basin (2,500–25,000 km^2) and continental scales have advanced with remote sensing. However, this has left an intermediate scale gap, where we lack spatial data describing watershed patterns and networks that could help us to understand emergent behavior of small watersheds.

With growing interest in watershed observatories, both hydrological and ecological, the focus of this review is to describe recent advances in soil water content measurement methods. We consider the issue of the intermediate scale gap and identify several emerging methods and technologies from geophysics and through the development of distributed sensors that may help fill this gap. We begin by reviewing the role of soil moisture at the continental scale and then move to watershed spatial patterns and the ecohydrological importance of soil moisture. In the main body of the review, we describe soil physical properties from which water content is determined and review instrumentation used for this purpose. We then examine the issue of how we bridge between measurements made at the point scale (<1 m^2) and the need for model areal estimates at scales of 10 to 100 m^2. Finally, we discuss some of the important advances needed to move the research forward.

Soil Moisture in the Global Hydrologic Cycle and Energy Balance

Over the oceans, approximately 90% of net radiation produces evaporation (Budyko, 1974), primarily in the tropics. Over continents, net radiation heats the surface, evaporates water from water bodies or moist soils, or provides plants with energy to remove water from soils (Pitman, 2003; Istanbulluoglu and Bras,

D.A. Robinson and R. Knight, Dep. of Geophysics, 397 Panama Mall, Stanford Univ., Stanford, CA 94305-2215; C.S. Campbell, Dep. of Crop and Soil Sciences, Washington State Univ., Pullman, WA 99164; J.W. Hopmans, Dep. of Land, Air and Water Resources, Univ. of California, Davis, CA 95616; B.K. Hornbuckle, Dep. of Agronomy, Iowa State Univ. of Science and Technology, Ames, IA 50011-1010; S.B. Jones, Dep. of Plants, Soils and Climate, Utah State Univ., Logan, UT 84322-4820; F. Ogden, Dep. of Civil & Architectural Engineering, Univ. of Wyoming, Laramie, WY 82071; J. Selker, Dep. of Biological and Ecological Engineering, Oregon State Univ., Corvallis, OR 97331-3906; O. Wendroth, Dep. of Plant and Soil Sciences, Univ. of Kentucky, Lexington, KY 40546-0091; D.A. Robinson, current address: Dep. of Food Production, Univ. of the West Indies, Trinidad and Tobago. Received 16 Aug. 2007. *Corresponding author (darearthscience@yahoo.com).

Vadose Zone J. 7:358–389
doi:10.2136/vzj2007.0143

2006; Rodriguez-Iturbe et al., 1999a,b). Continental averages indicate that approximately 58% of net radiation is used to drive evaporation and transpiration, while the remaining 42% heats the land surface (Ohmura and Raschke, 2005). Vegetation is quite efficient at removing water from soils and returning it to the atmosphere.

Entekhabi et al. (1996) identified preferred soil moisture states due to precipitation recycling in continental locations. In this case, soil moisture becomes an important source of atmospheric water, a fraction of which falls as precipitation back on the land surface downwind from the site of the original evapotranspiration. This feedback between land-surface evaporation and precipitation is a significant source of rainfall in larger mid-continental basins like the Mississippi and Amazon. Subsequently, when low soil water contents persist, precipitation is reduced, increasing the likelihood of dry conditions. Conversely, wet periods can help maintain soil moisture. This positive feedback creates a bimodal distribution of soil moisture probability over large watersheds, with important climatic implications. Many investigations have observed a strong relationship between soil moisture and precipitation variability (van der Schrier and Barkmeijer, 2007; Hong and Kalnay, 2000; Trenberth and Guillemot, 1996; Koster et al., 2004).

Watershed Soil Moisture Patterns

Spatial patterns of soil moisture are determined by a number of physiographic factors that affect the vertical and lateral redistribution of water in the vadose zone. The factors that influence vertical redistribution of soil moisture are better understood because of the preponderance of soil pit and column studies. Soil texture, layering, vegetation, and the depth to water table are the dominant factors. Identification of the factors that cause lateral redistribution is a relatively recent occurrence, albeit detailed space–time evaluation of soil moisture fields and their influence on runoff generation have been performed at only a few sites around the globe. Two such studies were performed in small catchments in Victoria, Australia, and the North Island of New Zealand (Western and Grayson 1998; Western et al., 1999; Grayson et al., 1997).

At the watershed scale, soil moisture is the major control for rainfall–runoff response, especially where saturation excess runoff processes dominate (Dunne and Black, 1970). The space–time evolution of soil moisture is controlled by a number of factors. Topography and landscape position are dominant during wet states, while slope aspect, vegetation, texture, and vertical structure are more important in dry states. Downslope flow through preferential pathways in the soil is highly effective at conveying water toward lower portions of hillslopes in humid regions (Uchida et al., 1999; Hewlett and Hibbert, 1963). This is in contrast with arid and semiarid regions, where surface runoff is produced during intense rainfall, increasing soil moisture in the downslope direction due to infiltration of run-on (Western et al., 2001). During nonrainy periods, slope-aspect and net radiation drive evapotranspiration, and the spatial variation in soil moisture is controlled by vegetation (Seyfried and Wilcox, 1995). The importance of soil moisture on continental hydrology necessitates better understanding of these abrupt transitions, semistable bimodal states, climatic influences, and thresholds. This improved understanding of emergent behavior in watersheds will only be achieved through better measurement capabilities over a range of space and time scales that can be successfully integrated into modeling frameworks.

Ecohydrological Contribution of Soil Moisture

In terms of the global hydrological cycle, the overall quantity of soil moisture is small ~0.05% (Dingman, 2002). However, soil moisture (θ) provides the plant-available transpirable pool of water for vegetative life on this planet and should be viewed as a valuable ecohydrological natural resource. Competition for water between agricultural irrigation and natural ecosystems continues to increase (FAO, 2006; World Bank, 2006). Water withdrawn for irrigation is lost to natural ecosystems and can lead to their decline. Understanding how much of the θ resource can be used without significantly damaging the natural ecosystem is one of the keys to sustainable development and the prevention of ecosystem decline. Particularly in drylands, θ is one of the major controls on ecosystem structure, function and diversity (Rodriguez-Iturbe and Porporato, 2005).

Soil moisture pulses are thought to be one of the controls on a hierarchy of physiological responses observed in plants in arid and semiarid ecosystems (Schwinning and Sala, 2004; Schwinning et al., 2004). Perhaps more than the physical amount of water, the ecologist is interested in the function of that pool of water (Ryel et al., 2008). It is often of more value to know the quantity of transpirable water within energy bounds, such as between saturation (0 MPa) and the permanent wilting point (~−1.5 MPa).

Letey (1985) introduced the concept of a nonlimiting water range in soils, describing optimum physical conditions for plant growth. It forms a useful conceptual framework for demonstrating the importance of θ on soil physical properties affecting plant growth (see Fig. 1a). Figure 1a illustrates that decreasing water content increases the mechanical resistance, making it harder for plant roots to penetrate into the soil, but conversely increases the temperature and aeration; increasing water content causes the reverse. Water, therefore, is the major control on soil physical properties affecting plant growth.

Water content also exerts a strong control on soil biogeochemistry (Fig. 1b), including microbial activity (Skoop et al., 1990), nitrogen mineralization (Stanford and Epstein, 1974), and biogeochemical cycling of nitrogen and carbon (Stanford and Epstein, 1974; Turcu et al., 2005; D'Odorico et al., 2003; Porporato et al., 2003; Ridolfi et al., 2003; Gower et al., 1992; Wildung et al., 1975). Focusing on the soil microbial population as the powerhouse of biogeochemical reaction, Skoop et al. (1990) presented a conceptual model showing the effect of water content on microbial growth (Fig. 2a) suggesting that aerobic microbial activity is constrained by diffusion limiting processes. In reality the curve is probably skewed. The quantity of air-filled porosity significantly impacts both the nitrogen and carbon cycles. Volumes of work have been written on the effects of θ and temperature on nitrogen mineralization (Sierra, 1997; Cassman and Munns, 1980; Stanford and Epstein, 1974; Drury et al., 2003; Myers et al., 1982; Reichman et al., 1966). Certainly no simple relation describes all soils. A particularly illustrative set of data was presented recently (Schjonning et al., 2003) and is reproduced in Fig. 2b. The data show both the net

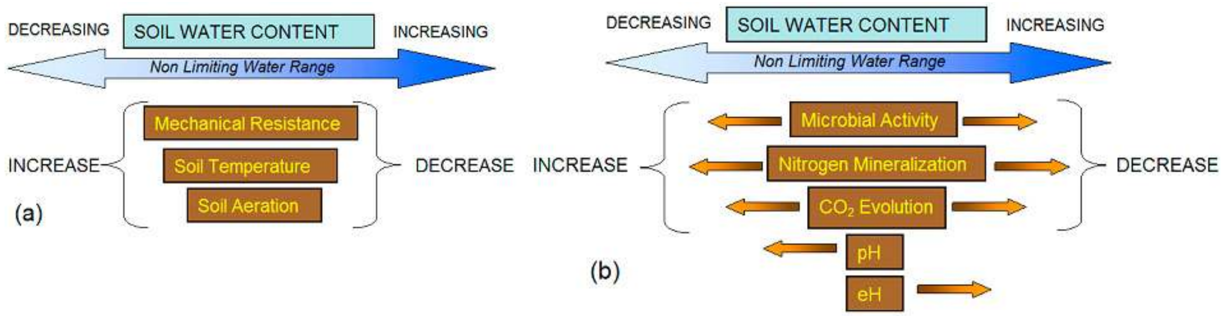

FIG. 1. (a) Soil water content control on soil physical properties affecting plant growth. (b) Soil water content control of soil biogeochemical reactions and processes including pH, acidity alkalinity, and Eh, the electrical potential of the system relative to the potential of a standard hydrogen electrode.

nitrification and the CO_2 evolution from three soils, with varying clay content from 11 to 22 to 34%, as a function of θ. The nitrification exhibits a clear maximum that depends on θ and clay content. The CO_2 evolution shows a linear increase as θ increases and then appears to reach a sill, although it would be expected to decrease at full saturation, which was not measured.

The Need for Observatory Scale Measurement

There is currently a gap in our ability to routinely measure θ at intermediate scales (subwatershed or catchment or vegetation stands) for hydrological, ecohydrological, and biogeochemical studies. For convenience in the discussion of scales, we adopt the Center for Watershed Protections definitions of watershed management units (Zielinski, 2002), with their approximate corresponding areas: basin (2500–25,000 km^2), subbasin (250–2,500 km^2), watershed (80–250 km^2), subwatershed (1–80 km^2), and catchment (0.1–1 km^2). Although these delineations are subjective, they guide the reader in relating water content measurements to hydrological scales of interest. Measurement constraints at the sample scale (~0.1–1 dm^3) and at the soil surface at large spatial scales using remote sensing have left significant gaps in our understanding, especially for intermediate-scale watershed processes, primarily because good quality data is lacking (Western et al., 2002). Measurement of θ at small watershed scales is particularly important for closing the water balance at small scales, understanding biogeochemical processes, continuing to develop

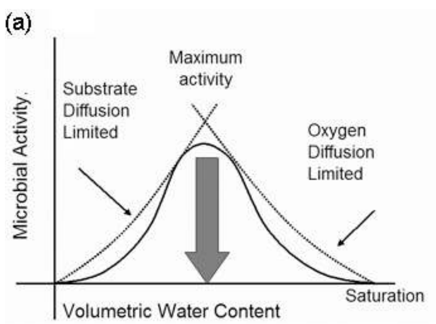

FIG. 2. (a) Schematic altered from Skoop et al. (1990) indicating conceptually how microbial activity is affected by soil water content. (b) Data from Schjonning et al. (2003) for a sand (L1), sandy loam (L2), and clay (L3) showing nitrification and CO_2 production as a function of water content.

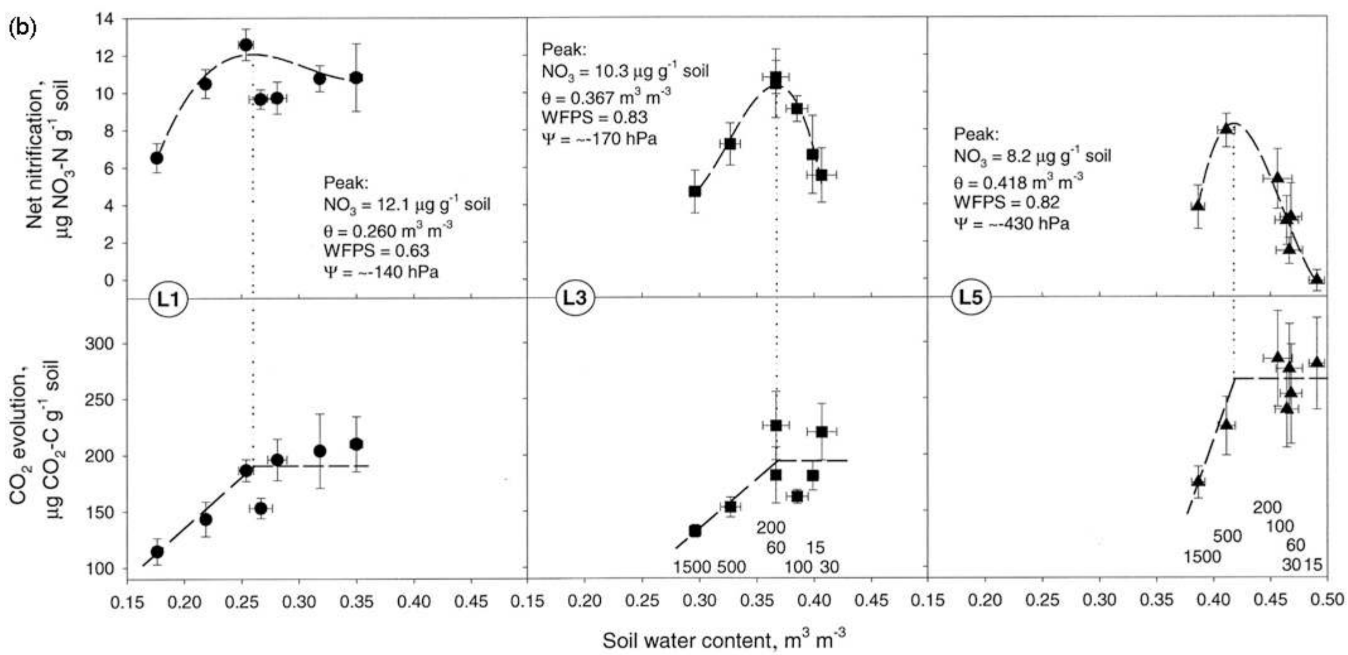

hydrologic models, and determining the pools of soil water that control emergent ecosystem structure and function.

The existence of this measurement gap may be caused in part by the two main historical directions from which the measurement of θ has developed. Point measurements have been predominantly developed for applications in agriculture, to understand field-scale soil water dynamics (Topp and Ferré, 2002), whereas more recently, satellite remote sensing has developed capabilities that contribute to understanding the hydrology of land–surface–atmosphere interactions, especially at river basin, continental, and global scales (Kerr et al., 2001). Figure 3 presents a space–time diagram relating measurement capabilities to scales at which hydrological process can be observed. Our present technological capabilities for measuring θ are shown within the boxes with solid lines and are generally constrained to the upper and left sides. However, we are often interested in the complex interaction of many processes that bring about the "emergent" or "system" behavior of a watershed or ecosystem. This scale of interest often falls between current measurement capabilities. New developments in instrumentation, geophysical networks, and sensor networks, shown in boxes with dashed lines, can help bridge the gap for process space–time scales of interest.

Pioneering small watershed-scale measurements using time domain reflectometry (TDR) instrumentation were presented by Western et al. (1999), Western and Grayson (1998), and Grayson et al. (1997) (see Fig. 4). These measurements were made using a mobile, stop-and-go TDR system in a 10-ha watershed in Australia. They illustrate how watershed patterns of soil moisture change in space and time, from structured when wet to random when dry. Understanding these patterns and dynamics is important for describing hydrological runoff response.

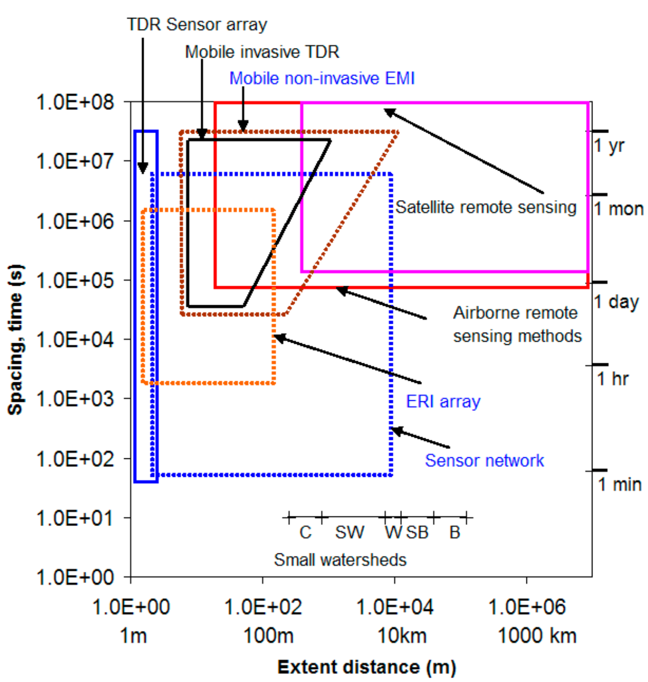

Fig. 3. Conceptual diagram showing the estimated extent (m) of measurements and the spacing in time. The extent of the watersheds is determined from the major axis of a 2:1 ellipse and surface areas according to Zielinski (2002). B, basin (2500–25,000 km^2); SB, subbasin (250–2,500 km^2); W watershed (80–250 km^2); SW, subwatershed (1–80 km^2); C, catchment (0.1–1 km^2). Current technology is constrained to measuring processes with space and time scales consistent with boxes having solid lines. The new technologies and methods (dashed lines) form a bridge between current sensor and remote sensing capabilities. They improve our ability to monitor rapid soil moisture change at small watershed scales.

Advances in wireless and sensor technology are increasing the feasibility of using distributed sensor networks, which may be one way to move toward observing soil water processes at these scales of interest, bridging ground-based sensors and remote sensing. Other promising avenues of research include continued improvement of remote sensing and advances in geophysical instrumentation. Perhaps some combination of these methods is required to provide comprehensive spatial and temporal coverage. The main question is how to advance the science and technologies to move forward and measure at intermediate scales.

The growing scientific emphasis on observatories in the United States, such as the National Ecological Observatory Network (NEON) and the WATERS network for hydrology, is stimulating research interest in measurement capability. The importance of observatories is that measurement efforts can be focused on and concentrated in specific locations to try and capture system response and emergent behavior. It provides an opportunity to link multiple point observations with regional response, by observing intermediate-scale processes. In particular, breakthroughs in sensor technology and lower costs make distributed sensing feasible; capitalizing on this is the next major challenge for hydrological and environmental science.

Physical Properties Used to Determine Water Content

Thermogravimetric Measurement

Soil moisture is a soil physical state variable that controls or modulates many physical, biological, and chemical processes. The amount of water in soils is expressed primarily in two different ways, either on a volumetric (θ_v) or a gravimetric (θ_g) basis. The volumetric measurement is as cubic meter per cubic meter and the gravimetric measurement is gram per gram of oven-dried soil at 105°C. Both of these quantities are related by

$$\theta_v = \theta_g(\rho_b/\rho_w) \qquad [1]$$

where ρ_b is the soil dry bulk density and ρ_w is the density of water. We are mostly interested here in measurements of volumetric water content, for which we use the symbol θ unless otherwise stated.

The standard reference method for determining θ in soils is to oven dry mineral soil samples, usually 100 g or less, at 105°C (ASTM, 1979; Gardner, 1986; Topp and Ferré, 2002). Exceptions are for organic soils and gypsiferous soils, when the temperature is usually decreased to 70°C. Samples are left in the oven until there is no further significant weight loss, which usually takes from 10 to 24 h. Volumetric water content is determined using samples with a known volume. Alternatives to oven drying have been suggested, such as microwaving 20 g of soil for 20 min in a 600 to 650 W microwave (Gee and Dodson, 1981), and more recently, a low-cost "lightbulb oven" has been proposed (Whitaker et al., 2006) for use by elementary and high school students who do not have access to laboratory ovens. Determining water content by oven drying remains a somewhat arbitrary measure, as Gardner

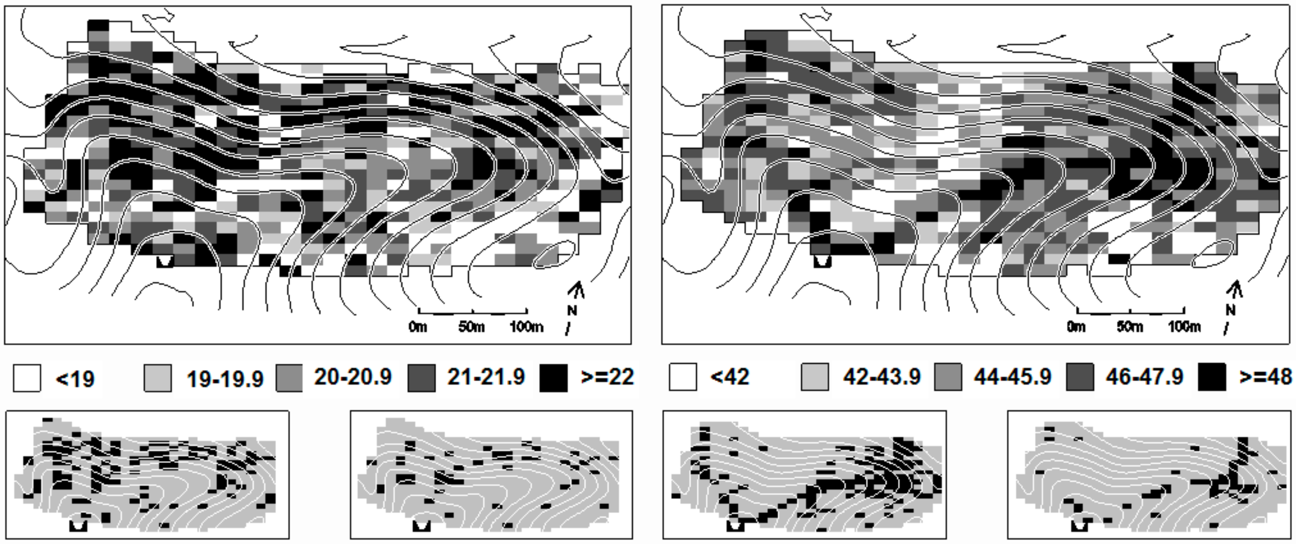

FIG. 4. Adapted from Western et al. (1999), soil moisture in the 10-ha Tarrawarra watershed in Australia when dry (left) and wet (right). Each pixel is one time domain reflectometry point measurement to 30 cm depth. The 75th (left) and 90th (right) percentile indicator plots are shown under each respective figure. During dry periods, the pattern is random, but an organized patter emerges as the soil becomes wet.

(1986) pointed out. Thermogravimetric analysis of clays demonstrated that 105°C is not a significant point (Earnest, 1991a,b). The choice of 105°C is a compromise between identifying water loss and preventing excessive weight loss due to oxidation and decomposition of organic materials. The point at which adsorbed water, but not crystalline water, is liberated appears to be about 160°C, particularly for montmorillonite clays (Fig. 5). However, 160°C would not serve as a practical temperature because of the problem with organic matter volatilization.

Neutron Thermalization

Neutrons carry no charge and are unaffected by electromagnetic fields. Released from a source, they will travel in a straight line unless they collide with the nucleus of an atom. A direct collision between a neutron and a hydrogen nucleus causes the neutron to lose all its energy and become thermalized. By comparison, direct collisions with oxygen, silicon, aluminum, or iron will lead to energy losses of 22, 14, 13, and 7%, respectively (Gardner et al., 2001). Collisions also cause the neutrons to change direction; the more collisions, the greater the likelihood of them returning to a detector near a source. Therefore, a count of the number of thermalized neutrons returning to a detector, over a sufficient period of time, gives a good estimate of the number of hydrogen nuclei in soils; this can be calibrated to determine θ. Restrictions on the use of radioactive materials are increasingly inflexible and have made active devices less attractive for determining θ.

Electrical Conductivity

Measurement of electrical conductivity was proposed as early as the end of the 19th century as a way of determining θ (Briggs, 1899). However, it never caught on significantly because of the dependence of the bulk electrical conductivity, σ_a, on both θ and the soil solution electrical conductivity, σ_w. Measurement of σ_a has become a common measurement used to assess soil salinity (Rhoades et al., 1989), infer solution electrical conductivity to predict soil nutrient content (Wraith et al., 1993; Kachanoski et al., 1992), or to parameterize models describing solute transport in soil (e.g., conductive tracers) (Dagan, 1987; Loague and Green, 1991; Seyfried and Rao, 1987; Singha and Gorelick, 2005). Depending on the method and scale, the electrical conductivity measurement includes any soil constituents that conduct electrical current. Soil solution electrical conductivity and θ are major contributors to σ_a. Other factors impacting σ_a include counter-ions adsorbed to charged particle surfaces (i.e., silt and clay particles), referred to as the surface conductivity, σ_s, and soil heterogeneity sensed in the orientation of the electrical field with respect to any significant soil structural anisotropy or layering (Friedman, 2005; Friedman and Jones, 2001). Soil temperature is also important to consider because of the dependence of the electrical conductivity of the solution phase on temperature (i.e., $\sim$2% °C^{-1}; (Rhoades

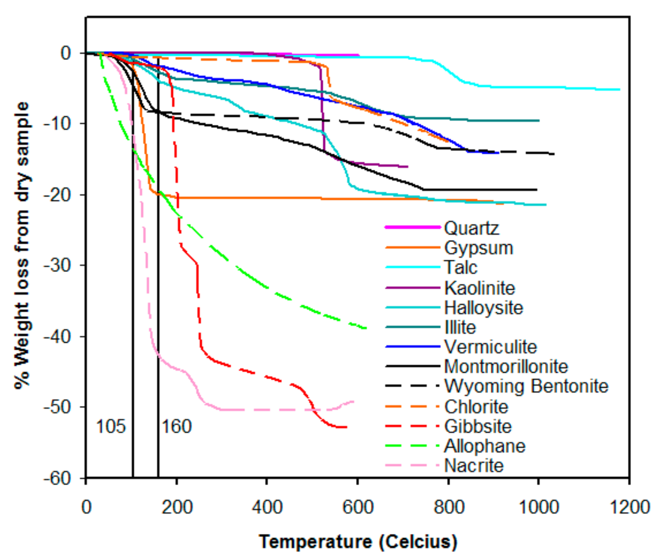

FIG. 5. Thermogravimetric analysis of common soil minerals and clay minerals. 105°C is the standard drying temperature; 160°C is the temperature at which most clays have undergone primary dehydration (adapted from Gardner, 1986).

et al., 1999). This dependence becomes a substantial problem for near-surface soil layers where both temperature and θ have the greatest variation, both spatially and temporally, and is the main reason why dielectric sensors, although more expensive, replaced resistivity to determine point measurements of θ.

Various empirical and physical models have been developed to describe σ_a as a function of these factors. One of the simplest expressions, considering only the solution phase conductivity, is given for saturated–unsaturated soils as (Mualem and Friedman, 1991)

$$\sigma_a = \sigma_w \theta_{sat}{}^{1.5} (\theta / \theta_{sat})^{2.5} \tag{2}$$

where θ_{sat} is the saturated water content. This model reduces to θ_{sat} being raised to an exponent of 1.5 for saturated soil. Equation [2] was found to describe σ_a in a wide range of coarse and stable structured soils. Adding the influence of σ_s, various authors (Friedman, 2005; Nadler, 2005; Rhoades et al., 1976) have suggested a general formulation of Archie's law (Archie, 1942) that can be extended to unsaturated soil (Telford et al., 1990):

$$\sigma_a = \frac{\sigma_w\ \phi^{(m-\eta)}\ \theta^{\eta}}{a} + \sigma_s(\sigma_w) \tag{3}$$

where the empirical parameters η, *m*, and *a* are often assigned common values or fit to measured data. The term η is approximately 2, *m* is the so-called cementation exponent taken as 1.5 ($1.3 < m < 2.5$) and *a* may be assumed to be 1 ($0.5 < a < 2.5$). Using these values, Eq. [3] can be rewritten in terms of θ indicating its dependence on the ratio of apparent and solution conductivities, porosity and surface conductance:

$$\theta = \left[\frac{\sigma_a\ \phi^{0.5}}{\sigma_w} - \sigma_s(\sigma_w)\right]^{0.5} \tag{4}$$

Electrical conductivity measurements applied to determining θ are reviewed in Freeland (1989). The ability of electrical geophysical methods to collect spatial data, such as direct current (DC) resistivity and electromagnetic induction (EMI) that are minimally or noninvasive, is leading to renewed interest in determining θ using electrical conductivity. These methods are considered later in this article under "Geophysical Methods."

Dielectric Properties

Sensors using dielectric properties to estimate θ include a broad spectrum of methods ranging from sample scale electrical sensors to geophysical methods and remote sensing. Water has many unique properties (Hasted, 1973), one of which is its permanent dipole moment. This is a displacement of positive and negative molecular charge due to the position of the hydrogen atoms in relation to the oxygen atom. The water molecule has a large permanent dipole compared to most other natural materials; as a result, water has a dielectric constant or relative permittivity of ∼80. Here, the relative permittivity is dimensionless, defined as $\varepsilon_r = \varepsilon/\varepsilon_o$, where ε is the permittivity of the material (pF m^{-1}) and ε_o is the permittivity of free space (8.854 pF m^{-1}); for brevity, the term *relative* is dropped in subsequent discussion and the term *permittivity* used. The permittivity of water is much higher than that of air, which is 1, or most soil minerals that are about 5. Therefore, the proportion of water strongly affects the measured bulk permittivity of the soil. It is permittivity that is exploited by both electromagnetic soil moisture sensors, many of which are now mature technologies (Evett and Parkin, 2005), and many remote sensing techniques used to determine θ.

Fundamental to understanding the response of dielectric sensor technology and water content measurement, is an understanding of the frequency dependence of composite dielectric materials such as soils. The frequency (*f*) dependence of a homogeneous dielectric was described in Debye's classic Nobel Prize–winning work (Debye, 1929). He considered that a molecule rotating in response to an applied electric field would experience an increasingly large frictional force, as the speed of rotation was increased, due to an increase in frequency of the applied electrical field. The result of the work was the Debye equations:

$$\varepsilon_r' = n^2 + \frac{\varepsilon_s - n^2}{1+\omega^2\tau^2} \tag{5}$$

$$\varepsilon_r'' = \frac{\left(\varepsilon_s - n^2\right)\omega\tau}{1+\omega^2\tau^2} + \frac{\sigma_{dc}}{\omega\varepsilon_o} \tag{6}$$

where a real part (ε_r') describes energy storage (related to θ), and an imaginary part (ε_r'') describes energy losses dissipated as heat. The σ_{dc} term only makes a contribution if the value is not zero and the material contains some ionic conduction. The term *n* is the refractive index, ε_s is the static relative permittivity, and τ describes the relaxation time (s) and is related to the frequency by $\tau = (1/\omega)$, where ω is the angular frequency $2\pi f$. This model provides a reasonable description of some solids and fluids but is not a useful description of the dielectric properties of soils, where many other processes occur. In particular, most natural materials, such as soils, are three-phase, and the geometry becomes important (Sihvola, 1999; Knight and Nur, 1987). Also, the solution phase containing ions leads to charge transport described by σ_{dc}.

An additional issue should be clarified in comparing actual laboratory or field measurements to the Debye response, and that is the difference between the real and imaginary parts of the total measured permittivity, ε_T' and ε_T'', and the defined Debye parameters, ε_r' and ε_r'':

$$\varepsilon_T'(\omega) = \varepsilon_r'(\omega) + \frac{\sigma''(\omega)}{\omega} \tag{7a}$$

$$\varepsilon_T''(\omega) = \varepsilon_r''(\omega) + \frac{\sigma'(\omega)}{\omega} \tag{7b}$$

where $\sigma''(\omega)$ is related to faradaic diffusion, and $\sigma'(\omega)$ represents ohmic conduction. The key point is that it is impossible to make a measurement that can fully separate dielectric from conduction phenomena. All that can be measured is the total amount of energy stored (ε_T') and the total amount of energy lost (ε_T''). At sufficiently high frequencies (typically above ∼100 kHz), it is usually assumed that $\sigma''(\omega) = 0$ and $\sigma'(\omega) = \sigma_{dc}$. With these assumptions in place, the term dielectric constant measured by an instrument (κ) is defined as

$$\kappa = \frac{\varepsilon_T'}{\varepsilon_o} = \frac{\varepsilon_r'(\omega)}{\varepsilon_o} \tag{8}$$

The full derivation of these expressions is given in Knight and Endres (2005).

Initially, it was considered that at the high frequencies used in most measurement systems, the permittivity response of soils was frequency independent. Recent studies have shown, however, that clay minerals show distinct dielectric dispersion (i.e., permittivity change with frequency) (Saarenketo, 1998; Ishida and Makino, 1999; Ishida et al., 2000). This dispersion effect is illustrated in Fig. 6, which shows the difference between a saturated quartz sand and partially saturated clay. Dispersion, therefore, presents some challenges to developing a single calibration model to describe the relationship between permittivity and θ.

The objective of soil sensor calibration should be twofold: to measure the real part of the permittivity (ε_r') by minimizing any contributions to this measurement from the imaginary component ε_r'' or σ'' and to work in a frequency window of operation that minimizes dielectric dispersion effects. Figure 6 also provides the measurement frequency or bandwidth of common sensors so that they can be placed in the context of soil dielectric properties. It becomes immediately apparent that many of the lower-cost sensors operate at frequencies that, in clay soils especially, will be susceptible to dielectric dispersion. This means that sensors measuring at different frequencies will have different κ–θ calibrations (Chen and Or, 2006). It also means that broadband θ measurements using TDR will change not only as a result of differences in θ but also from differences in clay content and temperature as they affect σ_a and $\varepsilon_r'(\omega)$. Operating in the frequency range between 0.5 and 1 GHz, TDR has been very successful since it minimizes many of the adverse effects (Fig. 6). Frequency shift capacitance probes operate between 0.10 and 0.25 GHz. Even at these frequencies, the imaginary permittivity can be considerable. It is also important to consider the growing trend of using low-frequency impedance sensors to calibrate remote sensing data. If this approach is taken, independent calibration of the low-frequency sensor must be obtained in terms of θ. Using the same calibration equation for both instruments in clay soils could lead to significant errors in determining θ. At lower frequencies, contributions from the term $\sigma''(\omega)/\omega$ will start to have a significant impact on the magnitude of the measured permittivity.

Soil Thermal Properties

Soil thermal measurements are increasingly considered as an alternative to other methodologies to determine soil properties and parameters, such as θ and soil water flux. Here, we define soil thermal properties as soil thermal conductivity (λ), volumetric heat capacity (C), and soil thermal diffusivity (α). Few direct measurement techniques are available to estimate soil thermal properties nondestructively since soil geometric parameters such as pore continuity and soil particle configurations control soil heat transport by both conduction and convection. Instead, soil thermal properties are most often estimated by matching analytical (curve-fitting) or numerical (inverse modeling) solutions of soil heat transport with experimental temperature data.

The soil volumetric heat capacity, C_{soil} (J m^{-3} K^{-1}), defining the amount of heat that can be stored in the soil, can be determined from the sum of the heat capacities of the individual constituents according to (Kluitenberg, 2002; De Vries, 1963)

$$C_{soil} = (\rho c)_s(1-\phi)+(\rho c)_w\theta+(\rho c)_a(\phi-\theta) \qquad [9]$$

where ρ is the density (kg m^{-3}), c is the specific heat (J kg^{-1} K^{-1}), ϕ and θ are as previously defined, and the subscripts s, w, and a indicate the soil's solid, water, and air phases, respectively. If the heat capacity of air is ignored and the solid phase is made up of mineral material only, setting $C_w = (\rho c)_w$ and $C_s = (\rho c)_s$ allows Eq. [9] to be rewritten as (Kluitenberg, 2002; Campbell, 1985)

$$C_{soil} = C_s(1-\phi)+C_w\theta \qquad [10]$$

Additional complications may arise if the soil solid phase has significant fractions of organic material, gravel, or other components. In that case, the calculation of C_s must include these other soil constituents requiring independent known values of the specific heat and density of each of these additional bulk soil fractions. It is clear from Eq. [10] that θ can be computed directly from measurement of C_{soil} if volumetric heat capacity values of the solid phase and water are known a priori. Direct measurements of C or c are usually obtained by calorimetric methods (Kluitenberg, 2002).

The bulk soil thermal conductivity (λ) describes the soil's ability to conduct heat (W m^{-1} K^{-1}) and is a function of mineral type, geometrical arrangement of the various phases, and θ (De

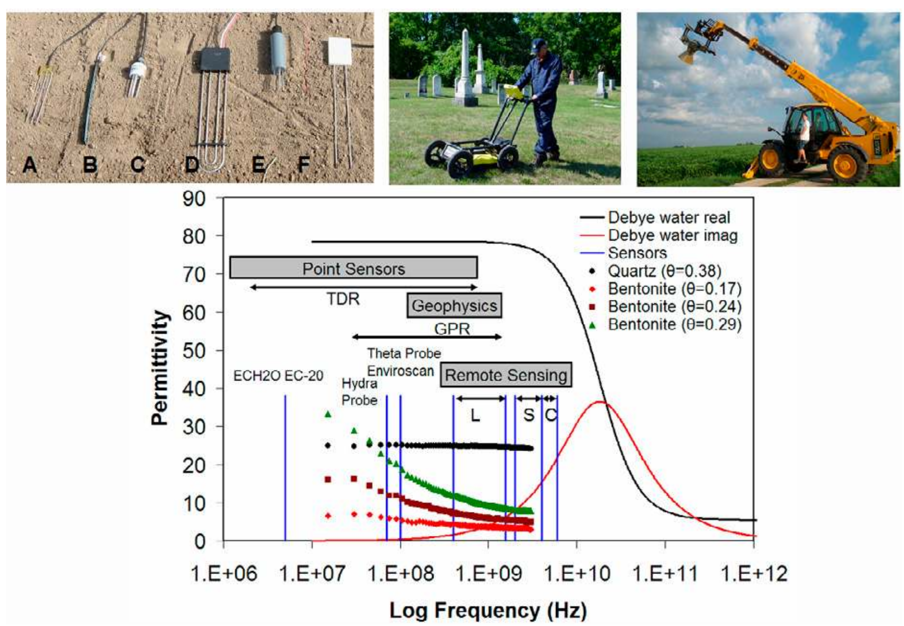

Fig. 6. Dielectric data for quartz sand with no dielectric dispersion and moist clays showing dielectric dispersion; the real (Eq. [7a]) and imaginary (Eq. [7b]) permittivity for water without ionic conductivity are indicated for reference. The upper-left figure shows six common soil water sensors: (A) time domain reflectometer, (B) ECH$_2$O EC-20 probe, (C) Hydra probe, (D) Acclima time domain transmission sensor, (E) ThetaProbe, (F) CS-616. The center figure shows a cart-mounted ground penetrating radar (GPR) (courtesy, Sensors & Software, Inc., Mississauga, ON); the top-right figure is a passive microwave remote sensing radiometer mounted on a crane.

Vries, 1963), and hence is soil specific. With the exception of the guarded hot-plate method (Bristow, 2002), available measurement techniques rely mostly on analytical solutions to the heat transport problem, by fitting thermal conductivity or thermal diffusivity to temperature measurements. For example, most recently, Mortensen et al. (2006), fitted a polynomial expression to the θ dependence of thermal conductivity from simultaneous measurements of temperature, θ, and solute concentration using numerical solution of the coupled flow and transport equations.

A general relationship between thermal conductivity and θ to account for soil composition and shape was introduced by De Vries (1963) and Campbell (1985) and was applied to laboratory data in Hopmans and Dane (1986). The theory of De Vries (1963) relating bulk soil thermal conductivity to mineral composition, θ, and temperature is extremely complicated and includes microscopic-scale pore and solid-phase geometry factors. Simpler macroscopic expressions were developed by Campbell (1985) and Chung and Horton (1987). At low θ, the thermal conductivity is mostly controlled by the volumetric air content, with slight variations determined by composition of the solid phase, such as organic matter and quartz. As θ increases, the bulk soil thermal conductivity is controlled by thermal contact between the various phases, such as the water films surrounding the soil particles.

In Situ Soil Sensing Instrumentation

Neutron Thermalization

The neutron probe has now been around for more than 50 yr. The method was first proposed in the 1940s (Pieper, 1949; Brummer and Mardock, 1945) and field tested by Blecher (1950). The first portable instrument was reported by Underwood et al. (1954) in the United States and by Holmes (1956) in Australia. Comprehensive descriptions of the practical and theoretical aspects of the use of these instruments are provided by Bell (1987) and Greacen (1981). The method has the advantage of providing a linear relationship between the count ratio and θ, thus making calibration more straightforward. The sampling volume is dependent on θ and generally described by a sphere of influence less than 0.15 m in wet soils and extending to as much as 0.5 m in dry soils. In addition to increasingly strict rules for using radioactive materials, the need for an operator and relatively slow data acquisition have led to reduced use of the neutron probe, other than for deep borehole work where there is little alternative (Yao et al., 2004).

Electromagnetic Sensors

High-frequency impedance measurements, often termed *capacitance probes* (Wobschall, 1978; Thomas, 1966; Saxena and Tayal, 1981; Hamid and Mostowy, 1976; Bell et al., 1987; Dean et al., 1987; Kuraz et al., 1970), and transmission line methods such as TDR (Fellner-Feldegg, 1969; Hoekstra and Delaney, 1974; Topp et al., 1980) have proved two distinct methods for determining θ using electrical sensors. Far more emphasis has been placed on the development of TDR since it can simultaneously determine θ and σ_a (Dalton and van Genuchten, 1986; Dasberg and Dalton, 1985; Dalton et al., 1984) and operates at frequencies above 0.5 GHz, making it less susceptible to interference by σ_a. Nonetheless, capacitance probes fill an important niche because their probe geometry is more adaptable than TDR for short electrodes and borehole applications.

Time domain reflectometry and time domain transmission (TDT) both use the propagation velocity of an electromagnetic signal along a pair of electrodes to determine the permittivity of the material in which they are imbedded. Commercially available TDR systems designed specifically for hydrology include the TRASE (Soil Moisture Equipment Corps, Santa Barbara, CA), Trime (IMKO, Ettlingen, Germany), and CS-TDR100 (Campbell Scientific, Logan, UT), among others. Time domain reflectometry instruments are often compared by the rise time of the step pulse—the shorter the time, the higher the frequency content of the signal. Generally, rise times shorter than 300 ps are desirable. Instruments such as the CS-616 have a longer rise time, ~2000 ps resulting in greater susceptibility to interference by soil σ_a. Digital TDT has recently been made commercially available. The Acclima (Acclima Inc, Meridian, ID) system is available for irrigation and has excellent performance characteristics with a rise time of less than 200 ps. The instrumentation is mounted on a chip in the head of the sensor, and resulting waveforms are particularly crisp (Blonquist et al., 2005b).

Time domain reflectometry methods provide the standard electromagnetic (EM) method for determining θ; its operation has formed the basis of a number of reviews, and the reader is referred to these for more detailed information (Noborio, 2001; Topp and Reynolds, 1998; Robinson et al., 2003; Pettinelli et al., 2002). The design and construction of the probe determine the quality of measurements made using the TDR technique. The support volume of TDR measurements depends on the probe design, which has been investigated thoroughly (Ferré et al., 1998).

A number of high-frequency (~100 MHz) impedance sensors using a fixed frequency, or frequency shift, have now been described in the literature. Many of these sensors are commercially available and generally operate in the frequency range between about 5 and 150 MHz. They include dedicated water content sensors such as the ThetaProbe (Gaskin and Miller, 1996) operating at about 100 MHz (Delta-T Devices, Ltd., Cambridge, UK), the 5 MHz ECH$_2$O EC-20 probe (Borhan and Parsons, 2004; McMichael and Lascano, 2003) (Decagon Devices, Pullman, WA), and the HMS9000 (SDEC, France) (Chanzy et al., 1998; Mohamed et al., 1997; Gaudu et al., 1993) and newer sensors such as the Delta-T SM200 and Decagon ECH$_2$O EC-5, which both operate around 100 MHz. A new generation of sensors combining determination of θ with σ_a and temperature include the Hydra probe (Campbell, 1990; Seyfried and Murdock, 2004; Seyfried et al., 2005; Ungar et al., 1992) (Stevens, Beaverton, OR), the Decagon ECH$_2$O-TE, and the Acclima TDT (Blonquist et al., 2005b).

Fundamental to all EM sensors is the relationship between the real part of the permittivity and θ. In their original article, Topp et al. (1980) indicated a firm relationship between permittivity and θ for the soils studied and which has proved to be the case in quartz-dominated soils. The diagram in Fig. 6 demonstrates that although quartz-dominated materials show negligible frequency dependence, some clay minerals do, termed *dielectric dispersion* (Saarenketo, 1998; Ishida and Makino, 1999; Ishida et al., 2000). Discussion of the phenomena that cause this frequency dependence is beyond the scope of this article, and the reader is referred to other literature (Chen and Or, 2006; Logsdon and Laird, 2004; Chelidze and Gueguen, 1999; Chelidze et al., 1999; Kelleners et al., 2005a). However, some important points arise from this: (i) fixed frequency sensors can be expected to have different calibration functions depending on their operating frequency, (ii) the least frequency dependence occurs above 500 MHz (Kelleners et al., 2005b), and (iii) accurate measurement of the real part of the permittivity is required to fully characterize the permittivity–θ relationship in the frequency domain.

Sensor calibration is a two-step process, from signal response to permittivity and from permittivity to θ. Any sensor used to exploit the permittivity–θ relationship must demonstrate its ability to accurately determine permittivity. Therefore, comparison of dielectric sensors should be based on their ability to determine the real permittivity accurately. This approach has been proposed by a number of authors (Seyfried and Murdock, 2004; Jones et al., 2005; Robinson et al., 1998). Blonquist et al. (2005a) used this approach to test seven water content sensors, including the Hydra probe, ThetaProbe, CS-616, ECH_2O EC-20 probe, Acclima TDT, Tektronix TDR, and the CS-TDR100 shown in Fig. 6 (note, a single TDR probe is shown for the last two). They found that the TDR and TDT sensors outperformed the impedance sensors. However, the ThetaProbe and Hydra probe gave the best performance of the impedance probes. The low-frequency sensors were susceptible to changes in σ_a. The CS-616 and the EC-20 probe both overestimated the real permittivity as σ_a increased. A comparison in a silt loam soil with a σ_a of 0.5 dS m^{-1} during wetting and drying is presented in Fig. 7. Only the TDT sensor accurately determined θ. The other sensors followed the trend with offsets most likely a result of sampling volume limitations and the effect of compaction around the electrodes during insertion. The CS-616 and the ECH_2O EC-20 probes both show strong diurnal fluctuation, a result of their susceptibility to σ_a, which changes with diurnal temperature.

Heat Pulse Sensors

The use of heat transport to estimate soil thermal properties was introduced by Campbell et al. (1991), who presented the dual-probe heat pulse (DPHP) method. By inducing a short heat pulse from one sensor needle and measuring the temperature response at a second sensor, the soil thermal properties (i.e., heat capacity, C; thermal conductivity, λ; and thermal diffusivity, α) and θ were estimated. This method has been tested in both laboratory settings (Bristow, 1998; Basinger et al., 2003; Bilskie et al., 1998; Bristow et al., 1994; Bristow et al., 1993) and in field soils (Heitman et al., 2003; Tarara and Ham, 1997). In the past few years, the DPHP probe has been refined and developed into various multisensor probes capable of simultaneously measuring a suite of soil properties. The so-called thermo-TDR was developed by combining the DPHP probe with TDR technology to achieve a probe that in addition to soil thermal properties, also estimates soil solute concentration from the simultaneous measurement of σ_a (Ren et al., 1999; Noborio et al., 1996). Bristow et al. (2001) showed the potential of measuring σ_a using a modified heat pulse probe by including two extra sensor needles in the DPHP probe to create a so-called four-electrode Wenner array. Since σ_a measurements depend on both solute concentration and water content, σ_a is an integral variable characterizing both water flow and solute transport that can be used to simultaneously estimate soil hydraulic and solute transport parameters (Šimůnek et al., 2002; Inoue et al., 2000).

The two-needle heat pulse probe (HPP) consists of thin needle-like heater and temperature probes (approximately 1 mm o.d.), which are mounted in parallel with a 6-mm separation distance. After application of a short-duration heat pulse, temperature responses are recorded by one or more thermistor needles. Campbell et al. (1991) presented the analytical solution for the temperature rise of an instantaneous heat pulse, allowing estimation of the soil's volumetric heat capacity and θ. Subsequently, Bristow et al. (1993) extended the probe to three needles to correct for drift in background temperature. Furthermore, they emphasized the relatively large sensitivity of θ estimations to errors in the heater-sensor spacing (r). Continued development of radial heat transport theory resulted in application of the HPP method to simultaneously estimate the soil's volumetric heat capacity, thermal conductivity (and hence, thermal diffusivity), and θ using a short-duration heat pulse from an infinite line source (Bristow, 1998). Error analyses by Kluitenberg et al. (1993, 1995) highlighted the importance of accurate r and time-to-maximum (t_{max}) temperature rise measurements for the accuracy of thermal and θ estimations. It was determined that rigid needles are required to minimize changes in mutual probe positions while inserting the HPP into soils. Typical heat pulse lengths used for making HPP measurements cause a temperature rise of about 1°C at the sensing probe, so that a 5% precision in heat capacity estimation requires temperature measurements with approximately 0.05°C precision (Kluitenberg et al., 1993).

Further developments have led to the simultaneous measurement of soil thermal properties, θ, and electrical conductivity using TDR combined with the HPP (Ren et al., 1999; Noborio et al., 1996). Bristow et al. (2001) showed that a simple modification of the dual probe with an additional two needles for bulk soil electrical conductivity measurements provides an alternative measure of the soil's electrical conductivity. In a subsequent study, Ren et al. (2000) reported on the possibility of using a

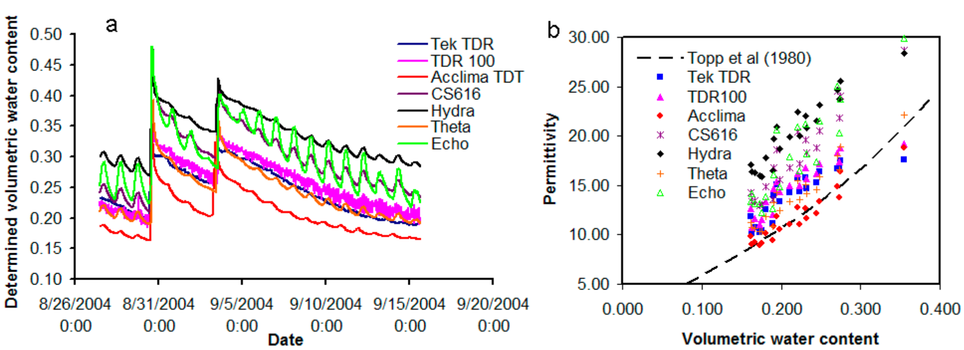

FIG. 7. (a) Water content measurements in a silt loam soil during two irrigation events for the seven sensors shown in Fig. 6. Diurnal fluctuations in sensor response occur as a result of temperature changing the bulk soil electrical conductivity to which certain instruments are sensitive. (b) The calibration indicating the Acclima is the only sensor to achieve accurate water content determination in this trial. Deviations from absolute values are considered to occur because of small sensor sampling volume.

three-needle HPP to estimate water flux density indirectly from temperature responses, measured upstream and downstream of the heat source. Their experimental results, using the maximum difference between upstream and downstream temperature signals, indicated that such analysis can be successful for flux density values larger than 0.864 m d^{-1} and suggested that the limit of sensitivity could be lowered to about 0.0864 m d^{-1}, using thermistors with a precision of 0.01°C. This lower limit was confirmed later by Mori et al. (2005), who demonstrated that multifunctional heat pulse probe technologies allow estimation of water fluxes for both saturated and unsaturated soils in the range of 0.5 to 27.0 m d^{-1}. In their modeling and sensitivity study, Hopmans et al. (2002) suggested that the limit at higher fluxes is caused by the thermal dispersion that can be taken into account by including an additional transverse thermistor needle. A comprehensive review of using heat as a tracer for groundwater studies was presented by Anderson (2005).

Distributed Wireless Sensor Networks

A critical feature of θ is its variability in time and space. Development of sensing systems that can enhance resolution in either of these dimensions has the potential to facilitate greater understanding of the natural and managed hydrosphere. It could be said that the significant contribution to hydrology would be to provide perfect data for soil water, since with this data, one could close the water balance both to the atmosphere and groundwater stores. By virtue of the spatial complexity of θ, measurement methods that enhance our ability to capture spatial θ dynamics are highly sought after. The ability to combine sensors with wireless data transfer for automated, seamless collection or even real-time monitoring is exceptionally appealing for observing hydrological processes.

For the purposes of wireless data collection, θ sensors can be divided into two classes: those that require direct connection to sophisticated data analysis equipment and those that are self-contained, only requiring connection to a power source and data logger. The first class of instruments includes passive TDR probes, HPPs, and gypsum block-type sensors. The second includes the ECH_2O probe, Hydraprobe, ThetaProbe, and Acclima, among others. These sensors must be hard-wired to a metering device that is programmed to read them according to a specified protocol. In the case of heat pulse and gypsum block-type sensors, many data-logging devices have sufficient capabilities to be programmed to read the sensor directly, while in the case of a passive TDR probe, a dedicated TDR instrument must be connected to the probe, which might be networked with a multiplexer to allow reading of an array of sensors from a single TDR with an automated controller. Excellent networked TDR solutions have been commercially available for more than 10 yr. However, TDR methods are expensive and constrained for making spatially distributed measurements in areas greater than 1 ha. This is because of the sensors need to be connected directly to the TDR instrument using cables, which, with lengths greater than 30 m, suffer signal dispersion and attenuation.

Of greatest current interest are sensing systems that use autonomous sensors by communicating their data to a base station or gateway without hard-wired connections, that is, via some kind of radio transmitter. The attraction is that they may operate over larger areas, monitor more points, and be situated in more remote locations, for example, without dedicated AC power.

In the past decade, the supporting communication and data-logging technology has matured greatly. Although still emerging, motes, or low-cost, low-power, low-to-intermediate distance radios are developing fast. The term *mote* derives from the notion that each sensing station might be like a speck of dust, most important, tiny and of low cost. To date, typical mote systems require on the order of microamps of power (and hence are capable of running on AA batteries on the order of a month) to communicate over 100 to 200 m with a per-station cost on the order of $100. Although these figures are constantly subject to change, this technology is in at least its third generation, and so we would not expect orders of magnitude changes in these figures in the coming 5 yr. Even with this progress, a final "plug and play" solution is still a little ways off, with much effort required in the total system integration area (Kevan, 2007, 2006). In summary, the basic sensor interface is likely to be about the size of a pack of cards, cost about $100, and need to be attended to several times a year depending primarily on maintenance of the energy supply. The energy draw is largely dictated by how often communication is required and the sensors' power consumption (Kevan, 2007). This leads to a preference for low energy-consumption soil moisture sensors. The most promising category of such sensors are those detecting soil permittivity, as described above. These sensors are well matched to the mote characteristics, in that they have prices that are of the same magnitude, reasonable factory calibration for a broad range of soils, and low energy consumption.

The simplest configuration of a mote network is a "single-hop" or end-node-to-gateway network in which all of the motes communicate directly with a base station. This protocol is well established and reasonably simple to develop and deploy. In addition, systems that will reach as much as 8 km or more, line of sight, and still run on as little as a few AA batteries are commercially available from several vendors. These systems offer considerable advantages over traditional wired systems by limiting the possibility of data loss due to cable failure and the expense and labor of constructing and burying the cable. One thing these networks do not offer is the ability for individual nodes to work together to pass data back to the gateway, which limits the spatial extent of the network to the span of one mote radio.

A more complicated configuration of motes is a "multihop" system, often referred to as a "wireless mesh network," illustrated schematically in Fig. 8. The goal of this configuration is to use intermediate "routing node" motes as relay stations from remote motes to the base station and to establish this communication without requiring the user to specify which mote shall communicate with which other mote. Although the electronic aspects of mesh networking technology are well established, the communication and control infrastructure for mote systems is still nascent. In principle, this self-organizing system would be robust in the sense that if one station malfunctions, the system could reroute the information along alternative communication pathways. This laudable goal presents many profound technical challenges that are yet to be resolved at a level accessible to nonexpert users (Kevan, 2007, 2006). To understand the nature of the instrumental challenge, it is instructive to consider how many possible branched interconnections could be made between even just 10 mote stations (many thousands). In the multihop or mesh modality, the network must periodically evaluate which of these is optimal on the basis of radio signal strength, network communication bottlenecks, and network reliability. This all must be done using the bare minimum of radio time to avoid draining the mote power. Among other requirements, precise temporal synchronization is essential, which is an unsolved technical challenge in this arena.

The landscape in mote type is changing quickly, with new user-friendly solutions on the horizon. Commercial, turn-key, single-hop, θ measuring systems are available from Decagon Devices and Campbell Scientific (Campbell has a mesh network solution, but it requires mainline or large battery power), among others. One such system in eastern Washington, with 12 remote radio data loggers (Em50R, Decagon Devices, Inc.) and a cell phone–enabled data collection and delivery system (CR850, Campbell Scientific, Inc.), collected soil moisture, temperature, and electrical conductivity from soil sensors for spatiotemporal modeling of soil water within a complex, polygenetic landscape (Brown et al., 2007). Field data were available in near real-time over the Internet anywhere in the world. Other exciting developments using the Acclima digital soil sensing technology are forthcoming. Commercial multihop solutions are also available (Crossbow Technology, Dust Networks, SensiCast Systems), but some problems remain to be solved for these to be viable θ monitoring devices. Research teams at the Ecole Polytechnique Fédérale de Lausanne (SensorScope) and the Center for Embedded Networked Sensing, for example, have demonstrated autonomous soil moisture sensing systems with more than 100 independent measurement stations. Clearly, in the very near future, this technology will be able to provide easily installed systems that measure θ and other environmental parameters at hundreds of points at costs only a few times the cost of the sensors themselves.

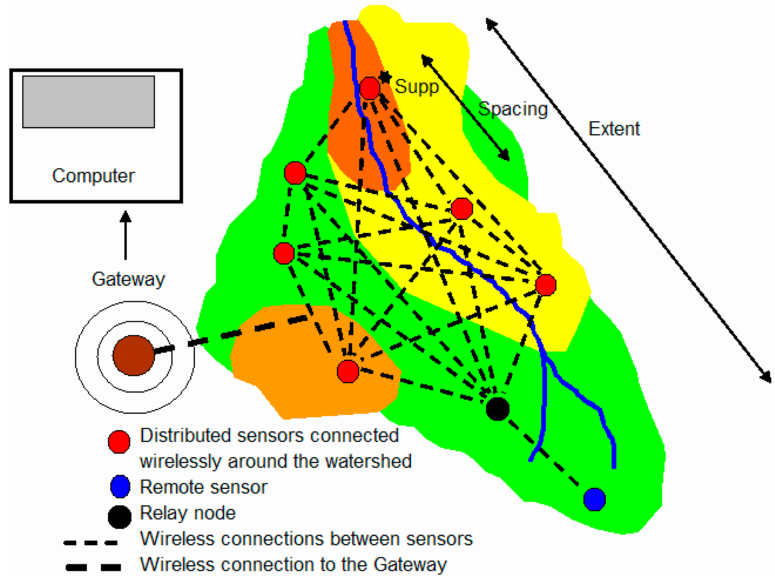

Fig. 8. A conceptual wireless mesh network or "multihop" system in a watershed. The sensors can all communicate to determine the most efficient wireless data transfer path to the gateway from where the data is transferred to the computer. The remote sensor sends data to a relay node, which passes it on to the gateway. Also shown are examples of the scale triplet (Blöschl and Sivapalan, 1995): support (Supp), spacing, and extent.

Geophysical and Mobile Sensing

Mobile TDR and Capacitance Sensors

The interest in being able to determine θ spatially has led to some innovative designs for mounting sensors to mobile platforms (Wraith et al., 2005). Most of these have been presented as designs for agricultural implements, since they require being dragged through the soil and can be combined with tillage practices. Whalley et al. (1992) presented an impedance-based sensor mounted on a plow and dragged through the soil at a depth of ~0.3m. More recently, TDR has been adapted to fit on mobile platforms, such as tractors, all-terrain vehicles (ATVs), or adapted spray rigs (Thomsen et al., 2005; Long et al., 2002; Inoue et al., 2001; Tyndale-Biscoe et al., 1998). Stop-and-go measurements for hydrological studies were presented by Tyndale-Biscoe et al. (1998) with an ATV-mounted TDR system and have been used by Grayson et al. (1997) for small watershed measurements (Fig. 4). The advantage of these measurements is that better spatial coverage is obtained, and θ is often averaged over 0.3 to 0.6 m down the profile. However, it is time consuming to make many stop-and-go measurements.

Two of the main design constraints for developing on-the-go sensing relate to (i) robustness and (ii) to obtaining a representative sampling volume. To drag anything through the soil, it must be robust. This usually means somehow mounting a probe at the base of a steel shank. This creates difficulties since the probe itself should not be connected to other pieces of metal that could act as extra sections of probe and affect the signal response. Friction, generating heat, caused by dragging a probe through the soil will also affect the reading, but to what extent remains unknown. The size of the sampling volume is also an important consideration. Inserting a small plow or torpedo shaped probe (Sun et al., 2006) will compact the soil around the sensor. Two blades might reduce this affect, but then there is the problem of putting the plates close enough together to achieve a representative sampling volume. If the plates are too close, clogging may result, preventing an even flow of soil between the sensor plates. Recent work presented by Jones et al. (2006) has tried to overcome some of these limitations by using a surface probe mounted in the body of a plow or shank (Fig. 9a). This design uses energy radiating from the end of the probe to estimate changes in θ. Because traditional travel-time measurements are hard to decipher using this design, methods are being investigated that use signal analysis to convert the waveform (Fig. 9b) to the frequency domain. Initial results appear promising, as shown in Fig. 9c.

It is not hard to imagine a time when all tillage machinery could be mounted with such sensors to collect on-the-go data. This type of development in measurement technology integrated into a measurement database could provide ground data to compare with routinely available remotely sensed data. Although this would be limited to agricultural ecosystems, it may form an important tool for understanding hydrologic response patterns in managed systems.

Geophysical Methods

Geophysical methods provide an interesting and exciting set of instruments for determining θ. The advantage of most geophysical tools is that they are noninvasive or min-

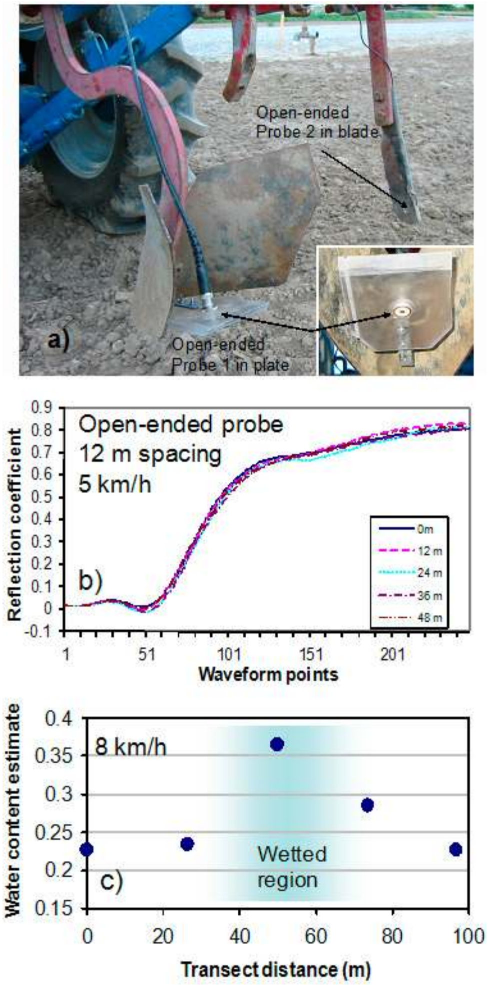

FIG. 9. (a) Picture of “blade-” and “sled-configured” prototype open-ended time domain reflectometry probes. (b) Waveforms measured with the blade probe in the field at uniform θ (i.e., Millville silt loam [coarse-silty, carbonatic, mesic Typic Haploxeroll]) along a 50-m transect. (c) θ interpreted from the blade open-ended probe reading in a nonuniformly wetted transect in the same field.

imally invasive and offer huge potential for spatial determination of soil properties in addition to θ. Those currently used for determining such properties fall into two categories: (i) those that measure ground electrical conductivity, which includes DC resistivity (Samouelian et al., 2005) and EMI (Sheets and Hendrickx, 1995), and (ii) those measuring electromagnetic wave propagation time through the ground, such as ground penetrating radar (GPR) (Knight, 2001; Huisman et al., 2003a).

Ground Penetrating Radar

Ground penetrating radar is an electromagnetic method that uses the transmission and reflection of high-frequency (1 MHz–1GHz) EM waves within the subsurface. The depth of investigation can be submeter to tens of meters or even greater in resistive materials. The measurements provide information about the permittivity of subsurface materials; because of the link between permittivity and θ, GPR offers the potential to obtain estimates of θ along transects within a watershed. Descriptions of the fundamental principles of GPR can be found in Daniels et al. (1988) and Davis and Annan (1989). An overview of its use for environmental applications is given by Knight (2001) and more specifically for the determination of θ, by Huisman et al. (2003a). Methods for determining water content include common offset profiling (Lunt et al., 2005), estimation of ground-wave velocity (Hubbard et al., 2002), common midpoint measurements (Greaves et al., 1996), and surface reflectivity (Serbin and Or, 2004; Redman et al., 2002).

A variety of methods have been adopted to determine θ from GPR data and have been reviewed in Huisman et al. (2003a) and Annan (2005a,b). Ground penetrating radar data can be collected using a surface-based system, where the transmitter and receiver antennas are moved across or above Earth’s surface, or using a crosshole system, where the antennas are positioned in boreholes, or a combination of the two. The various methods all involve measurement of the travel time of the EM waves and/or the amplitude of reflected EM energy, both of which are related to the dielectric constant ($\varepsilon_T'/\varepsilon_o$) of subsurface materials.

One relatively simple application of GPR for θ is measuring the travel time of the direct ground wave, which travels from the source to receiver antenna through the topmost layer of the soil (Huisman et al., 2003b; Hubbard et al., 2002). The uncertainty in this method is the true depth of the sampled region, which can vary from a few centimeters to a meter, depending on antenna frequency and θ (Galagedara et al., 2005).

Another surface-based method that yields an average θ of a volume of the subsurface involves measuring the change in travel time of EM waves, reflected off subsurface interfaces, as the antennas are moved apart (Greaves et al., 1996). In the past, the data acquisition for this method has been extremely time consuming, yielding θ estimates with spatial resolution on the order of meters to tens of meters. Recently, however, a new system has been developed with multiple antennas deployed on a moving platform; this will undoubtedly lead to increased use of this method.

The crosswell GPR method also uses measurements of the travel time of EM waves to estimate the variation in θ in the region between two boreholes (Redman et al., 2002). One of the challenges in applying this method is obtaining an accurate reconstruction of the dielectric properties between the boreholes used to estimate θ (Irving et al., 2007).

A method that has been applied successfully, which uses a measure of the amplitude of reflected energy, involves suspending the antennas above the ground to estimate θ of the surface layer (Chanzy et al., 1996). One source of uncertainty is determining the depth of the reflecting interface, which determines the thickness of the sampled surface layer.

Regardless of the GPR method used to obtain measurement of travel time or reflection amplitude, a critical step is transforming the determined dielectric constant κ to an estimate of θ. Calibration can be obtained at a field site using other forms of data, such as a neutron probe or TDR (Huisman et al., 2003b), but heterogeneity below the scale of the measurement has a large impact on the κ–θ relationship. Calibration with other forms of measurement with different supports, or the use of simple models or empirical relationships that neglect heterogeneity, can lead to significant errors in estimates of θ (Chan and Knight, 2001, 1999; Moysey and Knight, 2004). What is required is a means of quantifying (i) the support of the GPR measurement and (ii) the submeasurement-scale heterogeneity that exists within the sampled region if radar-based dielectric measurements are to be used to provide accurate estimates of water content.

Another way in which GPR methods could be used in studies of soil moisture is using GPR images to determine not the magnitude of θ but the spatial distribution in θ over large three-dimensional volumes of the subsurface, at submeter resolution. A recent study suggested that the correlation structure seen in the GPR image represents the correlation structure in θ, spatially averaged at a scale determined by the support of the GPR method (Knight et al., 2007). While further research is required to develop GPR as a reliable field method, it offers a new way to capture information about spatial heterogeneity in θ that cannot currently be obtained with any other method.

Ground penetrating radar is a high-resolution, noninvasive form of measurement that can be used to obtain estimates of the variation in dielectric properties over large regions of the surface and subsurface. A disadvantage of GPR, as with other geophysical methods, is the high degree of user knowledge required to obtain good-quality data and valid interpretations. An additional technical limitation occurs is in saline or some clay soils, where signal attenuation, due to bulk electrical conductivity >1 dS m^{-1}, makes it increasingly difficult to obtain good results (Weihermuller et al., 2007). As interest in the use of GPR in hydrology, soil science, and agriculture continues to grow, we will undoubtedly see advancements in both the technology and the science that will lead to improvements in methods of data acquisition and improvements in the accuracy of θ estimates.

Electromagnetic Induction

One of the more promising technologies for determining soil properties including estimations of θ is EMI. It was first described as a noninvasive borehole-logging geophysical technique (Keller and Frischknecht, 1966). The instrument measures ground conductivity and has a receiver at one end and a transmitter loop at the other. The transmitter is energized and creates magnetic field loops in the ground. These magnetic loops produce electrical field loops, which in turn create a secondary magnetic field. At low induction numbers, the combined primary and secondary magnetic fields measured in the receiver are proportional to the ground conductivity (McNeill, 1980). Different instruments have different loop separations. The greater the spacing of the loops, the deeper the penetration into the ground. The orientation of the loops also affects the field penetration into the ground (Wait, 1955). The nominal depth of penetration for these tools is 0.75 times the transmitter–receiver loop spacing for a horizontal electromagnetic dipole configuration and 1.5 times the spacing for a vertical dipole. Callegary et al. (2007) have shown that this penetration depth depends on the conductivity of the soil, the penetration depth reducing slightly as the soil becomes more conductive. An instrument with a 1-m loop separation in the vertical orientation may integrate a volume of several cubic meters of soil in each measurement. The EMI method has been used extensively for mapping soils after first being reported by DeJong et al. (1979). It has been used for mapping soil salinity (Rhoades et al., 1999), within precision agriculture (Corwin and Lesch, 2003), and increasingly in mapping clay content of soils (Jung et al., 2005; Triantafilis and Lesch, 2005). The instruments are robust, are relatively simple to use, and can be linked to a field computer and global positioning systems to provide spatially exhaustive data over comparatively large areas, 50 to 500 ha.

Kachanoski et al. (1988) were the first to report using EMI to determine water content explicitly; more recent work includes Reedy and Scanlon (2003), Sheets and Hendrickx (1995), and Scanlon et al. (1999). The major difficulty with this method is interpreting the signal and the causes of the response. Sherlock and McDonnell (2003) proposed that simply using the signal response to provide spatial information has merit. They called the signal information collected in this way *soft data*, in contrast to what might be termed *hard data* from a soil moisture sensor such as TDR.

Understanding how best to use and interpret the signal response for hydrological applications is an important area of needed research. Such study would involve quantifying the spatial covariance between the EMI data and any other "hard data," such as gravimetric or TDR measurements. Using cross-correlation statistics would be one way to analyze the results of such indirect measurements. The area of spatial covariance analysis needs research for the application of methodologies suitable for hydrology. One approach taken by agricultural scientists has been to try to calibrate the signal response using directed soil sampling based on the signal response surface and using a multiple linear regression (Lesch et al., 1995a,b). An alternative approach might be to use the instrument to assess changes in ground conductivity before and after rainfall events (Fig. 10). On a 12-ha field site in Utah, 5000 data points were collected before (Fig. 10a) and after rainfall (Fig. 10b). Hydrological changes can be observed by differencing the maps, where differences in the observed ground conductivity (Fig. 10c) are primarily the result of changes in θ. As with the data presented in Fig. 4, more structured patterns occur after wetting, indicating the presence of subsurface flow paths. Alternatively, this "soft data" could be combined with more sparse data such as TDR measurements of θ, which are harder and more time consuming to obtain. A vision for the future is to combine EMI measurements with ground-based sensor networks, either using the EMI data to place sensors in hydrological locations of interest or using the data collected from the sensor network to constrain calibration of the EMI measurements. This method in the hands of a skilled user holds great promise for hydrological applications, especially since

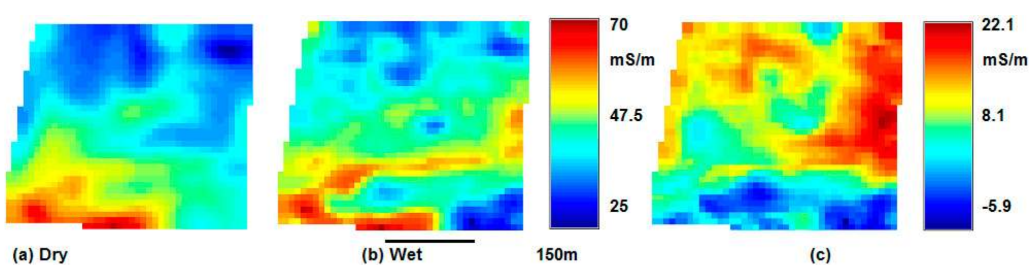

Fig. 10. Maps of bulk soil electrical conductivity measured with electromagnetic induction across a 12-ha field, rendered with 10- by 10-m pixels. (a) Dry soil before a major rainfall event, (b) soil after ~75 mm of rain, and (c) the difference between the two. The field slopes from right to left, with the bottom-left corner the lowest point. The red areas in (a) and (b) indicate what appears to be the emergence of subsurface flow paths after rainfall. The red areas in (c) indicate zones of increased electrical conductivity after rainfall.

a number of soil properties of hydrological interest can be inferred (texture, water content) from spatially exhaustive data.

Direct Current Resistivity

Direct current resistivity is defined here as imaging from the ground surface, whereas electrical resistance tomography is used to describe borehole measurements. Direct current resistivity is a direct current (or low-frequency alternating current) method of determining resistivity, where electrodes are inserted in the ground along a line at even spacing, typically from 0.5 to 5 m between each. The use of DC resistivity to determine soil moisture was described as long ago as the end of the 19th century (Briggs, 1899). Use of the four-probe resistance method was described by Edlefsen and Anderson (1941) using the Wenner array (Wenner, 1915) designed for measuring earth resistivity. Interest in the measurement of θ using resistivity declined because of its dependence on other soil properties and the advance of other methods such as the neutron probe. However, it still found some application for θ determination in rapid laboratory measurements in saline soils (Gupta and Hanks, 1972).

The method of using resistivity developed mostly through mineral and oil exploration (Archie, 1942; Keller and Frischknecht, 1966) and more recently in near-surface geophysics applications. Multiple resistance data are now collected by creating an electrical gradient between two source electrodes and measuring the resultant potential distribution at two or more receiving electrodes along a line of multiple electrodes. Advances in electronic switching means that tens of electrodes can be measured in a few tens of minutes, providing spatially exhaustive data along transects. This advanced capability has created a renewed interest in monitoring soil properties and processes using the method (Samouelian et al., 2005; Michot et al., 2003; Zhou et al., 2001; Goyal et al., 1996). The resistivity measurements provide a two-dimensional profile and can be used to determine static properties such as subsurface structure and texture, as well as temporal changes associated with θ, or water chemistry (Samouelian et al., 2005). The advantage of using DC resistivity was illustrated by Michot et al. (2003), who studied changes in θ under a corn crop. Rapid data acquisition means that it is highly useful for monitoring spatial processes, and when calibrated or linked to point measurements with water content sensors, it can provide strong insight into subsurface processes including changes in θ. Figure 11, adapted from Michot et al. (2003), shows how the resistivity image gives a two-dimensional slice so that θ changes can be observed spatially in the soil profile. Resistivity imaging as illustrated here is possible at submeter- to tens-of-meter scales in the field and has been used mostly for monitoring tracer tests (Singha and Gorelick, 2005) and qualitative changes in θ (Amidu and Dunbar, 2007; Goyal et al., 1996).

Remote Sensing

By definition, remotely sensed measurements of θ are made using instruments that are not in direct contact with the soil. Changes in θ are inferred through the soil's influence on potential fields, such as the electric, magnetic, and gravitational fields. These "measurements at a distance" have distinct advantages and challenges compared with ground-based techniques. There are currently three main remote sensing methods used to measure θ. The first two methods consider either the electromagnetic radiation naturally emitted by the target (passive remote sensing); or the radiation scattered by the target after the target has been illuminated with a known source of radiation (active remote sensing). In the third method, changes in the gravity potential field above the soil, which are related to changes in the density of the soil, and thus θ, are detected. At present, measurements of θ using the third method are only available at very large scales, 600 to 1000 km (Tapley et al., 2004). Only the first and second methods can produce measurements at the observatory (small watershed) scale, and hence, only these two methods are considered here.

Passive Remote Sensing

In the first method, a remote sensing instrument called a radiometer is used to measure radiation naturally emitted by the soil. This technique is called radiometry or passive remote sensing (Njoku and Entekhabi, 1996; Njoku and Kong, 1977; Eagleman and Lin, 1976; Jackson et al., 1997). A picture of a mobile radiometer system is shown in the upper-right corner of Fig. 6. Soil, like all matter, emits radiation, and this emission increases with temperature. The dielectric properties of the soil and the physical nature of the soil surface (roughness) determine how closely the soil surface resembles a perfect emitter, or blackbody. The fraction of the total possible radiation (blackbody radiation) that is emitted is called the emissivity of the soil. Emissivity varies between zero and 1. At infrared wavelengths, soil emissivity is close to unity regardless of θ. Consequently, infrared radiometry is an effective method of soil surface temperature measurement. In the microwave region (frequencies from hundreds of MHz to hundreds of GHz, or wavelengths from meters to millimeters), soil emissivity is a strong function of θ (Hallikainen et al., 1985; Schmugge et al., 1974).

To illustrate the theory of passive remote sensing, consider a smooth bare soil surface with a uniform temperature, *T*, and

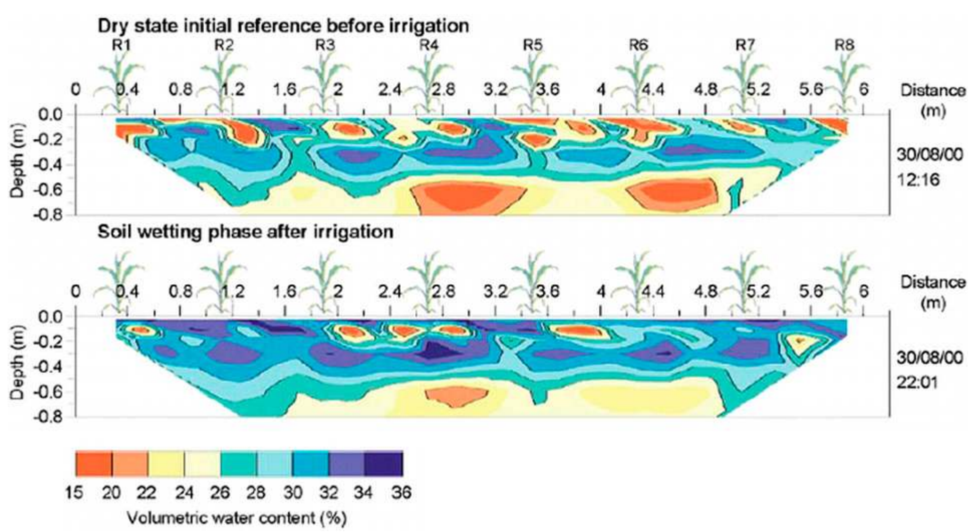

FIG. 11. Characteristic soil moisture under a corn crop before and after soil wetting. θ is determined from DC resistivity measurements; figure altered from Michot et al. (2003).

a uniform soil moisture profile. The brightness temperature of this soil surface,

$$T_B = eT \quad [11]$$

is equal to the product of the soil temperature and the microwave emissivity, e. Since e is dimensionless, brightness temperature has units of Kelvin. At microwave frequencies, the brightness temperature is directly proportional to the radiant power emitted. As a result, a simple linear calibration can be used to relate the radiant power measured by a radiometer to the brightness temperature. If the soil temperature is known, then changes in the brightness temperature of the soil reflect changes in e, and hence, θ, of the soil surface.

The value of e is essentially a linear function of θ. It also depends on soil texture, which along with θ determines the dielectric properties of the soil; the roughness of the soil surface, as previously mentioned; the observation view angle; and polarization. As θ increases, e decreases. Low brightness temperatures correspond to wet and/or cold soils. Because of the significant changes in e with θ, the brightness temperature of a wet and dry soil can differ by nearly 100 K. This is large in relation to the precision of a typical microwave radiometer (≤1 K) and results in an excellent signal-to-noise ratio, making it possible to measure changes in θ of less than 1%. Soil surface roughness tends to decrease the sensitivity of the brightness temperature to θ (Schneeberger et al., 2004; Choudhury et al., 1979). The dependence on observation view angle and polarization is well known for quasi-specular (effectively smooth) surfaces (e.g., Ulaby et al., 1981). In practice, the horizontally polarized (H) and vertically polarized (V) components of the emitted radiation are measured.

Two important distinctions between infrared radiometry and microwave radiometry must be made. First, space-borne infrared radiometers cannot view the Earth's surface through clouds or precipitation, which are effectively transparent at low microwave frequencies. Second, an infrared radiometer is sensitive to the temperature of an extremely thin layer of soil at the soil surface, much less than a micrometer in depth. Hence, the brightness temperature measured with an infrared radiometer is often called the skin temperature. A much thicker layer of soil contributes to the emission measured by a microwave radiometer. The depth of this contributing soil layer, called the emitting depth, scales with wavelength. At a frequency of 1.4 GHz (a wavelength of 21 cm), the emitted radiation is typically sensitive to the upper 3 to 5 cm (Laymon et al., 2001), while at 19 GHz (a wavelength of 1.6 cm), the emission is determined by only the upper few millimeters. For a soil with a nonuniform temperature and soil moisture profile, the emitting depth can change depending on how sharply the soil dielectric properties vary with depth. When the soil moisture profile is sharp (very wet just at the surface), the emitting depth is decreased (Jackson et al., 1998). On the other hand, when the soil is dry or the moisture profile is uniform, the first several centimeters determine the emitted radiation (Schmugge and Choudhury, 1981).

When vegetation is present, its radiative properties must also be considered. Vegetation is semitransparent at microwave frequencies: vegetation attenuates the radiation emitted by the soil and also self-emits. Attenuation is due to both absorption and scattering. The most useful models of microwave emission from a vegetated surface consider three main components of the brightness temperature (Jackson et al., 1982), $T_B = T_{Bsoil} + T_{Bveg\uparrow} + T_{Bveg\downarrow}$, where T_{Bsoil} is emission from the soil attenuated by the canopy, $T_{Bveg\uparrow}$ is upwelling emission from the canopy, and $T_{Bveg\downarrow}$ is downwelling emission from the canopy reflected by the soil and attenuated by the canopy. This treatment assumes that the absorption and scattering properties of the vegetation can be effectively modeled with two parameters, the optical depth and the single-scattering albedo, respectively. This has been found to be true for many different types of vegetation (Jackson and Schmugge, 1991).

Active Remote Sensing

In the second method, remote sensors measure radiation scattered by the soil. This technique is called active remote sensing. The illumination that causes the scattering can originate either from a natural source or from the remote sensor itself. Cameras and other visible and near-infrared detectors, including our own eyes, are active remote sensors since they detect scattered solar radiation. On the other hand, radar launches an electromagnetic wave toward the soil surface and then records the radiation scattered by the soil. In either case, the fraction of radiation scattered by a soil surface is a function of θ.

Radar at microwave frequencies is considered to be the most effective active remote sensing technique for the measurement of θ for several reasons. First, radars do not depend on illumination from the sun. Furthermore, radars that operate at lower microwave frequencies can penetrate through clouds and precipitation. Low-frequency radar can therefore be used in all weather conditions and at all times of day. Another reason is the depth of the soil volume that influences the scattered radiation, the penetration depth. At visible and near-infrared wavelengths, the penetration depth is extremely thin (less than the emitting depth for infrared radiometry), while in the microwave region the penetration depth at frequencies between 1 and 2 GHz is approximately 5 cm (Ulaby et al., 1996). Finally, visible and near-infrared techniques are affected by soil organic matter, roughness, texture, color, and incidence angle more than microwave techniques. In the future, hyperspectral visible and near-infrared active remote sensing may be useful at smaller (subfield) scales as new technology is developed and more ancillary data become available (Kaleita et al., 2005).

Since radar transmits and receives radiation, the configuration of the transmitting and receiving antennas must be specified. Bistatic radars have separate transmitting and receiving antennas but are rarely used. Normally, a single antenna transmits and receives the radiation, resulting in a measurement of backscatter from the soil. The ratio of the power received, P_r, to the power transmitted, P_t, is directly proportional to effective scattering area of the target, called the backscattering cross-section, σ:

$$\frac{P_r}{P_t} \propto \sigma \quad [12]$$

The proportionality constant depends on the configuration geometry, characteristics of the antenna, and the wavelength of observation. The backscattering coefficient, σ^o, is the backscattering cross-section per unit area, an intrinsic property of the soil surface (analogous to the visible–near-infrared reflectance of a surface) that can be used to determine θ.

The backscattering coefficient of a soil surface is related to the reflectivity, R, of the surface, the fraction of incident radiation scattered. Note that under conditions of thermodynamic equilibrium, e and R of a surface are related by Kirchoff's law, which states that $e = 1 - R$ (Peake, 1959). R depends on the dielectric properties of the soil surface and (for smooth surfaces) varies with incidence angle and polarization according to the Fresnel reflection coefficients. For a surface that is not perfectly smooth, incident radiation is scattered in many directions, which is the case for nearly all natural surfaces. R and σ^o increase with θ. As the soil surface roughness increases, σ^o increases in magnitude but the sensitivity of σ^o to θ decreases (Ulaby et al., 1986). A polarimetric radar can measure the HH, VV, HV, and VH backscattering coefficients, where the first letter denotes the polarization of the transmitted radiation and the second the polarization of the received radiation. By reciprocity, HV = VH. The phase difference between transmitted and received radiation is also measured by a polarimetric radar, and it is useful in certain situations. The magnitude of σ^o can vary greatly and is normally expressed in decibels. A typical radar has a precision of ≤1 dB, and the change in σ^o of a wet and dry soil can be up to 10 dB.

Low-frequency radar can penetrate through modest amounts of vegetation, unlike visible and near-infrared techniques. There are three categories of scattering mechanisms that determine σ^o of a vegetated surface (Ulaby et al., 1996): $\sigma^o = \sigma^o_v + \sigma^o_g + \sigma^o_{vg}$. One mechanism is direct canopy backscatter, σ^o_v. Another is direct backscatter from the ground, σ^o_g, attenuated by scattering and absorption as it passes through the canopy. A variety of other mechanisms that involve multiple scattering between the canopy the soil surface, here grouped together as σ^o_{vg}, also contribute to σ^o. The number of multiple scattering mechanisms that must be considered depends on the type of vegetation and, specifically, on its architecture. For example, some scattering mechanisms can be neglected for canopies that do not have large vertical stems (De Roo et al., 2001).

Advantages and Challenges

There are two primary advantages of remote sensing: the ability to make measurements over large spatial areas with a single instrument on a mobile platform (such as an airplane or satellite), which is more cost-effective and eliminates errors introduced by sensor-to-sensor variability, and the ability to make measurements in isolated locations where it is not possible or feasible to make in situ θ measurements. Consequently, remote sensing is the only measurement technique capable of regular and reliable large-scale measurements of θ, including global measurements (Kerr et al., 2001).

As noted earlier, low microwave frequencies are favorable for soil moisture remote sensing. At lower frequencies, the effects of vegetation and roughness on the remote sensing signal decrease, the emitting or penetration depth increases, and clouds and precipitation are essentially transparent. Given the remote sensing technology that is currently available, L-band (frequencies between 1 and 2 GHz) has been identified as optimal for soil moisture remote sensing (Entekhabi et al., 2004). At L-band, both radiometry and radar are sensitive to θ through vegetation. The opacity of a vegetation canopy is primarily determined by its water column density, the mass of water contained within the vegetation canopy per area. At 1.4 GHz, a radiometric sensitivity of at least 1.5 K per percent θ has been measured through maize (*Zea mays* L.) up to a vegetation water column density of 6.3 kg m^{-2} corresponding to a 3.0-m canopy; the highest water column density observed during a full growing season (Hornbuckle and England, 2004). Reliable models of the microwave emission at L-band have been developed for column densities up to 4 to 5 kg m^{-2} (Wigneron et al., 2007). Hence, microwave radiometry at 1.4 GHz can be used in virtually all nonforested areas of low relief (strong variations in topography currently preclude the use of radiometry in mountainous areas). For L-band radar, θ retrieval is only possible for vegetation canopies of up to approximately 0.5 kg m^{-2} (Ulaby et al., 1996).

The coherent nature of the radar signal makes this technique much more susceptible to the effects of vegetation and surface roughness than radiometry. On the other hand, radar can provide higher spatial resolution images because of its ability to discriminate the arrival of separate pulses of radiation in range. For radiometers and radars mounted on aircraft, the difference in spatial resolution is not significant, and both techniques can provide maps of θ on the scale of tens to hundreds of meters. At the satellite scale, radiometers typically have resolutions of tens of kilometers, while radar resolution can be much less than a kilometer. Although radar cannot be used in most vegetated areas by itself, it has been hypothesized that for short periods of time (1–3 d), changes in the radar signal are primarily caused by changes in θ (Narayan et al., 2006). Using this change detection strategy, it may be possible to use combined radiometer and radar satellite measurements to produce a θ product in nonforested areas with a spatial resolution of approximately 10 km by using high-resolution radar measurements to disaggregate lower-resolution radiometer measurements (Entekhabi et al., 2004).

Recall that L-band radiometry and radar are sensitive to only the upper few centimeters of soil because the emitting depth and penetration depth at L-band is approximately 5 cm. While this near-surface θ is an important hydrologic variable because of its effect on infiltration, runoff, and the surface energy balance, the total amount of water in the vadose zone is also an important hydrologic variable. L-band measurements of near-surface θ can be used to estimate θ in the vadose zone when these measurements are assimilated into land surface water and energy balance models, as long as the observations of near-surface θ are made with sufficient frequency (Wigneron et al., 1999; Galantowicz et al., 1999). In the future, it may be possible to make direct measurements of vadose zone θ with low-frequency radar in the UHF and VHF bands (Kuo and Moghaddam, 2007).

Promising Avenues of Instrumentation Research

Over the years, many methods for determining θ have been examined, some developing into the sensors we currently use and some requiring improved technology to exploit contrasts allowing for water detection. The development of each methodology requires a critical set of ingredients to make it successful. Cost, adaptability, and robustness are fundamentally important, but so are their abilities to explore phenomena we have been unable to detect so far. Developments described in this article have advanced our understanding of high temporal resolution processes at the sample scale. Now we are looking for instruments that will improve spatial measurements over the root zone at a temporal resolution that allows us to monitor hydrological processes and characterize the hydrological connectivity. Timing is also important, and the right instrument needs to become available at the right time. This section looks at some of the promising methods being developed and the principles on which they are founded.

Acoustic Waves

The sensitivity of acoustic wave propagation to θ was reported by Brutsaert and Luthin (1964) and Mack and Brach (1966). Mack and Brach (1966) showed that measurements at low ultrasonic frequencies (16–20 MHz) were sensitive to both θ and solution ionic concentration. However, increasing the frequency to between 114 and 142 MHz reduced the sensitivity to ionic concentration and linearized the relationship. Recent developments include work by Adamo et al. (2004) and acoustic tomography to study unsaturated flow (Blum et al., 2004), as well as a phase shift method for studying acoustics in soils (Lu, 2007b). Recently, Lu (2007a) proposed that the acoustic properties are more closely related to the matric potential of the soil than the water content and may provide a means for determining matric potential over a wide range.

Optical Methods

Optical methods work in a number of ways; some exploit the contrast in refractive index between the water and material in which it resides, some use near-infrared reflectance, and others measure indirectly by detecting changes in other properties related to changes in θ. Measurements of changes in the refractive index have proved a valuable laboratory technique for measuring two-dimensional flow in hele-shaw cells. Tidwell and Glass (1994) demonstrated that using a light source behind a cell and measuring the transmission could be used to determine the spatial distribution of θ in the cell. One of the experimental difficulties was providing uniform light, but developments in light-emitting materials such as luminous films (www.luminousfilm.com) should help overcome these limitations. However, these methods are limited to the laboratory (Darnault et al., 2001).

Infrared reflectance spectroscopy is used to determine θ in minerals for planetary exploration (Yen et al., 1998). These methods are also applied in the food industry where a uniform homogeneous material can be monitored rapidly for θ (Wrolstad et al., 2004). However, the heterogeneity and surface roughness of soils combined with sample penetration limited to less than 1 mm or so makes the method currently impractical for environmental applications.

The exciting developments that are currently being made for environmental sensing are based on modified fiber optic systems. Older methods used attenuation (Alessi and Prunty, 1986) or reflection measurements (Garrido et al., 1999) and tend to measure across very limited volumes. Newer methods exploit brillouin scattering along a fiber optic cable (Texier and Pamukcu, 2003). The equivalent to metallic-TDR for light is the O-TDR, or optical time domain reflectometer. Commercial systems for sensing temperature along fiber optic cables are available and have been used in environmental sensing (Selker et al., 2005). These systems reportedly have a 1-m spatial resolution along the cable and detect temperature differences of as little as 0.1°C or better. Fiber optic systems have also been tested to determine the location of moisture spills using polymers that swell and create a localized loss along the fiber optic cable (MacLean et al., 2001). More recent fiber optics have been wrapped in hydrogel, where expansion and contraction of the hydrogel with changing θ cause strain gauges to give a measurable optical response (Texier and Pamukcu, 2003; Pamukcu et al., 2006). One of the current constraints to long-term monitoring encountered in soils is the degradation of the polymer by soil microbes. The potential of optical methods is exciting for environmental applications since cables can be buried in the ground over long distances and monitored, offering high temporal resolution data over the length of the transect. The possibility of determining temperature (Selker et al., 2005), θ (Pamukcu et al., 2006), and chemical signature (Yuan et al., 2001; Michie et al., 1995) makes fiber optic methods an exciting area of research.

Gravity Measurements

Gravity measurements can be used to determine temporal changes in the mass of a conceptual column of water in the near surface. Unlike many sensors that measure at a point, gravity measurements offer the potential to determine water content change from local to regional scales. The measurement of microgravity is made using an absolute gravimeter. Gravimeters operate by measuring the rate of fall of a control mass. The value of g is measured at a given location to accuracies on the order of 1 μGal (Nabighian et al., 2005), and they do not require comparison to another control location. However, the cost of these instruments is currently expensive, in excess of $250,000.

As the gravimeter determines a spatially weighted cumulative measure of changes in water content in the subsurface the measurements should be part of a coupled hydrologic instrument response framework (Blainey et al., 2007). Pool and Eychaner (1995) presented the first example of this application. Time-lapse gravity measurements were used together with water-level measurements in monitoring wells to infer aquifer specific yield. The interpretation required the use of a hydrologic conceptual model of complete drainage throughout the vadose zone and a flat-lying water table. The ability to make continuous measurements of this type holds promise for application to ecohydrological problems such as monitoring transpiration from trees.

Nuclear Magnetic Resonance

Nuclear magnetic resonance (NMR), first demonstrated in 1946 (Purcell, 1952; Bloch, 1952), has been developed extensively by the food industry for noninvasive θ determination (Wrolstad et al., 2004). Hydrogen nuclei (^{1}H) possess the strongest nuclear magnetic moment. These are randomly aligned in the absence of a strong magnetic field. On supply of an external magnetic field, the magnetic moments align with the field, parallel or antiparallel. An excess of antiparallel alignment provides a detectable macroscopic magnetization. The modulus of the magnetization vector aligned with the external field is proportional to the number of ^{1}H nuclei in the sample. Assuming that θ is proportional to the number of ^{1}H nuclei, the proportion of θ can be determined. Nuclear magnetic resonance relaxation measurements are also used to characterize porous media in the laboratory and include T_1, the spin lattice relaxation time, and T_2, the spin-spin relaxation time (Barrie, 2000). Laboratory investigations include water content determination in porous media (Liaw et al., 1996) and more specifically in soil (Bird et al., 2005; Hinedi and Chang, 1999; Kinchesh et al., 2002; Hinedi et al., 1993). Laboratory NMR and magnetic resonance imaging offer perhaps some of the most exciting methods of determining θ in situ in column experiments.

Field-based NMR systems have been developed for industrial applications and are described in Wolter and Krus (2005). The OSA-NMR system (Perlo et al., 2005) can be placed flat on a surface and measures to a depth of 5 to 30 mm. No reports of environmental application appear to have been made yet. Geophysical field systems have been deployed with application to hydrogeology (Lubczynski and Roy, 2004; Legchenko et al., 2004; Legchenko et al., 2002). At present the only commercial field system is the NUMIS MRS equipment (IRIS Instruments, Orleans, France) designed to determine θ and porosity to depths of up to 1500 m. The system requires a knowledgeable user to conduct experiments and interpret the data. The major obstacle to environmental NMR is that problems can occur in the presence of ferromagnetic materials. A second limitation is that if T_2 is very short, the hydrogen nuclei may have already relaxed in the dead time of the NMR instrument; this can occur with clay minerals.

Thermalized Neutron Detection

Satellite measurements of neutrons have been used to detect water in planetary exploration. Mitrofanov et al. (2004) reported the use of an instrument measuring θ in the Martian polar regions. Exciting research is being conducted at the University of Arizona where a team of scientists reported the development of a technique named the cosmic-ray neutron probe (Zreda et al., 2005). The technique is described as addressing the intermediate-scale detection zone between point measurements and remote sensing. The instrument uses cosmic-ray neutrons as the source and detects changes in neutron flux. Reported accuracy in the measurement of the change in θ is about 1% with an integrated measurement sensitive to the root zone and with a footprint of 10 to 100 m^2. The maximum sensitivity of the instrument is obtained buried around 0.2 m or 100 to 200 m above the ground mounted on a balloon or aircraft (Zreda et al., 2005). This type of method holds great promise for observatory measurements, and with no radioactive source, it overcomes many regulatory hurdles encountered using active neutron probes.

Scaling Issues: Bridging Measurement and Modeling

As much as measurement has improved at the point scale, the data are still incommensurate with modeling data requirements (Beven, 2001). This means that the scale at which a measurement is made (<1 m^2) differs from the scale represented by a model grid cell (>10 m^2), and θ at these scales is not the same quantity. One of the aims of watershed observatories is to improve our understanding of watershed processes using intensive monitoring. And so the question of how to bridge between measurement and modeling scales is pertinent. A desirable long-term goal is to transfer this new understanding gained at the watershed scale to watersheds that have minimal monitoring (Wagener et al., 2004). This raises a series of questions in terms of how we get from a series of point measurements to improving our understanding of ungauged watersheds: (i) What is the uncertainty associated with individual sensor measurements? (ii) How can we upscale from point measurements to areal mean soil moisture, compatible with a model grid square? (iii) How best can we sample soil moisture within the watershed? (iv) Can we determine characteristic watershed-scale soil moisture behavior, given certain watershed characteristics, such as soil type, vegetation, and topography? (v) Assuming some underlying behavior or pattern, can we use this to classify soil moisture behavior that can be transferred to ungauged watersheds? (vi) Are there measurements that allow estimation of areally distributed (e.g., grid-scale) model parameters? (vii) Do solutions exist for simulating the time-evolution of soil moisture at scales larger than point scale?

These questions underpin many current research efforts and although we cannot address them all, the following sections outline some of the issues and current research in more detail.

Determining Measurement Uncertainty

Gardner (1986) presented a comprehensive overview of the measurement errors associated with the standard method of oven drying soils and weighing. In general, error values are less than 1% depending on the mass of soil used and the accuracy of the balance. Perhaps the most significant source of error for determining volumetric water content from the field is obtaining an accurate volume of soil. For field calibration of an instrument, obtaining measurements of 2% or better is considered good. For example, in calibration measurements using a neutron probe (Campbell Pacific Nuclear hydroprobe, Model 503), Katul et al. (1993) investigated the relationship between the θ and the neutron probe count ratio. The count ratio was the ratio between actual and standard count. They found that the standard error of estimation was 2.1 volume percent of water.

In this discussion of errors, we limit ourselves to discussion of point sensors and GPR. The measurement error for most point sensors can generally be divided into two components: the precision of the measurement, characterized conveniently by the root mean square error, RMSE, and the accuracy, often described by an offset error. As an example, we analyzed the offset error and the RMSE after removing the offset error from the data shown in Fig. 7; the results are presented in Table 1. The Acclima gives the best performance, most notably with no offset error. This is due in part to its higher operating power and larger support volume. The TDRs, Theta, and Hydra probes all perform well with RMSE values ~0.02 $m^3\ m^{-3}$ commonly found for laboratory calibration of TDR (Topp et al., 1980; Malicki et al., 1996). Most of the sensors show some offset error, most likely resulting from soil compaction around the electrodes; this may change in time as soil redistributes around the electrodes caused by wetting and drying. Time domain reflectometry measurements are widely used in hydrology, and Hook et al. (2004) suggested a convenient method of assessing the quality of TDR measurements. They demonstrated that the error in θ increased as the rise-time of the TDR waveform increased. The rise-time of the waveform can increase due to poor probe construction, dielectric dispersion (Robinson et al., 2003), or soil salinity. For rise-times of <6 ns, errors were less than 0.1. For increasing rise times of 10 and 15 ns, the θ determination errors also increased nonlinearly to 0.15 $m^3\ m^{-3}$ and 0.4 $m^3\ m^{-3}$, respectively. Since the waveform rise-time is easily measured, they suggested (Hook et al., 2004) it be collected routinely as a way of ensuring data quality and checking for errors.

The CS-616 and ECH_2O EC-20 performed reasonably, but not as well as the other sensors (Table 1), but this has to be

Table 1. Errors associated with θ determination. Values for electrical sensors from data presented in Fig. 7. dual-probe heat pulse (DPHP) error determination from Heitman et al. (2003), Enviroscan errors from Baumhardt et al. (2000), and ground penetrating radar (GPR) errors from Huisman et al. (2001) for aggregated soil moisture data. Offset errors for instruments will vary depending on method of installation.

Sensor	RMSE after offset adjustment	Offset error	Water content range	Soil type
	$m^3\ m^{-3}$			
Acclima	± 0.014	0.002	0.17–0.36	Silt loam
Theta	± 0.017	0.056	0.17–0.36	Silt loam
TDR100	± 0.022	0.081	0.17–0.36	Silt loam
Hydra	± 0.024	0.194	0.17–0.36	Silt loam
Tektronix TDR	± 0.025	0.060	0.17–0.36	Silt loam
CS-616	± 0.031	0.140	0.17–0.36	Silt loam
ECH_2O EC-20	± 0.041	0.136	0.17–0.36	Silt loam
Enviroscan	± 0.027	–	0–0.4	
Enviroscan	± 0.026	–	0–0.4	
Enviroscan (FC)†	± 0.05	–	~0.40	
DPHP	± 0.012	0.1	0.00–0.33	Broad range
DPHP	± 0.022	0.1	0.02–0.59	Broad range
GPR (WARR)†	± 0.030		0.02–0.39	Sands and loams
GPR (STA)†	± 0.037		0.02–0.39	Sands and loams

† FC, factory calibration; WARR, wide angle reflection and refraction; STA, single trace analysis.

weighed against their low cost. However, the performance of these sensors is likely to decline further in 2:1 clays or saline soils, especially if temperature is variable, and RMSE values may be significantly greater. This was demonstrated for the CS-616 by Kelleners et al. (2005b). The Enviroscan errors are similar to the TDR errors for nonsaline coarse-textured soils (Baumhardt et al., 2000; Paltineanu and Starr, 1997). Again, Kelleners et al. (2004) demonstrated that the errors can significantly increase in saline or 2:1 clay soils. A further cause of measurement error in clay soils is failing to take into account the deformable, or shrink–swell, behavior of the clay. Kim et al. (2000) demonstrated the importance of accounting for shrinkage in forest soils using TDR.

Errors associated with the heat pulse method can be found in Basinger et al. (2003) and Heitman et al. (2003). Both showed an offset error of ~0.1, and the former presented RMSE values ~0.02 $m^3\ m^{-3}$ for a broad range of soils (Table 1). Basinger et al. (2003) also demonstrated that error may result because of the spacing of the electrodes changing when inserted into the soil. They showed that a 5% error in the spacing causes errors in θ determination of 0.024 $m^3\ m^{-3}$ at air dry to 0.084 $m^3\ m^{-3}$ at saturation 0.6 $m^3\ m^{-3}$.

Of the geophysical instruments, GPR methods are of significant interest. They have a support volume that is intermediate between point sensors and remote sensing, and the fundamental principle of determining dielectric response makes the technique an attractive bridge between TDR and active microwave remote sensing. The most comprehensive studies of measurement error for θ are presented in Huisman et al. (2003b, 2001, 2002). Huisman et al. (2001, 2002) demonstrated that RMSE values for θ were quite similar to those associated with TDR, of 0.030 $m^3\ m^{-3}$, for the same experiment. An interesting observation was that the θ–κ calibration model error was dominant. This suggested that comparisons between TDR, GPR, and Active microwave remote sensing are perhaps better in terms of dielectric response than conversion to θ.

From Point to Areal Average: How Best Can We Sample?

Mader (1963) raised an important question with respect to soil sampling: "How many soil samples do I need to be reasonably sure that the results of analysis on the samples collected are representative of the area being studied?" In the context of soil moisture, various studies have attempted to address this question. Hills and Reynolds (1969) presented a study in which they showed that their field site fell into two spatial categories, <950 m^2 and 950 to 6000 m^2. They found that maintaining a standard error below 2.5 at the 95% level required 4 to 19 and 44 to 80 samples, respectively. This only attempted to capture spatial variation, but of course θ varies temporally. Monumental sampling studies have been reported for spatial and temporal watershed soil moisture variability by Loague (1992a) for the R-5 watershed in Oklahoma. In a companion paper, Loague (1992b) demonstrated that the incorporation of the spatial variability of the antecedent soil moisture in the modeling approach improved peak flow prediction. Central to incorporating soil moisture measurements into distributed models is overcoming the incommensurate nature of point measurements and model grid squares (Beven, 2001). This involves the upscaling (Blöschl and Sivapalan, 1995; Western et al., 2002) of point measurements to provide areal averages, which has been considered in recent literature (de Lannoy et al., 2007, 2006; Pachepsky et al., 2003).

As a framework for discussion, the scale triplet (Blöschl and Sivapalan, 1995; Western et al., 2002) is considered to characterize the scale of measurements. Three scale aspects are identified. First is the support, the volume over which a measurement is integrated; in the case of a 30-cm-long TDR probe, this might be 600 cm^3. Next is the spacing, which is the distance between measurements. Finally is the extent, the length scale between the two farthest measurements in a group of measurements (see Fig. 8). Consideration of the scale triplet is important in developing a sampling scheme. Knowing the support volume is important because it determines the sphere of influence of an individual measurement (Table 2). The smaller the sphere of influence of an instrument, the larger the local fluctuations of measurements will be, and the less local variation would be attenuated. In other words, if the support is too large, small-scale variation will be lost. When comparing measurements at different scales and with different instruments, there will likely be a change of support, which is important because each instrument attenuates the variance within the support volume in both space and time. Therefore, an observed scale variance of soil water content, that is, the spatial or temporal semivariance, differs at each observation scale; this can be caused to a great extent by differing support sizes of the individual instruments. In addition, distribution of the water content itself can affect the support size, as demonstrated by Ferré et al. (2002); this may become more important with the transition to using geophysical instruments where support size may vary due to the instrumentation and the water content distribution. If the extent is too small, the large-scale variation is lost, whereas if the spacing is too large the small-scale variability is lost (Blöschl and Grayson, 2000).

As a detailed example, we consider a gravimetric soil moisture data set using the scale triplet along a transect. We consider first, the impact of sampling distance or spacing, and, second, how data aggregation or the support size affects the resulting $θ_g$ and its variance behavior and relationship to other

TABLE 2. Estimated support volume for a range of soil water content sensing instrumentation. Techniques measuring between 1 and 10 m^3 are very limited in availability. The values given for remote sensing are typical values reported in the literature; all assume a penetration depth of 0.05 m.

Instrument or measurement method†	Approximate support volume	Support changes depending on θ
	m^3	
ECH_2O	0.000010	x
Heat pulse probe	0.000010	
ThetaProbe	0.000015	
Hydra Probe	0.000015	
Gravimetric sample	0.0001	
0.15-m TDR	0.0003	
0.3-m Acclima	0.0006	
Neutron probe	0.1131	x
GPR (100 MHz antenna)	0.5–1	x
EMI (1-m coil spacing)	1	x
Remote sensing (typical values)		
Vehicle mounted Passive (5 × 5 m)	1.25	x
Vehicle mounted Active (5 × 5 m)	1.25	x
Aircraft passive (300 × 400 m) Passive/active L/S-band sensor	6,000	x
Aircraft active (300 × 400 m) Passive/active L/S-band sensor	6,000	x
Satellite passive (18,000 × 18,000m) Tropical rainfall mapping mission with EMI	16,200,000	x
Satellite active (30 × 30 m) ASAR systems†	45	x

† TDR, time domain reflectometry; GPR, ground penetrating radar, EMI, electromagnetic induction; ASAR, Advanced Synthetic Aperture Radar.

variables. For this purpose, measurements were taken along a 500-m moraine landscape transect at 5-m intervals. θ_g was measured at 10-cm-vertical depth increments down to 1 m. Soil sand content was measured at 0 to 10 cm depth, and surface elevation was determined. A few θ_g samples were taken in four nests at closer distances of 1 m (Wendroth et al., 2006). Increasing point sample spacings of 5, 15, 25, 35, 45, and 55 m were considered in the following analysis, with samples in between dropped. Conversely, the same spacings were applied with an increasing support size, yielded from data aggregation over increasing distances, while avoiding any overlapping. For example, at 15-m spacing, the distance over which data were aggregated was also 15 m (a scenario that could manifest with remote sensing measurements).

In Fig. 12, all point measurements of θ_g and topographic elevation, as well as point and aggregated measurements for 25- and 55-m spacings, are presented. While there is a considerable smoothing effect associated with the aggregation of θ_g measurements compared with point measurements, the spacing and different aggregation levels of elevation data do not create a large difference at the spacings analyzed here.

The mean values of θ_g point measurements at 0 to 10 cm [SWC(10)] increase with increasing spacing of point observations (Fig. 13); the same was found for the 80 to 90 cm depth increment [SWC(90)]. The standard deviation of θ_g point measurements rises with increasing spacing owing to the large impact of some high or low values found at large spacings.

Next, relations between θ_g at 0 to 10, 40 to 50 [SWC(50)], and 80 to 90 cm depth, elevation, sand content, and their behavior at different spacings and support sizes are quantified using Spearman rank correlation coefficients. In general, relations between SWC(10) and any of the other variables are closer for aggregated data than for point observations. There is no common or general trend observable for point observations whether ranking correlation coefficients increase or decrease with increasing spacing (Fig. 14). From this graph, we conclude that there is an obvious change of relations between different variables depending on the scale of observation.

Results from regression analysis presented in Table 3 reveal not only changes in the magnitude of slope and intercept with different spacing but also whether aggregated or point measurements are considered in the same extent and spacing distance. This result manifests the changing relationship between variables being observed across different scales; similar results are often observed in soil science and agronomy. For example, at the regional scale, a close relation between biomass production and soil texture may exist. Conversely, at the field scale and smaller, this relation can hardly be found because of a smaller variation of one or both variables and other influences relevant at the field scale (Wendroth et al., 1997).

Semivariograms (Isaaks and Srivastava, 1989; Nielsen and Wendroth, 2003) are shown in Fig. 15 for point and aggregated measurements. The only sampling designs resulting in a spatially structured variance are the original sampling and sampling at 15-m intervals, regardless of whether point or aggregated measurements are considered. If the spatial process of θ_g has to be sampled within this extent, observations should be taken at 15 m or less. At distances greater than 15 m, spatial variation is random. It is important to note that no interpolation of θ_g could be based on samples taken at spacings of 25 m or more. In general, point observations yield a larger variance than do aggregated data, regardless of sampling distance. Selecting point observations at

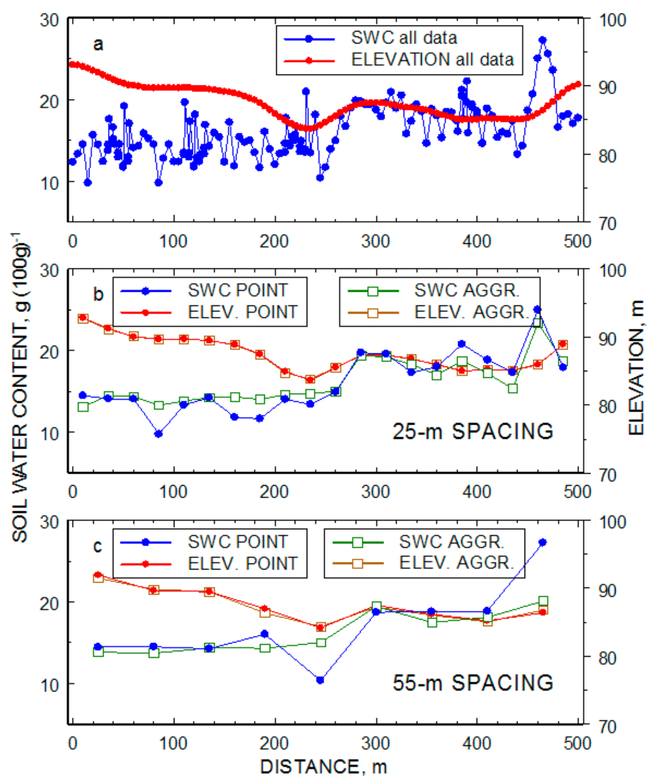

FIG. 12. Original soil water content (SWC) data (a) at the 0 to 10 cm depth and elevation, and point and aggregated measurements for (b) 25-m, and (c) 55-m spacing, respectively.

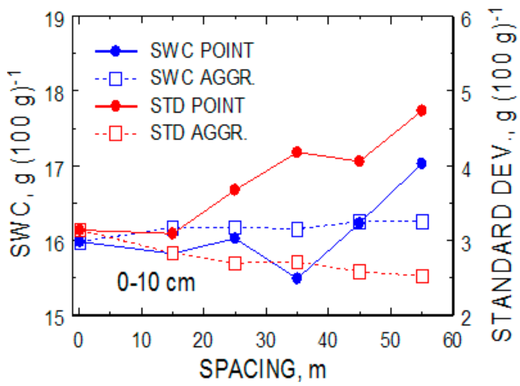

FIG 13. Soil water content (SWC) at 0–10 cm, measured at different spacings and aggregated over different distances, and their respective standard deviations.

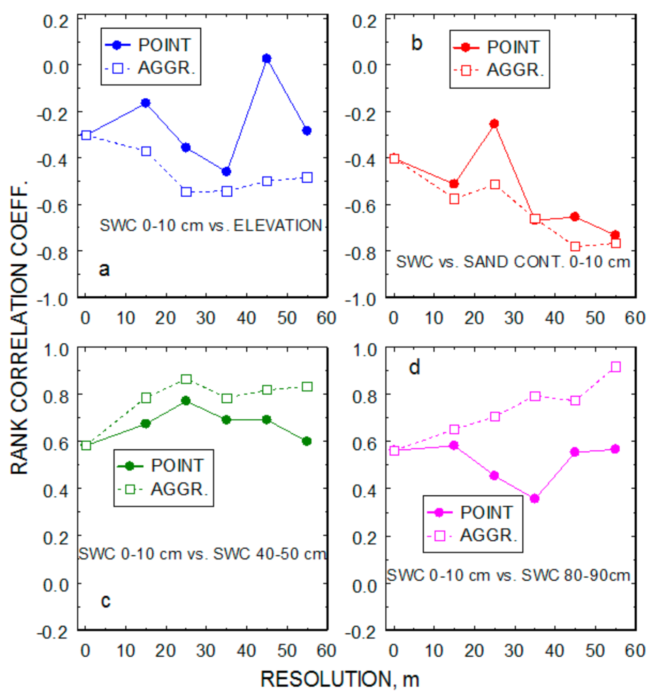

FIG. 14. Spearman rank correlation coefficients for various pairs of variables as a function of spacing for point and aggregated measurements. SWC = soil water content.

increasing spatial intervals raises the variance. This is one reason for the previous result of less-pronounced correlations for point-based observations compared with aggregated data. To identify a spatial variability structure for aggregated or point measurements taken at distances larger than 15 m, the spatial extent would have to be increased beyond 500 m, based on the assumption that the variance at the next higher scale exceeds the one observed within our 500-m extent.

The spatial distribution of soil water content at a given point in time depends on several landscape factors, including topography, soil texture, and vegetation. We consider a final analysis, in which the impact of measurement resolution and the inclusion of static data (sand content) with water content is used to evaluate the spatial process of θ_g in three scenarios (Fig. 16). In the first, SWC(10) is aggregated over a distance of 55 m and is based on sand content (0–10 cm) in a first-order autoregressive state-space model (Nielsen and Wendroth, 2003). The 95% confidence interval of estimation manifests the general behavior of data, following an increasing trend. Of course, fluctuations of data observed at a smaller scale are not represented by this model with very limited θ information (Fig. 16a). In the second scenario, small-scale behavior of θ_g is estimated based on 55-m point observations of θ_g and sand content, measured at a smaller scale of 5 m distance (Fig. 16b); not all the θ_g fluctuations are conserved in this scenario. However, the process of θ_g at a smaller scale is represented by introducing another variable, that is, sand content, sampled at the smaller scale and being statistically related to the spatial process of θ_g. At the 5-m scale, the coincidence between θ_g and sand content provides a narrow confidence band of estimation and appropriately represents fluctuations typical at this scale (Fig. 16c), which remains only slightly conserved in scenario 2 (Fig. 16b) and not conserved at all in the case of aggregated data, scenario 1 (Fig. 16a). This indicates the effect that including static and dynamic secondary data can have on improving the determination of the spatial pattern. The inclusion of the secondary data has the important consequence of reducing the uncertainty of the θ estimation in space.

The above example focused on spatial analysis; however, soil moisture also has a temporal variation component. The question, "How often, do we need to sample θ?" is as important as the question, "What soil water process do we want to represent at what scale, and what other variables do we need to sample that are related to θ, and support transition between scales"? Ranking correlation indicates increasing relationships between two variables with increasing aggregation level. However, small-scale information is lost, as is the spatial or temporal representation of a process. Moreover, linear regression coefficients change, manifesting the fact that there is not a unique answer between two variables measured across the landscape, but the answer is at least strongly affected by the support size and spacing.

One approach to address the issue of linking point measurements to provide areal space-time estimates of θ follows the methodology presented by Vachaud et al. (1985), who found the existence of time-stable θ monitoring sites. In essence, these are monitoring sites that capture the spatial and temporal average behavior of θ for a defined spatial area. This work was performed on a site with minimal slope, and Kachanoski and de Jong (1988) were quick to point out that the spatial variability of hydrological processes creates a lack of time stability in landscapes where topographic redistribution occurs. However, Grayson and Western (1998) showed that although time stable sites do not generally exist in watersheds with slopes, a few catchment average soil moisture monitoring (CASMM) sites could be found. Thierfelder et al. (2003) have continued with this theme in identifying CASMM

TABLE 3. Constant and slope values for linear regression between soil water content 0–10 cm (SWC10) and sand content at 0–10 cm (S10).

Resolution	All data: SWC10 = 34.066 – 0.326 S10			
	Aggregated		Point	
	Constant	Slope	Constant	Slope
15 m	41.394	–0.462	39.538	–0.437
25 m	41.485	–0.462	24.004	–0.148
35 m	46.611	–0.553	66.213	–0.916
45 m	49.692	–0.610	66.682	–0.915
55 m	60.413	–0.802	63.503	–0.862

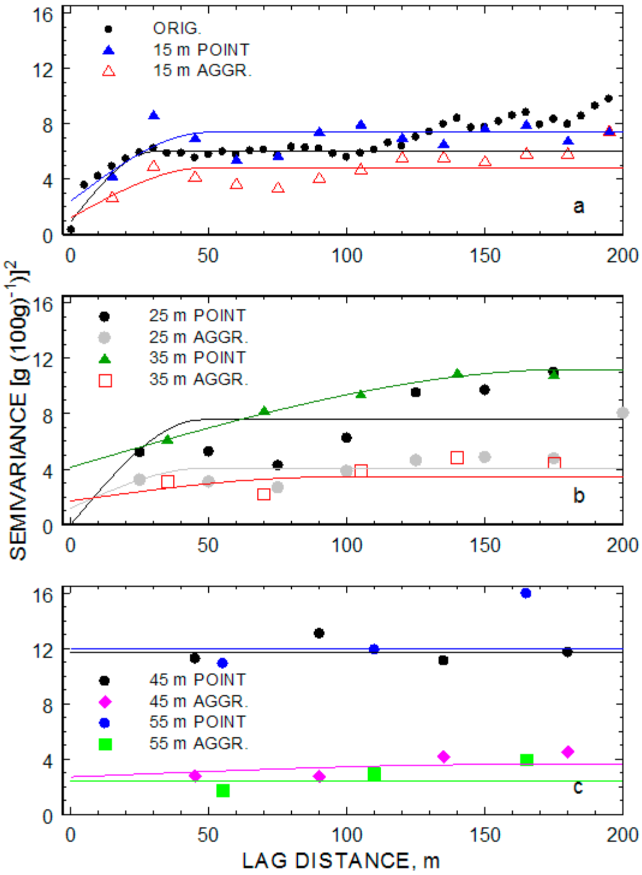

FIG. 15. Semivariograms obtained from soil water content at 0 to 10 cm depth for point and aggregated measurements at different spacings as a function of lag distance. The lines are semivariogram models fitted to the data.

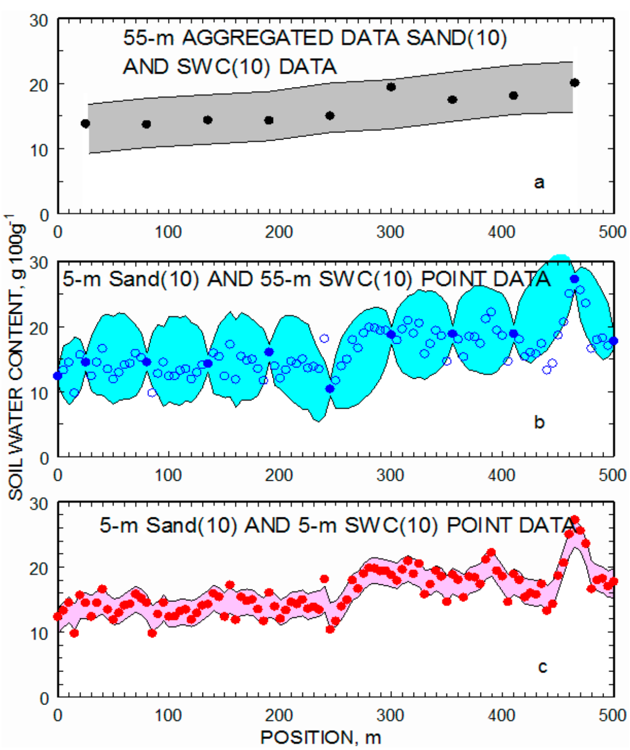

FIG. 16. Soil water content at 0 to 10 cm [SWC(10)] estimated with sand content at 0 to 10 cm [Sand(10)] for three scenarios based on different data spacing of point or aggregated measurements.

sites using database information. Research is now needed to determine how to rapidly identify such sites given limited data.

At a variety of scales, and for a variety of support, spacings, and extents, the range of structured variation needs to be explored, as does the magnitude of the variance with changing measurement resolution. As long as measurements and even aggregated data exhibit nonstructured variation, the spatial or temporal process remains undersampled, where undersampling refers to either sampling distances that are too long, aggregation volumes that are too large, sampling extents that are too small, or any of these reasons in combination with any other.

Moreover, statistical tools exist to quantify the length over which different variables are related to each other, and can be coregionalized with each other. However, another challenge is to combine the spatial and temporal domain of θ (Cahill et al., 1999; Wendroth et al., 1999) and take advantage of smaller measurement uncertainty in either one of these domains. Statistical filtering techniques (e.g., Kalman, 1960) allow the combination of process models and measurements. Wherever the model's capability of describing a process is limited, additional measurements may support the description of the process while lowering the uncertainty levels (Parlange et al., 1993; Bierkens et al., 2001; Walker et al., 2002; Margulis et al., 2002).

Is There Such a Thing as Characteristic Watershed Soil Moisture Behavior?

The growing interest in predicting hydrological response in ungauged basins, considered by Sivapalan (2003) the grand challenge of theoretical hydrology, prompts the question, "Does a characteristic watershed soil moisture exist?" If it were possible to discover such a behavior, then some form of classification of watersheds might be established on the basis of measurable characteristics (McDonnell and Woods, 2004; Wagener et al., 2007). McDonnell et al. (2007) recently argued that a change of emphasis is required in our modeling approach to understanding and describing watershed processes. They suggested moving from distributed physical models to exploring network models and conceptual models capturing dominant processes. While it is always good to explore different directions, perhaps a leading cause of frustration is not our lack of modeling ability but our inability to obtain data that can constrain more physically based models.

Soil moisture patterns have long been considered to be heavily intertwined with watershed topography. Digital elevation models are widely used for this purpose (Wilson et al., 2005). However, the analysis presented in the previous section indicates the importance of other landscape attributes. In the example given, the correlation with percentage sand was greater than with elevation (Fig. 14a and b). Recently, Wilson et al. (2004) showed that soil type and vegetation are at least as important as topography in explaining the spatial and temporal variance of soil moisture within a watershed. They called for improved measurement of soils and vegetation alongside topography to explain observed patterns. It is clear, comparing Fig. 16a and b, that uncertainty can be reduced by the incorporation of such texture data and the spatial process can be better identified. Whether one approaches watershed description through the concept of identifying dominant processes or networks or from physically distributed watershed models, advances in quantifying of soil and plant spatial variability and structure within the watershed can only be helpful. The key is finding relevant scales at which to describe these watershed attributes without getting lost in the endless description of unnecessary spatial variability. It is therefore fitting to consider here some of the measurement advances being made in other fields that could greatly contribute to hydrological description and understanding.

Recent attempts at identifying such measurement methods include a review and vision of hydrological methods (Loescher et al., 2007) and a similar work for the incorporation of geophysical methods into hydrology (Robinson et al., 2008). The former, identifies light detection and ranging (LIDAR) in particular as a transformative method of obtaining detailed topographic information. Used at watershed scales, LIDAR can reveal detailed structure of earth surface features (Carter et al., 2001; Frankel and Dolan, 2007). In addition, LIDAR is attractive because it can see through many vegetation types, while obtaining information on vegetation height and density (Dubayah and Drake, 2000; Su and Bork, 2007).

Geophysical methods also need to be further incorporated into hydrological investigation. Electromagnetic induction, covered in an earlier section, is particularly suited to identifying soil root-zone spatial variability. Having originally been developed for measuring field-scale soil salinity, it is increasingly being used to map soil texture (Lesch et al., 2005). A paradigm shift is needed in the way soils are mapped for scientific studies, requiring greater emphasis on quantitative over qualitative data. Instruments such as EMI can often, but not always, provide this, as demonstrated in Fig. 10. One of the fundamental challenges is how to incorporate these types of data into hydrological prediction.

Can We Measure Relevant Parameters to Simulate Soil Moisture Evolution over Areas?

There are surprisingly few physics-based approaches for simulating the time evolution of soil moisture, and these are "point-process" schemes. Beginning with the Buckingham (1907) and the Green and Ampt (1911) approach through Richards' equation (Richards, 1931) and up to and including various approximations thereof (Philip, 1957, 1969; Smith and Parlange, 1978; Smith et al., 1993; Salvucci and Entekhabi, 1995; Ogden and Saghafian, 1997), simulation methodologies vary by approximations and assumptions but fundamentally simulate the same process. Richards' equation remains the standard, of which other methodologies are approximate solutions under various circumstances. One impediment to the general use of Richards' equation in modeling the time evolution of soil moisture is that it requires fine spatial discretization and a highly significant computational burden (Downer and Ogden, 2004).

A physics-based solution of variably saturated flow requires detailed knowledge of soil suction and hydraulic conductivity as a function of water content for different layers in the soil. Empirical approximations are universally used to functionally describe soil suction and conductivity. The hydraulics associated with macroporosity due to mesofauna (Gupta et al., 2001) and vegetation (Seguis and Bader, 1997) are not included in these empirical relations. Furthermore, flow through macropores is increasingly understood to be very important (Zehe et al., 2007) but is not solvable using the Richards' (1931) solution. Macroporosity is highly heterogeneous (Seguis and Bader, 1997) and to date is widely ignored because it is seen as an intractable problem.

In many watersheds, lateral downslope subsurface flow is a highly important process at the hillslope scale. Conceptual models can implicitly simulate this phenomena at the watershed scale and its effect on the hydrology of runoff. However, the effect of lateral downslope subsurface flow on soil moisture is not well simulated using physics-based approaches at hillslope scales because of a lack of understanding of the multidimensional properties of the soil, including the influence of downslope macroporosity.

Areally applicable (either watershed or computational element) methods are recent advances that can represent areally averaged infiltration. Kim et al. (2005) developed a stochastic differential-equations approach for simulating areally averaged infiltration in a heterogeneous field that performed well compared with a Monte Carlo average of point-scale Richards' (1931) solutions. Talbot et al. (2006) described a discrete water-content solution methodology for flow through variably saturated media that is areally applicable provided that large-area measurements of suction and conductivity are available. Other new approaches likely remain to be discovered. And these new approaches will probably require large-scale estimates of soil hydraulic properties, macroporosity density and size distributions, and vertical variability—measurements that may come about through the synergy between geophysics, soils research, and hydrology.

Vision

Developments in technology and data handling are undoubtedly required to advance watershed research and to increase our understanding sufficiently to allow better predictions of ungauged watersheds. Both LIDAR and geophysical methods will help us to improve the characterization of watershed properties, while the development of wireless sensor networks will bring the opportunity to obtain more comprehensive spatial coverage to measure hydrological processes. However, we need to understand and develop modeling and data collection frameworks to get the most use out of the technology. We need to understand how to deploy them correctly, how to analyze the data and upscale, and how to relate the data to other measurements of interest.

Once we plan to obtain soil water content measurements across a spatial extent or time period, we must consider what other processes in space or time we want to relate these to. In the case of observatory watershed monitoring, this question is at least as important as the questions concerning what soil water content measurement method we should use, and where the measurements should be taken. It is essential to know the answer to this before the experiment. At a particular space and time-scale combination, each process has its characteristic length. Over this length, a large portion of the variation in the magnitude of the variable is passed. Moreover, each process depends on other processes that have their own characteristic lengths. Some of them may be identical or similar to the length of the main process of interest. How are measurements of the same or a different variable, taken at the same locations or times, or at different locations or times related to each other? In other words, how should we spatially distribute or schedule measurements so that we can identify their coincidence or association and explain phenomena of interest? The answer to this question can be complicated because of experimental restrictions in situations when measurements cannot be taken at exactly the same spatial location or the same time or both. Therefore, the measurement design framework for distributed sensing must consider the method, where measurements should be taken, how often, and what other measures they are to be related to. The framework also needs to have flexibility for the practical considerations of installation and maintenance.

Within this framework, it is therefore important to know not only the sphere of influence, which is linked to the technology needs, but also the range of spatial and temporal correlation. This is the above-mentioned characteristic length of a process and is not technologically but ecosystem-structure driven. Moreover, spatial and temporal cross-correlation needs to be quantified to know over what distance or what time increment two variables are related to each other and when they are no longer related. The calculation is simple; however, there is no unique answer. Depending on the overall magnitude of variance in a given spatial or temporal domain, the correlation and cross-correlation lengths differ. See the above example of gravimetric water content measurements for different spatial sampling distances. Moreover, depending on the scale of measurement and the domain size, the answer differs as well. The scientific challenge is to identify with what sensitivity a process itself, and associated processes, needs to be measured to identify characteristic correlation and cross-correlation lengths. In other words, the auto- and cross-covariance structure of a system, and their change across different scales, needs to be determined. Another challenge is to identify whether the variable related to a specific process at one scale allows scale-up to the specific process at another scale, or which other variable deserves consideration for the purpose of scale transition.

A further step is to bridge between data collected from sensor networks and data collected from remote sensing (Krajewski et al., 2006). Bridging this gap must be seen as one way to understand cross-scale soil moisture patterns in watersheds. Efforts to date have relied on scheduling sampling campaigns with remote sensing data collection (Western and Grayson, 1998; Jackson et al., 1999, 1995). More sophisticated long-term experiments could be established through the use of validation sites utilizing nested sensor networks, at which all the relevant environmental variables affecting the remotely sensed measurement of soil moisture could be observed and quantified. A conceptual illustration of such a validation site is shown in Fig. 17. Truck- and tower-based remote sensing instruments could be used to capture the smallest spatial scales and shortest temporal scales. At small spatial scales on the order of 10 m^2, the characterization of the variability of other environmental variables such as soil texture, soil surface roughness, and vegetation could be captured with networks of in situ sensors and related to the remotely sensed measurement. A wide range of time scales from minutes to seasons could be investigated. Subsequent remote sensing platforms could then be used to transfer, in space and time, the measurements made with truck- and tower-based instruments to larger spatial scales and longer time scales. These platforms could include remote sensing instruments on board unmanned aerial vehicles at the next level (100–1000 m^2, hours), to airplanes (10,000–100,000 m^2, day), and finally to the satellite scale (1–100 km^2, days). Traditional approaches to comparing measurements have focused on the instrumentation. While this is important, there is a need to integrate measurement campaigns like this with watershed process studies. If nothing else, linking these together will determine at what scales we need to

Fig. 17. An example of a nested calibration site; the blue disks represent sensor arrays, and the yellow vehicle has a crane-mounted passive remote sensing device (as in Fig. 6). The airborne methods include drone-mounted, aircraft-mounted, and satellite remote sensing devices. All the data are telemetered back to the office via the Internet so that the site can be continuously monitored.

focus measurement efforts to understand patterns and linkages. Parallel efforts should be focused on measurement campaigns that not only consider quantification but also test our understanding of watershed soil moisture patterns and behavior. The Tarrawarra data set (Western and Grayson, 1998) demonstrates how combined measurement and modeling efforts can increase our understanding across scales.

The above discussion articulates and demonstrates the need for an experimental design framework for integrated water content measurement across watersheds. At the same time, a range of advances is required in terms of the instrumentation, especially those that can be used to capture spatial patterns within watersheds. In the following sections, we list some of the perceived areas of research needed to improve our ability to measure, monitor, and understand the watershed water content spatial process.

Lab Challenges

- Consider the development of a standard energy definition for θ to integrate measurements with ecological observation and relevance.
- Determination of permittivity underlies many of the techniques—TDR, GPR, remote sensing. Therefore, measure and model dielectric spectra across a wide range of frequencies to more accurately measure θ and σ. Concurrently, investigate the possibility of determining other properties, possibly mineralogy and sample geometry.

Equipment Challenges

- Develop inexpensive, noninvasive, or easily installed soil moisture devices capable of measuring and monitoring the root zone, especially instruments that could integrate measurement over a volume of $\sim$1 m^3.

- Reduce power consumption.
- Quantify the sampling volume or support of new sensors and geophysical instruments such as GPR, EMI, and NMR.
- Develop sensors that can be made mobile with measurements made on the go, such as TDR or NMR.

Monitoring Challenges

- Design fully buriable sensors without the need for surface wires to stop animals eating or trampling them. Ultimately, develop data upload links via satellite.
- Develop fully integrated wireless networks (we have many pieces, but are far from a simple, usable system). Wireless challenges include reducing power consumption, increasing broadcast range, and lowering costs.
- Determine where we place sensors. Can we optimize their placement locations using other data? An experimental design framework needs to be developed.
- As the cost of sensors decreases, determine whether we could place networks over the land surface to link with data collected by satellite remote sensing to help calibrate. Nationwide networks might follow the soil climate analysis network (SCAN) run by USDA (www.wcc.nrcs.usda.gov/scan/).
- Determining and describing macroporosity.
- Estimating soil water parameters over areas.
- Observations of vertical decreases in hydraulic conductivity and downslope macroporosity that promote lateral downslope subsurface flow.

Remote Sensing Challenges

- Improve the modeling of the soil surface (roughness) and the effect of intervening materials (vegetation) on the measurement.
- Develop a more sophisticated change detection approach to interpret the radar response, since other transient effects besides θ, like water residing on the vegetation either from dew or the interception of precipitation, can significantly affect backscatter.
- Remote sensing instruments make spatially averaged measurements of θ, while in situ measurements used to validate remotely sensed measurements are point observations. The challenge in remote sensing of θ is to develop useful models that effectively integrate the important variables affecting remotely sensed measurements of θ at each spatial scale and to construct sensor networks that can provide the data needed by these models to validate remotely sensed measurements of θ.

Modeling Challenges

- Move beyond the point-process modeling paradigm and develop infiltration and soil moisture modeling approaches that are areally applicable.
- Improve process-level descriptions to explicitly include the effects of macroporosity.
- Research relations between multisensor technologies, vegetation, mesofauna, and the timing, occurrence, and distribution of macroporosity both in the vertical and downslope directions.

This summary outlines and identifies some areas of research needs with the aim of increasing our understanding of the collective or emergent behavior of watersheds. The importance of water content to both hydrological and ecological processes means that its study should form one of the research cornerstones of the emerging ecohydrology discipline.

Appendix: Nomenclature

α	soil thermal diffusivity
ε	material permittivity
ε_r'	real part of the permittivity ($\varepsilon'/\varepsilon_o$)
ε_r''	imaginary part of the permittivity ($\varepsilon''/\varepsilon_o$)
ε_o	permittivity of free space
ε_s	static relative permittivity
ε_T'	real part of the measured relative permittivity
ε_T''	imaginary part of the measured relative permittivity
η	cementation index in Archie's law
θ	water content
θ_g	gravimetric water content
θ_{sat}	saturated water content
θ_v	volumetric water content
κ	relative permittivity measured by a soil sensor or GPR
λ	soil thermal conductivity
π	mathematical constant 3.214
ρ	density
ρ_b	bulk density
ρ_w	density of water
σ	backscattering cross-section
σ'	electrical conductivity due to ohmic conduction
σ''	electrical conductivity due to faradaic diffusion
σ_a	bulk electrical conductivity
σ_{dc}	DC electrical conductivity
σ_s	surface electrical conductivity
σ_w	porous medium solution electrical conductivity
σ^o	backscattering coefficient
$\sigma^o{}_g$	direct ground backscatter
$\sigma^o{}_v$	direct canopy backscatter
$\sigma^o{}_{vg}$	other multiple scattering between ground and canopy
τ	relaxation time
ϕ	porosity
ω	angular frequency ($2\pi f$, where f = frequency)

Acknowledgments

The authors would like to thank Keith Beven, Keith Loague, and Andrew Western for assistance in preparing this manuscript. We would like to thank Vicente Urdanoz and Hiruy Abdu for the data used in Fig. 10. This material is based on work supported by the National Science Foundation under Grants 03-26064 and 04-47287. Any opinions, findings, and conclusions or recommendations expressed in this material are those of the authors and do not necessarily reflect the views of the National Science Foundation. The use of firm, trade, and brand names in this report is for identification purposes only and does not constitute endorsement by CUAHSI, NSF, the U.S. government, or the authors and their respective institutions.

References

Adamo, F., G. Andria, F. Attivissimo, and N. Giaquinto. 2004. An acoustic method for soil moisture measurement. IEEE Trans. Instrum. Meas. 53:891–898.

Alessi, R.S., and L. Prunty. 1986. Soil-water determination using fiber optics. Soil Sci. Soc. Am. J. 50:860–863.

Amidu, S.A., and J.A. Dunbar. 2007. Geoelectric studies of seasonal wetting and drying of a Texas vertisol. Vadose Zone J. 6:511–523.

Anderson, M.P. 2005. Heat as a groundwater tracer. Ground Water 6:951–968.

Annan, A.P. 2005a. GPR methods for hydrogeological studies. p. 185–213. *In* Y. Rubin and S. Hubbard (ed.) Hydrogeophysics. Water Science and Technology Library Vol. 50. Springer, The Netherlands.
Annan, A.P. 2005b. Ground-penetrating radar. p. 351–432. *In* D.K. Butler (ed.) Near surface geophysics. Investigations in Geophysics 13. Society of Exploration Geophysicists, Tulsa, OK.
Archie, G.E. 1942. The electrical resistivity log as an aid in determining some reservoir characteristics. Trans. Am. Inst. Miner. Metall. Petrol. Eng. 146:54–62.
ASTM. 1979. Standard method of laboratory determination of moisture content of soil: Procedure D2216-71. p. 290–291. *In* Annual book of ASTM standards. Am. Soc. Test. Mater., Philadelphia, PA.
Barrie, P.J. 2000. Characterization of porous media using NMR methods. Annu. Rep. NMR Spectrosc. 41:265–316.
Basinger, J.M., G.J. Kluitenberg, J.M. Ham, J.M. Frank, P.L. Barnes, and M.B. Kirkham. 2003. Laboratory evaluation of the dual-probe heat pulse method for measuring soil water content. Vadose Zone J. 2:389–399.
Baumhardt, R.L., R.J. Lascano, and S.R. Evett. 2000. Soil material, temperature, and salinity effects on calibration of multisensor capacitance probes. Soil Sci. Soc. Am. J. 64:1940–1946.
Bell, J.P. 1987. Neutron probe practice. 3rd ed. Hydrology Report 19. Available at http://www.ceh.ac.uk/products/publications/hydrology.html (verified 22 Jan. 2008). Institute of Hydrology, Wallingford, Oxon, UK.
Bell, J.P., T.J. Dean, and M.G. Hodnett. 1987. Soil-moisture measurement by an improved capacitance technique: 2. Field techniques, evaluation, and calibration. J. Hydrol. 93:79–90.
Beven, K.J. 2001. Rainfall–runoff modelling: The primer. John Wiley & Sons, Chichester, UK.
Bierkens, M.F., M. Knotters, and T. Hoogland. 2001. Space–time modeling of water table depth using a regionalized time series model and the Kalman filter. Water Resour. Res. 37:1277–1290.
Bilskie, J.R., R. Horton, and K.L. Bristow. 1998. Test of a dual-probe heat-pulse method for determining thermal properties of porous materials. Soil Sci. 163:346–355.
Bird, N.R.A., A.R. Preston, E.W. Randall, W.R. Whalley, and A.P. Whitmore. 2005. Measurement of the size distribution of water-filled pores at different matric potentials by stray field nuclear magnetic resonance. Eur. J. Soil Sci. 56:135–143.
Blainey J. B., T. P. A. Ferré, and J. T. Cordova. 2007. Assessing the likely value of gravity and drawdown measurements to constrain estimates of hydraulic conductivity and specific yield during unconfined aquifer testing, Water Resour. Res. 43:W12408, doi:10.1029/2006WR005678.
Blecher, D.J. 1950. The measurement of soil moisture by neutron and gamma ray scattering. p. 98–120. *In* Civil Aeronautics Administration technical development report. No. 127. Civil Aeronautics Administration, Washington, DC.
Bloch, F. 1952. The principle of nuclear induction. *In* Nobel lectures, physics 1942–1962. Elsevier, Amsterdam, The Netherlands
Blonquist, J.M., S.B. Jones, and D.A. Robinson. 2005a. Standardizing characterization of electromagnetic water content sensors: Part 2. Evaluation of seven sensing systems. Vadose Zone J. 4:1059–1069.
Blonquist, J.M., S.B. Jones, and D.A. Robinson. 2005b. A time domain transmission sensor with TDR performance characteristics. J. Hydrol. 314:235–245.
Blöschl, G., and R.B. Grayson. 2000. Spatial observations and interpolation. p. 17–50. *In* R.B. Grayson and G. Blöschl (ed.) Spatial patterns in hydrology. Cambridge Univ. Press, Cambridge, UK).
Blöschl, G., and M. Sivapalan. 1995. Scale issues in hydrological modelling: A review. Hydrol. Proc. 9:251–290.
Blum, A., I. Flammer, T. Friedli, and P. Germann. 2004. Acoustic tomography applied to water flow in unsaturated soils. Vadose Zone J. 3:288–299.
Borhan, M.S., and L.R. Parsons. 2004. Monitoring of soil water content in a citrus grove using capacitance ECH_2O probes. Paper no. 042110. *In* Proc. ASAE Annu. Meeting. Ottowa, Canada. 1–4 Aug. 2004. American Society of Agricultural and Biological Engineers, St. Joseph, MI.
Briggs, L.J. 1899. Electrical instruments for determining the moisture, temperature, and soluble salt content of soils. USDA Div. Soils Bull. 10. U.S. Gov. Print. Office, Washington, DC.
Bristow, K.L. 2002. Thermal conductivity. p. 1209–1226. *In* J.H. Dane, and G.C. Topp (ed.) Methods of soil analysis: Part 4. Physical methods. SSSA Book Ser. 5. SSSA, Madison, WI.
Bristow, K.L. 1998. Measurement of thermal properties and water content of unsaturated sandy soil using dual-probe heat-pulse probes. Agric. For. Meteorol. 89:75–84.
Bristow, K.L., G.J. Kluitenberg, C.J. Goding, and T.S. Fitzgerald. 2001. A small multi-needle probe for measuring soil thermal properties, water content and electrical conductivity. Comput. Electron. Agric. 31:265–280.
Bristow, K.L., G.J. Kluitenberg, and R. Horton. 1994. Measurement of soil thermal properties with a dual-probe heat-pulse technique. Soil Sci. Soc. Am. J. 58:1288–1294.
Bristow, K.L., G.S. Campbell, and K. Calissendorff. 1993. Test of a heat-pulse probe for measuring changes in soil water content. Soil Sci. Soc. Am. J. 57:930–934.
Brown, D.J., J.C. Crupper, C.S. Campbell, D.R. Cobos, C.A. Perillo, and D.R. Huggins. 2007. Constructing a field-scale dynamic landscape model of soil hydrology using data from a distributed wireless sensor network. *In* Agronomy Abstracts, ASA-CSSA-SSSA Annu. Meeting, New Orleans, LA. 4–8 Nov. 2007. ASA, Madison, WI.
Brummer, E., and E.S. Mardock. 1945. A neutron method for measuring saturation in laboratory flow measurements. Proc. Am. Inst. Mining and Metal Engineering.
Brutsaert, W., and J.N. Luthin. 1964. The velocity of sound in soils near the surface as a function of moisture content. J. Geophys. Res. 69:643–652.
Buckingham, E. 1907. Studies on the movement of soil moisture. Bull. 38. USDA, Bureau of Soils, Washington, DC.
Budyko, M.I. 1974. Climate and life. Academic Press, New York.
Cahill, A.T., F. Ungaro, M.B. Parlange, M. Mata, and D.R. Nielsen. 1999. Combined spatial and Kalman filter estimation of optimal soil hydraulic properties. Water Resour. Res. 35:1079–1088.
Callegary, J.B., T.P.A. Ferré, and R.W. Groom. 2007. Spatial sensitivity of low-induction-number frequency-domain electromagnetic induction instruments. Vadose Zone J. 6:158–167.
Campbell, G.S. 1985. Soil physics with BASIC. Elsevier, New York.
Campbell, G.S., C. Calissendorff, and J.H. Williams. 1991. Probe for measuring soil specific heat using a heat-pulse method. Soil Sci. Soc. Am. J. 55:291–293.
Campbell, J.E. 1990. Dielectric properties and influence of conductivity in soils at one to 50 Megahertz. Soil Sci. Soc. Am. J. 54:332–341.
Carter, W., R. Sherestha, G. Tuell, D. Bloomquist, and M. Sartori. 2001. Airborne laser swath mapping shines new light on Earth's topography. Trans. Am. Geophys. Union 82(46):549–550, 555.
Cassman, K.G., and D.N. Munns. 1980. Nitrogen mineralization as affected by soil-moisture, temperature, and depth. Soil Sci. Soc. Am. J. 44:1233–1237.
Chan, C.Y., and R. Knight. 1999. Determining water content and saturation from dielectric measurements in layered materials. Water Resour. Res. 35:85–93.
Chan, C.Y., and R.J. Knight. 2001. Laboratory measurements of electromagnetic wave velocity in layered sands. Water Resour. Res. 37:1099–1105.
Chanzy, A., J. Chadoeuf, J.C. Gaudu, D. Mohrath, G. Richard, and L. Bruckler. 1998. Soil moisture monitoring at the field scale using automatic capacitance probes. Eur. J. Soil Sci. 49:637–648.
Chanzy, A., A. Tarussov, A. Judge, and F. Bonn. 1996. Soil water content determination using a digital ground-penetrating radar. Soil Sci. Soc. Am. J. 60:1318–1326.
Chelidze, T.L., and Y. Gueguen. 1999. Electrical spectroscopy of porous rocks: A review—I. Theoretical models. Geophys. J. Int. 137:1–15.
Chelidze, T.L., Y. Gueguen, and C. Ruffet. 1999. Electrical spectroscopy of porous rocks: A review- II. Experimental results and interpretation. Geophys. J. Int. 137:16–34.
Chen, Y.P., and D. Or. 2006. Geometrical factors and interfacial processes affecting complex dielectric permittivity of partially saturated porous media. Water Resour. Res. 42:W06423.
Choudhury, B.J., T.J. Schmugge, A. Chang, and R.W. Newton. 1979. Effect of surface roughness on the microwave emission from soils. J. Geophys. Res. 84:5699–5706.
Chung, S.-P., and R. Horton. 1987. Soil heat and water flow with a partial surface mulch. Water Resour. Res. 23:2175–2186.
Corwin, D.L., and S.M. Lesch. 2003. Application of soil electrical conductivity to precision agriculture: Theory, principle, and guidelines. Agron. J. 95:455–471.

Dagan, G. 1987. Theory of solute transport by groundwater. Annu. Rev. Fluid Mech. 19:183–213.

Dalton, F.N., W.N. Herkelrath, D.S. Rawlins, and J.D. Rhoades. 1984. Time-domain reflectometry: Simultaneous measurement of soil-water content and electrical-conductivity with a single probe. Science 224:989–990.

Dalton, F.N., and M.Th. van Genuchten. 1986. The time-domain reflectometry method for measuring soil-water content and salinity. Geoderma 38:237–250.

Daniels, D.J., D.J. Gunton, and H.F. Scott. 1988. Introduction to subsurface radar. Radar Signal Process. 135:278–320.

Darnault, C.J.G., D.A. DiCarlo, T.W.J. Bauters, A.R. Jacobsen, J.A. Throop, C.D. Montemagno, J.-Y. Parlange, and T.S. Steenhuis. 2001. Measurement of fluid contents by light transmission in transient three phase oil-water-air systems in sand. Water Resour. Res. 37:1859–1868.

Dasberg, S., and F.N. Dalton. 1985. Time domain reflectometry field-measurements of soil-water content and electrical-conductivity. Soil Sci. Soc. Am. J. 49:293–297.

Davis, J.L., and A.P. Annan. 1989. Ground-penetrating radar for high-resolution mapping of soil and rock stratigraphy. Geophys. Prospect. 37:531–551.

de Lannoy, G.J.M., P.R. Houser, N.E.C. Verhoest, V.R.N. Pauwels, and T.J. Gish. 2007. Upscaling of point soil moisture measurements to field averages at the OPE test site. J. Hydrol. 343:1–11.

de Lannoy, G.J.M., N.E.C. Verhoest, P.R. Houser, T.J. Gish, and M. Van Meirvenne. 2006. Spatial and temporal characteristics of soil moisture in an intensively monitored agricultural field (OPE^3). J. Hydrol. 331:719–730.

De Roo, R.D., Y. Du, F.T. Ulaby, and M.C. Dobson. 2001. A semi-empirical backscattering model at L-band and C-band for a soybean canopy with soil moisture inversion. IEEE Trans. Geosci. Remote Sens. 39:864–872.

De Vries, D.A. 1963. Thermal properties of soils. p. 210–235. *In* W.R. van Wijk (ed.) Physics of plant environment. North Holland Publishing, Amsterdam, The Netherlands.

Dean, T.J., J.P. Bell, and A.J.B. Baty. 1987. Soil-moisture measurement by an improved capacitance technique: 1. Sensor design and performance. J. Hydrol. 93:67–78.

Debye, P. 1929. Polar molecules. Chemical Catalog, New York.

DeJong, E., A.K. Ballantyne, D.R. Cameron, and D.W.L. Read. 1979. Measurement of apparent electrical conductivity of soils by an electromagnetic induction probe to aid salinity surveys. Soil Sci. Soc. Am. J. 43:810–812.

Dingman, S.L. 2002. Physical hydrology. 2nd ed. Prentice Hall, Upper Saddle River, NJ.

D'Odorico, P., F. Laio, A. Porporato, and I. Rodriguez-Iturbe. 2003. Hydrologic controls on soil carbon and nitrogen cycles: II. A case study. Adv. Water Resour. 26:59–70.

Downer, C.W., and F.L. Ogden. 2004. Appropriate vertical discretization of Richards' equation for two-dimensional watershed-scale modelling. Hydrol. Process. 18:1–22.

Drury, C.F., T.Q. Zhang, and B.D. Kay. 2003. The non-limiting and least limiting water ranges for soil nitrogen mineralization. Soil Sci. Soc. Am. J. 67:1388–1404.

Dubayah, R.O., and J.B. Drake. 2000. LIDAR remote sensing for forestry. J. For. 98:44–46.

Dunne, T., and R.D. Black. 1970. An experimental investigation of runoff production in permeable soils. Water Resour. Res. 6:478–490.

Eagleman, J.R., and W.C. Lin. 1976. Remote sensing of soil moisture by a 21-cm passive radiometer. J. Geophys. Res. 81:3660–3666.

Earnest, C.M. 1991a. Thermal analysis of selected illite and smectite clay minerals: Part I. Illite clay minerals. p. 270–286. *In* W. Smykatz-Kloss and S.S.J. Warne (ed.) Thermal analysis in the geosciences. Vol. 38. Springer-Verlag, Berlin.

Earnest, C.M. 1991b. Thermal analysis of selected illite and smectite clay minerals: Part II. Smectite clay minerals. p. 288–312. *In* W. Smykatz-Kloss and S.S.J. Warne (ed.) Thermal analysis in the geosciences. Vol. 38. Springer-Verlag, Berlin.

Edlefsen, N.E., and A.B.C. Anderson. 1941. The four-electrode resistance method for measuring soil-moisture content under field conditions. Soil Sci. 51:367–376.

Entekhabi, D., I. Rodriguez-Iturbe, and F. Castelli. 1996. Mutual interaction of soil moisture state and atmospheric processes. J. Hydrol. 184:3–17.

Entekhabi, D., E.G. Njoku, P. Houser, M. Spencer, T. Doiron, Y.J. Kim, J. Smith, R. Girard, S. Belair, W. Crow, T.J. Jackson, Y.H. Kerr, J.S. Kimball, R. Koster, K.C. McDonald, P.E. O'Neill, T. Pultz, S.W. Running, J.C. Shi, E. Wood, and J. van Zyl. 2004. The hydrosphere state (Hydros) satellite mission: An earth system pathfinder for global mapping of soil moisture and land freeze/thaw. IEEE Trans. Geosci. Remote Sens. 42:2184–2195.

Evett, S.R., and G.W. Parkin. 2005. Advances in soil water content sensing: The continuing maturation of technology and theory. Vadose Zone J. 4:986–991.

FAO. 2006. AQUASTAT. Available at http://www.fao.org/nr/water/aquastat/main/index.stm (verified 22 Jan. 2008). FAO, Rome.

Fellner-Feldegg, H. 1969. Measurement of dielectrics in time domain. J. Phys. Chem. 73:616–623.

Ferré, P.T.A., J.H. Knight, D.L. Rudolph, and R.G. Kachanoski. 1998. The sample areas of conventional and alternative time domain reflectometry probes. Water Resour. Res. 34:2971–2979.

Ferré, P.T.A., H.H. Nissen, and J. Simunek. 2002. The effect of the spatial sensitivity of TDR on inferring soil hydraulic properties from water content measurements made during the advance of a wetting front. Vadose Zone J. 1:281–288.

Frankel, K.L., and J.F. Dolan. 2007. Characterizing arid region alluvial fan surface roughness with airborne laser swath mapping digital topographic data: J. Geophys. Res. Earth Surface

Freeland, R.S. 1989. Review of soil-moisture sensing using soil electrical-conductivity. Trans. ASAE 32:2190–2194.

Friedman, S.P. 2005. Soil properties influencing apparent electrical conductivity: A review. Comput. Electron. Agric. 46:45–70.

Friedman, S.P., and S.B. Jones. 2001. Measurement and approximate critical path analysis of the pore-scale-induced anisotropy factor of an unsaturated porous medium. Water Resour. Res. 37:2929–2942.

Galagedara, J.D., J.D. Redman, G.W. Parkin, A.P. Annan, and A.L. Endres. 2005. Numerical modeling of GPR to determine the direct ground water sampling depth. Vadose Zone J. 4:1096–1106.

Galantowicz, J.F., D. Entekhabi, and E.G. Njoku. 1999. Tests of sequential data assimilation for retrieving profile soil moisture and temperature from observed L-band radiobrightness. IEEE Trans. Geosci. Remote Sens. 37:1860–1870.

Gardner, C.M.K., D.A. Robinson, K. Blyth, and J.D. Cooper. 2001. Soil water content. p. 1–64. *In* K.A. Smith and C.E. Mullins (ed.) Soil and environmental analysis: Physical methods. 2nd ed. Marcel Dekker, New York.

Gardner, W.H. 1986. Water content. p. 493–544. *In* A. Klute (ed.) Methods of soil analysis: Part 1. Physical and mineralogical properties. 2nd ed. ASA and SSSA, Madison, WI.

Garrido, F., M. Ghodrati, and M. Chendorain. 1999. Small-scale measurement of soil water content using a fiber optic sensor. Soil Sci. Soc. Am. J. 63:1505–1512.

Gaskin, G.J., and J.D. Miller. 1996. Measurement of soil water content using a simplified impedance measuring technique. J. Agric. Eng. Res. 63:153–159.

Gaudu, J.C., J.M. Mathieu, J.C. Fumanal, L. Bruckler, A. Chanzy, P. Bertuzzi, P. Stengel, and R. Guennelon. 1993. Soil-moisture measurement using a capacitive probe. Agronomie 13:57–73.

Gee, G.W., and M.E. Dodson. 1981. Soil water content by microwave drying: A routine procedure. Soil Sci. Soc. Am. J. 45:1234–1237.

Gower, S.T., K.A. Vogt, and C.C. Grier. 1992. Carbon dynamics of Rocky Mountain Douglas-fir: Influence of water and nutrient availability. Ecol. Monogr. 62:43–65.

Goyal, V.C., P.K. Gupta, S.M. Seth, and V.N. Singh. 1996. Estimation of temporal changes in soil moisture using resistivity method. Hydrol. Proc. 10:1147–1154.

Grayson, R.B., and A.W. Western. 1998. Towards areal estimation of soil water content from point measurements: Time and space stability of mean response. J. Hydrol. 207:68–82.

Grayson, R.B., A.W. Western, F.H.S. Chiew, and G. Blöschl. 1997. Preferred states in spatial soil moisture patterns: Local and non-local controls. Water Resour. Res. 33:2897–2908.

Greacen, E.L. 1981. Soil water assessment by the neutron method. CSIRO, Melbourne, Australia.

Greaves, R.J., D.P. Lesmes, J.M. Lee, and M.N. Toksoz. 1996. Velocity variations and water content estimated from multi-offset, ground-penetrating radar. Geophysics 61:683–695.

Green, W.H., and C.A. Ampt. 1911. Studies on soil physics: I. Flow of air and water through soils. J. Agric. Sci. 4:1–24.

Gupta, S.C., and R.J. Hanks. 1972. Influence of water content on electrical conductivity of the soil. Soil Sci. Soc. Am. J. 36:855–857.

Gupta, S.C., A. Bhattacharjee, J.F. Moncrief, E.C. Berry, and J.E. Zachmann. 2001. Influence of earthworm species and depth of residue placement on macropore characteristics and preferential transport, in preferential flow, water movement, and chemical transport in the environment. p. 153–156. *In* D.D. Bosch and K.W. King (ed.) Proc. 2nd Int. Symp. Honolulu, HI. 3–5 Jan. 2001. ASAE, St. Joseph, MI.

Hallikainen, M.T., F.T. Ulaby, M.C. Dobson, M.A. El-Rayes, and L.-K. Wu. 1985. Microwave dielectric behavior of wet soil: Part I. Empirical models and experimental observations. IEEE Trans. Geosci. Remote Sens. 23:25–34.

Hamid, M.A.K., and N.J. Mostowy. 1976. Capacitive moisture probe for prefab concrete industry. IEEE Trans. Indust. Electron. Control Instrum. 23:462–465.

Hasted, J.B. 1973. Aqueous dielectrics. Chapman and Hall, London.

Heitman, J.L., J.M. Basinger, G.J. Kluitenberg, J.M. Ham, J.M. Frank, and P.L. Barnes. 2003. Field evaluation of the dual-probe heat pulse method for measuring soil water content. Vadose Zone J. 2:552–560.

Hewlett, J.D., and A.R. Hibbert. 1963. Moisture and energy conditions within a sloping soil mass during drainage. J. Geophys. Res. 68:1081–1087.

Hills, R.C., and S.G. Reynolds. 1969. Illustrations of soil moisture variability in selected areas and plots of different sizes. J. Hydrol. 8:27–47.

Hinedi, Z.R., D.B. Borchard, and A.C. Chang. 1993. Probing soil and aquifer material porosity with nuclear magnetic resonance. Water Resour. Res. 29:3861–3866.

Hinedi, Z.R., and A.C. Chang. 1999. Probing pore characteristics in a sandy soil with nuclear magnetic resonance. p. 413–422. *In* M.Th. van Genuchten, F.J. Leij, and L. Wu (ed.) Characterization and measurement of the hydraulic properties of unsaturated porous media: Part 1: Proceedings of the International workshop on characterization and measurement of the hydraulic properties of unsaturated porous media, Riverside, CA. 22–24 Oct. 1999. Univ. of California, Riverside.

Hoekstra, P., and A. Delaney. 1974. Dielectric properties of soils at UHF and microwave-frequencies. J. Geophys. Res. 79:1699–1708.

Hook, W.R., T.P.A. Ferré, and N.J. Livingston. 2004. The effects of salinity on the accuracy and uncertainty of water content measurement. Soil Sci. Soc. Am. J. 68:47–56.

Holmes, J.W. 1956. Calibration and field use of the neutron scattering method of measuring soil water content. Aust. J. Appl. Sci. 7:45–58.

Hong, S.Y., and E. Kalnay. 2000. Role of sea surface temperature and soil-moisture feedback in the 1998 Oklahoma-Texas drought. Nature 408:842–844.

Hopmans, J.W., and J.H. Dane. 1986. Thermal conductivity of two porous media as a function of water content, temperature, and density. Soil Sci. 142:187–195.

Hopmans, J.W., J. Šimůnek, and K.L. Bristow. 2002. Indirect estimation of soil thermal properties and water flux from heat pulse measurements: Geometry and dispersion effects. Water Resour. Res. 38:1006, doi:10.1029/2000WR000071.

Hornbuckle, B.K., and A.W. England. 2004. Radiometric sensitivity to soil moisture at 1.4 GHz through a corn crop at maximum biomass. Water Resour. Res. 40:W10204, doi:10.1029/2003WR002931.

Hubbard, S., K. Grote, and Y. Rubin. 2002. Mapping the soil volumetric water content of a California vineyard using high-frequency GPR ground wave data. Leading Edge 21:552–559.

Huisman, J.A., S.S. Hubbard, J.D. Redman, and A.P. Annan. 2003a. Measuring soil water content with ground penetrating radar: A review. Vadose Zone J. 2:476–491.

Huisman, J.A., J.J.J.C. Snepvangers, W. Bouten, and G.B.M. Heuvelink. 2002. Mapping spatial variation in surface soil water content: Comparison of ground-penetrating radar and time domain reflectometry. J. Hydrol. 269:194–207.

Huisman, J.A., J.J.J.C. Snepvangers, W. Bouten, and G.B.M. Heuvelink. 2003b. Monitoring temporal development of spatial soil water content variation: Comparison of ground penetrating radar and time domain reflectometry. Vadose Zone J. 2:519–529.

Huisman, J.A., C. Sperl, W. Bouten, and J.M. Verstraten. 2001. Soil water content measurements at different scales: Accuracy of time domain reflectometry and ground-penetrating radar. J. Hydrol. 245:48–58.

Inoue, M., J. Šimůnek, S. Shiozawa, and J.W. Hopmans. 2000. Simultaneous estimation of soil hydraulic and solute transport parameters from transient infiltration experiments. Adv. Water Resour. 23:677–688.

Inoue, Y., T. Watanabe, and K. Kitamura. 2001. Prototype time-domain reflectometry probes for measurement of moisture content near the soil surface for applications to “on-the-move” measurements. Agric. Water Manage. 50:41–52.

Irving, J., M. Knoll, and R. Knight. 2007. Improving crosshole GPR travel-time tomography between closely spaced boreholes at the Boise Hydrogeophysical Research Site. Geophysics 72:J31–J41.

Isaaks, E.H., and R.M. Srivastava. 1989. Applied geostatistics. Oxford Univ. Press, New York.

Ishida, T., and T. Makino. 1999. Effects of pH on dielectric relaxation of montmorillonite, allophane, and imogolite suspensions. J. Colloid Interface Sci. 212:152–161.

Ishida, T., T. Makino, and C.J. Wang. 2000. Dielectric-relaxation spectroscopy of kaolinite, montmorillonite, allophane, and imogolite under moist conditions. Clays Clay Miner. 48:75–84.

Istanbulluoglu, E., and R.L. Bras. 2006. On the dynamics of soil moisture, vegetation, and erosion: Implications of climate variability and change. Water Resour. Res. 42:W06418.

Jackson, T.J., D.M. Le Vine, A.Y. Hsu, A. Oldak, P.J. Starks, C.T. Swift, J.D. Isham, and M. Haken. 1999. Soil moisture mapping at regional scales using microwave radiometry: The Southern Great Plains Hydrology Experiment. IEEE Trans. Geosci. Remote Sens. 37:2136–2151.

Jackson, T.J., D.M. Le Vine, C.T. Swift, T.J. Schmugge, and F.R. Schiebe. 1995. Large area mapping of soil moisture using the ESTAR passive microwave radiometer in Washita’92. Remote Sens. Environ. 54:27–37.

Jackson, T.J., P.E. O’Neill, and C.T. Swift. 1997. Passive microwave observation of diurnal surface soil moisture. IEEE Trans. Geosci. Remote Sens. 35:1210–1222.

Jackson, T.J., and T.J. Schmugge. 1991. Vegetation effects on the microwave emission of soils. Remote Sens. Environ. 36:203–212.

Jackson, T.J., T.J. Schmugge, P.E. O’Neill, and M.B. Parlange. 1998. Soil water infiltration observation with microwave radiometers. IEEE Trans. Geosci. Remote Sens. 36:1376–1383.

Jackson, T.J., T.J. Schmugge, and J.R. Wang. 1982. Passive microwave remote sensing of soil moisture under vegetation canopies. Water Resour. Res. 18:1137–1142.

Jones, S.B., J.M. Blonquist, D.A. Robinson, V.P. Rasmussen, and D. Or. 2005. Standardizing characterization of electromagnetic water content sensors. Part 1: Methodology. Vadose Zone J. 4:1048–1058.

Jones, S.B., D.A. Robinson, and S.P. Friedman. 2006. Development of a subsurface open-ended TDR probe for on-the-go mapping of water content. Proceedings TDR 2006, 3rd Int. Symp. and Workshop on Time Domain Reflectometry for Innovative Soils Applications, Purdue University, West Lafayette, IN. 17–20 Sept. 2006. Available at https://engineering.purdue.edu/TDR/ (verified 22 Jan. 2008).

Jung, W.K., N.R. Kitchen, K.A. Sudduth, R.J. Kremer, and P.P. Motavalli. 2005. Relationship of apparent soil electrical conductivity to claypan soil properties. Soil Sci. Soc. Am. J. 69:883–892.

Kachanoski, R.G., and E. de Jong. 1988. Scale dependence and the temporal persistence of spatial patterns of soil water storage. Water Resour. Res. 24:85–91.

Kachanoski, R.G., E.G. Gregorich, and I.J. Van Wesenbeeck. 1988. Estimating spatial variations of soil water content using non-contacting electromagnetic inductive methods. Can. J. Soil Sci. 68:715–722.

Kachanoski, G., E. Pringle, and A. Ward. 1992. Field measurement of solute travel times using time domain reflectometry. Soil Sci. Soc. Am. J. 56:47–52.

Kaleita, A.L., L.F. Tian, and M.C. Hirschi. 2005. Relationship between soil moisture content and soil surface reflectance. Trans. ASAE 48:1979–1986.

Kalman, R.E. 1960. A new approach to linear filtering and prediction problems. Trans. ASME J. Basic Eng. 8:35–45.

Katul, G.G., O. Wendroth, M.B. Parlange, C.E. Puente, and D.R. Nielsen. 1993. Estimation of in situ hydraulic conductivity function from nonlinear filtering theory. Water Resour. Res. 29:1063–1070.

Kelleners, T.J., R.W.O. Soppe, J.E. Ayers, and T.H. Skaggs. 2004. Calibration capacitance probe sensors in a saline silty clay soil. Soil Sci. Soc. Am. J. 68:770–778.

Kelleners, T.J., D.A. Robinson, P.J. Shouse, J.E. Ayars, and T.H. Skaggs. 2005a. Frequency dependence of the complex permittivity and its impact on dielectric sensor calibration in soils. Soil Sci. Soc. Am. J. 69:67–76.

Kelleners, T.J., M.S. Seyfried, J.M. Blonquist, Jr., J. Bilskie, and D.G. Chandler. 2005b. Improved interpretation of water content reflectometer measurements in soils. Soil Sci. Soc. Am. J. 69:1684–1690.

Keller, G.V., and F.C. Frischknecht. 1966. Electrical methods in geophysical prospecting. Pergamon Press, New York.

Kerr, Y.H., P. Waldteufel, J.P. Wigneron, J.M. Martinuzzi, J. Font, and M. Berger. 2001. Soil moisture retrieval from space: The soil moisture and ocean salinity (SMOS) mission. IEEE Trans. Geosci. Remote Sens. 39:1729–1735.

Kevan, T. 2006. Coming to terms with wireless. Available at http://www.sensorsmag.com/sensors/article/articleDetail.jsp?id=390789 (verified 22 Jan. 2008). Sensors (Dec.).

Kevan, T. 2007. Power management: Critical choices for wireless. Available at http://www.sensorsmag.com/sensors/article/articleDetail.jsp?id=402154 (verified 22 Jan. 2008). Sensors (Jan.).

Kim, D.J., S.I. Choi, O. Ryszard, J. Feyen, and H.S. Kim. 2000. Determination of moisture content in a deformable soil using time-domain reflectometry (TDR). Eur. J. Soil Sci. 51(1):119–127.

Kim, S., M.L. Kavvas, and J. Yoon. 2005. Upscaling of vertical unsaturated flow model under infiltration condition. J. Hydrol. Eng. 10(2):151–159.

Kinchesh, P., A.A. Samoilenko, A.R. Preston, and E.W. Randall. 2002. Stray field nuclear magnetic resonance of soil water: Development of a new, large probe and preliminary results. J. Environ. Qual. 31:494–499.

Kluitenberg, G.J. 2002. Heat capacity and specific heat. p. 1201–1208. *In* J.H. Dane and G.C. Topp (ed.) Methods of soil analysis: Part 4. Physical methods. SSSA Book Ser. 5. SSSA, Madison, WI.

Kluitenberg, G.J., K.L. Bristow, and B.S. Das. 1995. Error analysis of the heat pulse method for measuring soil heat capacity, diffusivity and conductivity. Soil Sci. Soc. Am. J. 59:719–726.

Kluitenberg, G.J., J.M. Ham, and K.L. Bristow. 1993. Error analysis of the heat pulse method for measuring soil volumetric heat capacity. Soil Sci. Soc. Am. J. 57:1444–1451.

Knight, R. 2001. Ground penetrating radar for environmental applications. Annu. Rev. Earth Planet. Sci. 29:229–255.

Knight, R., and A.L. Endres. 2005. An introduction to rock physics principles for near-surface geophysics. p. 31–70. *In* D.K. Butler (ed.) Near surface geophysics. Investigations in Geophysics 13. Society of Exploration Geophysicists, Tulsa, OK.

Knight, R., J. Irving, P. Tercier, G. Freeman, C. Murray, and M. Rockhold. 2007. A comparison of the use of radar images and neutron probe data to determine the horizontal correlation length of water content. p. 31–44. *In* D.W. Hyndman, F.D. Day-Lewis, and K. Singha (ed.) Subsurface hydrology: Data integration for properties and processes. AGU Geophys. Monogr. Series 171. AGU, Washington, DC.

Knight, R., and A. Nur. 1987. The dielectric constant of sandstones, 60 kHz to 4 MHz. Geophysics 52:644–654.

Koster, R.D., P.A. Dirmeyer, Z.C. Guo, G. Bonan, E. Chan, P. Cox, C.T. Gordon, S. Kanae, E. Kowalczyk, D. Lawrence, P. Liu, C.H. Lu, S. Malyshev, B. McAvaney, K. Mitchell, D. Mocko, T. Oki, K. Oleson, A. Pitman, Y.C. Sud, C.M. Taylor, D. Verseghy, R. Vasic, Y.K. Xue, and T. Yamada. 2004. Regions of strong coupling between soil moisture and precipitation. Science 305:1138–1140.

Krajewski, W.F., M.C. Anderson, W.E. Eichinger, D. Entekhabi, B.K. Hornbuckle, P.R. Houser, G.G. Katul, W.P. Kustas, J.M. Norman, C. Peters-Lidard, and E.F. Wood. 2006. A remote sensing observatory for hydrologic sciences: A genesis for scaling to continental hydrology. Water Resour. Res. 42:W07301.

Kuo, C.-H., and M. Moghaddam. 2007. Electromagnetic scattering from multilayer rough surfaces with arbitrary dielectric profiles for remote sensing of subsurface soil moisture. IEEE Trans. Geosci. Remote Sens. 45:349–366.

Kuraz, V., M. Kutilek, and I. Kaspar. 1970. Resonance-capacitance soil moisture meter. Soil Sci. 110:278–279.

Laymon, C.A., W.L. Crosson, T.J. Jackson, A. Manu, and T.D. Tsegaye. 2001. Ground-based passive microwave remote sensing observations of soil moisture at S-band and L-band with insight into measurement accuracy. IEEE Trans. Geosci. Remote Sens. 39:1844–1858.

Legchenko, A., J.M. Baltassat, A. Beauce, and J. Bernard. 2002. Nuclear magnetic resonance as a geophysical tool for hydrogeologists. J. Appl. Geophys. 50:21–46.

Legchenko, A., J.M. Baltassat, A. Bobachev, C. Martin, H. Robain, and J.M. Vouillamoz. 2004. Magnetic resonance sounding applied to aquifer characterization. Ground Water 42:363–373.

Lesch, S.M., D.L. Corwin, and D.A. Robinson. 2005. Apparent soil electrical conductivity mapping as an agricultural tool for arid zone soil. Comput. Electron. Agric. 46:351–378.

Lesch, S.M., D.J. Strauss, and J.D. Rhoades. 1995a. Spatial prediction of soil salinity using electromagnetic induction techniques: 1. Statistical prediction models—A comparison of multiple linear regression and cokriging. Water Resour. Res. 31:373–386.

Lesch, S.M., D.J. Strauss, and J.D. Rhoades. 1995b. Spatial prediction of soil salinity using electromagnetic induction techniques: 2. An efficient spatial sampling algorithm suitable for multiple linear regression model identification and estimation. Water Resour. Res. 31:387–398.

Letey, J. 1985. Relationship between soil physical properties and crop production. Adv. Soil Sci. 1:277–294.

Liaw, H.K., R. Kulkarni, S. Chen, and A.T. Watson. 1996. Characterization of fluid distributions in porous media by NMR techniques. AIChE J. 42:538–546.

Loague, K. 1992a. Soil water content at R-5: Part 1. Spatial and temporal variability. J. Hydrol. 139:233–251.

Loague, K. 1992b. Soil water content at R-5: Part 2. Impact of antecedent conditions on rainfall-runoff simulations. J. Hydrol. 139:253–261.

Loague, K., and R. Green. 1991. Statistical and graphical methods for evaluating solute transport models: Overview and application. J. Contam. Hydrol. 7:51–73.

Loescher, H.W., J. Jacobs, O. Wendroth, D.A. Robinson, G.S. Poulos, K. McGuire, P. Reed, B. Mohanty, J.B. Shanley, and W. Krajewski. 2007. Enhancing water cycle measurements for future hydrologic research. Bull. Am. Meteorol. Soc. 88:669–676.

Logsdon, S., and D. Laird. 2004. Cation and water content effects on dipole rotation activation energy of smectites. Soil Sci. Soc. Am. J. 68:1586–1591.

Long, D.S., J.M. Wraith, and G. Kegel. 2002. A heavy-duty time domain reflectometry soil moisture probe for use in intensive field sampling. Soil Sci. Soc. Am. J. 66:396–401.

Lu, Z. 2007a. Monitoring climate and seasonal effects on field soil properties using sound speed measurement: A long-term survey. *In* Abstracts, ASA-CSSA-SSSA Annu. Meeting, New Orleans, LA. 4–8 Nov. 2007. ASA, Madison, WI.

Lu, Z. 2007b. The phase shift method for studying nonlinear acoustics in a soil. Acta Acustica United with Acustica 93:542–554.

Lubczynski, M., and J. Roy. 2004. Magnetic resonance sounding: New method for ground water assessment. Ground Water 42:291–303.

Lunt, I.A., S.S. Hubbard, and Y. Rubin. 2005. Soil moisture content estimation using ground-penetrating radar reflection data. J. Hydrol. 307:254–269.

Mack, A.R., and E.J. Brach. 1966. Soil moisture measurement with ultrasonic energy. Soil Sci. Soc. Am. Proc. 30:544–548.

MacLean, A., C. Moran, W. Johnstone, B. Culshaw, D. Marsh, and G. Andrews. 2001. Distributed fiber optic sensors for the detection of liquid spills. *In* TDR 2001: Second symposium and workshop on time domain reflectometry for innovative geotechnical applications. Available at http://www.iti.northwestern.edu/tdr/tdr2001/proceedings/ (verified 22 Jan. 2008). Northwestern University, Evanston, IL. 5–7 Sept. 2001. Infrastructure Technology Inst., Evanston, IL.

Mader, D.L. 1963. Soil variability: A serious problem in soil site studies in the Northeast. Soil Sci. Soc. Am. Proc. 27:707–709.

Malicki, M.A., R. Plagge, and C.H. Roth. 1996. Improving the calibration of dielectric TDR soil moisture determination taking into account the solid soil. Eur. J. Soil Sci. 47:357–366.

Margulis, S.A., D. McLaughlin, D. Entekhabi, and S. Dunne. 2002. Land data assimilation and estimation of soil moisture using measurements from the Southern Great Plains 1997 field experiment. Water Resour. Res. 38:1299, doi:10.1029/2001WR001114.

McDonnell, J.J., M. Sivapalan, K. Vache, S. Dunn, G. Grant, R. Haggerty, C. Hinz, R. Hooper, J. Kirchner, M.L. Roderick, J. Selker, and M. Weiler. 2007. Moving beyond heterogeneity and process complexity: A new vision for watershed hydrology. Water Resour. Res. 43:W07301.

McDonnell, J.J., and R. Woods. 2004. On the need for catchment classification. J. Hydrol. 299:2–3.

McMichael, B., and R.J. Lascano. 2003. Laboratory evaluation of a commercial dielectric soil water sensor. Vadose Zone J. 2:650–654.

McNeill, J.D. 1980. Electromagnetic terrain conductivity measurement at low induction numbers. Technical Note TN-6. Available at http://www.geonics.com/html/technicalnotes.html (verified 22 Jan. 2008). Geonics, Ontario, Canada.

Michot, D., Y. Benderitter, A. Dorigny, B. Nicoullaud, D. King, and A. Tabbagh. 2003. Spatial and temporal monitoring of soil water content with an irrigated corn crop cover using surface electrical resistivity tomography. Water Resour. Res. 39:1138, doi:10.1029/2002WR001518.

Michie, W.C., B. Culshaw, M. Konstantaki, I. McKenzie, S. Kelly, N.B. Graham, and C. Moran. 1995. Distributed pH and water detection using fiber-optic sensors and hydrogels. J. Lightwave Technol. 13:1415–1420.

Mitrofanov, I.G., M.L. Litval, A.S. Kozyrev, A.B. Sanin, V.I. Tret'yakov, V. Yu Grin'kov, W.V. Boynton, C. Shinohara, D. Hamara, and R.S. Saunders. 2004. Soil water content on Mars as estimated from neutron measurements by the HEND instrument onboard the 2001 Mars Odyssey spacecraft. Solar Syst. Res. 38:253–257.

Mohamed, S.O., P. Bertuzzi, A. Bruand, L. Raison, and L. Bruckler. 1997. Field evaluation and error analysis of soil water content measurement using the capacitance probe method. Soil Sci. Soc. Am. J. 61:399–408.

Mori, Y., J.W. Hopmans, A.P. Mortensen, and G.J. Kluitenberg. 2005. Estimation of vadose zone water flux from multi-functional heat pulse probe measurement. Soil Sci. Soc. Am. J. 69:599–606.

Mortensen, A.P., J.W. Hopmans, Y. Mori, and J. Simunek. 2006. Multi-functional heat pulse probe measurements of coupled vadose zone flow and transport. Adv. Water Resour. 29:250–267.

Moysey, S., and R.J. Knight. 2004. Modeling the field-scale relationship between dielectric constant and water content in heterogeneous systems. Water Resour. Res. 40:W03510, doi:10.1029/2003WRR002589.

Mualem, Y., and S.P. Friedman. 1991. Theoretical prediction of electrical-conductivity in saturated and unsaturated Soil. Water Resour. Res. 27:2771–2777.

Myers, R.J.K., C.A. Campbell, and K.L. Weier. 1982. Quantitative relationship between net nitrogen mineralization and moisture-content of soils. Can. J. Soil Sci. 62:111–124.

Nabighian, M.N., M.E. Ander, V.J.S. Grauch, R.O. Hansen, T.R. LaFehr, Y. Li, W.C. Pearson, J.W. Peirce, J.D. Phillips, and M.E. Ruder. 2005. The historical development of the gravity method in exploration. Geophysics 70:63ND–89ND.

Nadler, A. 2005. Methodologies and the practical aspects of the bulk soil EC (σ_a)–soil solution EC (σ_w) relations. Adv. Agron. 88:273–312.

Narayan, U., V. Lakshmi, and T.J. Jackson. 2006. High-resolution change estimation of soil moisture using L-band radiometer and radar observations made during the SMEX02 experiments. IEEE Trans. Geosci. Remote Sens. 44:1545–1554.

Nielsen, D.R., and O. Wendroth. 2003. Spatial and temporal statistics: Sampling field soils and their vegetation. Catena, Reiskirchen, Germany.

Njoku, E.G., and D. Entekhabi. 1996. Passive microwave remote sensing of soil moisture. J. Hydrol. 184:101–129.

Njoku, E., and J.A. Kong. 1977. Theory for passive microwave remote sensing of near-surface soil moisture. J. Geophys. Res. 82:3108–3118.

Noborio, K. 2001. Measurement of soil water content and electrical conductivity by time domain reflectometry: A review. Comput. Electron. Agric. 31:213–237.

Noborio, K., K.J. McInnes, and J.L. Heilman. 1996. Measurements of soil water content, heat capacity, and thermal conductivity with a single TDR probe. Soil Sci. 161:22–28.

Ogden, F.L., and B. Saghafian. 1997. Green and Ampt infiltration with redistribution. J. Irrig. Drain. Eng. 123:386–393.

Ohmura, A., and A. Raschke. 2005. Energy budget at the earth's surface. Chap. 10. *In* M. Hantel (ed.) Observed Global Climate. Landolt-Börnstein New Series 6 (Group V: Geophysics). Springer Verlag, Berlin.

Pachepsky, Y., D.E. Radcliffe, and H. Magdi Selim. 2003. Scaling methods in soil physics. CRC Press, Boca Raton, FL.

Paltineanu, I.C., and J.L. Starr. 1997. Real-time soil water dynamics using multisensor capacitance probes: Laboratory calibration. Soil Sci. Soc. Am. J. 61:1576–1585.

Pamukcu, S., S. Texier, and J. Toulouse. 2006. Advances in water content measurement with distributed fiber-optic sensor. p. 7–12. *In* D.J. DeGroot, J.T. DeJong, J.D. Frost, and L.G. Baise (ed.) Proc. of GeoCongress 2006: Geotechnical Engineering in the Information Technology Age, Atlanta, GA. 26 Feb.–1 Mar. 2006. ASCE, Reston, VA.

Parlange, M.B., G.G. Katul, M.V. Folegatti, and D.R. Nielsen. 1993. Evaporation and the field scale soil water diffusivity function. Water Resour. Res. 29:1279–1286.

Peake, W.H. 1959. Interaction of electromagnetic waves with some natural surfaces. IEEE Trans. Antennas Propagation AP-7:S324–S329.

Perlo, J., V. Demas, F. Casanova, C. Meriles, J. Reimer, A. Pines, and B. Blumich. 2005. High resolution spectroscopy with a portable single-sided sensor. Science 308:1279.

Pettinelli, E., A. Cereti, A. Galli, and F. Bella. 2002. Time domain reflectometry: Calibration techniques for accurate measurement of the dielectric properties of various materials. Rev. Sci. Instrum. 73:3553–3562.

Philip, J.R. 1957. Theory of infiltration. Soil Sci. 83:345–357.

Philip, J.R. 1969. Theory of infiltration. p. 215–296. *In* V.T. Chow (ed.) Advances in Hydroscience. Vol. 5. Academic Press, New York.

Pieper, G.F. 1949. The measurement of the moisture content of soil by the slowing of neutrons. Ph.D. thesis, Cornell University, Ithaca, NY.

Pitman, A.J. 2003. The evolution of, and revolution in, land surface schemes designed for climate models. Int. J. Climatol. 23:479–510.

Pool, D.R., and J.H. Eychaner. 1995. Measurements of aquifer-storage change and specific yield using gravity surveys. Ground Water 33:425–432.

Porporato, A., P. D'Odorico, F. Laio, and I. Rodriguez-Iturbe. 2003. Hydrologic controls on soil carbon and nitrogen cycles: I. Modeling scheme. Adv. Water Res. 26:45–58.

Purcell, E.M. 1952. Research in nuclear magnetism. *In* Nobel lectures, physics 1942–1962. Elsevier, Amsterdam, The Netherlands.

Redman, J.D., J.L. Davis, L.W. Galagedara, and G.W. Parkin. 2002. Field studies of GPR air launched surface reflectivity measurements of soil water content. Proc Ninth Int. Conf. on Ground Penetrating Radar. Proc. SPIE 4758:156–161

Reedy, R.C., and B.R. Scanlon. 2003. Soil water content monitoring using electromagentic induction. J. Geotech. Geoenviron. Eng. 129:1028–1039.

Reichman, G.A., D.L. Grunes, and F.G. Viets. 1966. Effect of soil moisture on ammonification and nitrification in 2 northern plains soils. Soil Sci. Soc. Am. Proc. 30:363–366.

Ren, T., G.J. Kluitenberg, and R. Horton. 2000. Determining soil water flux and pore water velocity by a heat pulse technique. Soil Sci. Soc. Am. J. 64:552–560.

Ren, T., K. Noborio, and R. Horton. 1999. Measuring soil water content, electrical conductivity, and thermal properties with a thermo-time domain reflectometry probe. Soil Sci. Soc. Am. J. 63:450–457.

Rhoades, J.D., F. Chanduvi, and S. Lesch. 1999. The use of saline waters for irrigation. FAO Irrigation and Drainage Paper No. 48. FAO, Rome.

Rhoades, J.D., N.A. Manteghi, P.J. Shouse, and W.J. Alves. 1989. Soil electrical conductivity and soil salinity: New formulations and calibrations. Soil Sci. Soc. Am. J. 53:433–439.

Rhoades, J.D., P.A.C. Raats, and R.J. Prather. 1976. Effects of liquid-phase electrical conductivity, water content, and surface conductivity on bulk electrical conductivity. Soil Sci. Soc. Am. J. 40:651–655.

Richards, L.A. 1931. Capillary conduction of liquids in porous mediums. Physics 1:318–333.

Ridolfi, L., P. D'Odorico, A. Porporato, and I. Rodriguez-Iturbe. 2003. The influence of stochastic soil moisture dynamics on gaseous emissions of NO, N_2O, and N_2. Hydrol. Sci. J. 48:781–798.

Robinson, D.A., A. Binley, N. Crook, F.D. Day-Lewis, T.P.A. Ferré, V.J.S. Grauch, R. Knight, M. Knoll, V. Lakshmi, R. Miller, J. Nyquist, L. Pellerin, K. Singha, and L. Slater. 2008. Advancing process-based watershed hydrological research using near-surface geophysics: A vision for, and review of, electrical and magnetic geophysical methods. Hydrol. Process. (in press).

Robinson, D.A., C.M.K. Gardner, J. Evans, J.D. Cooper, M.G. Hodnett, and J.P. Bell. 1998. The dielectric calibration of capacitance probes for soil hydrology using an oscillation frequency response model. Hydrol. Earth Syst. Sci. 2:111–120.

Robinson, D.A., S.B. Jones, J.A. Wraith, D. Or, and S.P. Friedman. 2003. A review of advances in dielectric and electrical conductivity measurement in soils using time domain reflectometry. Vadose Zone J. 2:444–475.

Rodriguez-Iturbe, I., P. D'Odorico, A. Porporato, and L. Ridolfi. 1999a. On the spatial and temporal links between vegetation, climate, and soil moisture. Water Resour. Res. 35:3709–3722.

Rodriguez-Iturbe, I., and A. Porporato. 2005. Ecohydrology of water-controlled ecosystems: Soil moisture and plant dynamics Cambridge Univ. Press, Cambridge, UK.

Rodriguez-Iturbe, I., A. Porporato, L. Ridolfi, V. Isham, and D.R. Cox. 1999b.

Probabilistic modelling of water balance at a point: The role of climate, soil, and vegetation. Proc. R. Soc. London, Ser. A 455:3789–3805.
Ryel, R.J., C.I. Ivans, M.S. Peek, and A.J. Leffler. 2008. Functional differences in soil water pools: A new perspective on plant water use in water limited ecosystems. p. 397–422. *In* U. Lüttge, W. Beyschlag, and J. Murata (ed.) Progress in botany 69. Springer, New York.
Saarenketo, T. 1998. Electrical properties of water in clay and silty soils. J. Appl. Geophys. 40:73–88.
Salvucci, G.D., and D. Entekhabi. 1995. Ponded infiltration into soils bounded by a water table. Water Resour. Res. 31:2751–2759.
Samouelian, A., I. Cousin, A. Tabbagh, A. Bruand, and G. Richard. 2005. Electrical resistivity survey in soil science: A review. Soil Tillage Res. 83:173–193.
Saxena, S.C., and G.M. Tayal. 1981. Capacitive moisture meter. IEEE Trans. Ind. Electron. Control Instrum. 28:37–39.
Scanlon, B.R., J.G. Paine, and R.S. Goldsmith. 1999. Evaluation of electromagnetic induction as a reconnaissance technique to characterize unsaturated flow in an arid setting. Ground Water 37:296–299.
Schjonning, P., I.K. Thomsen, P. Moldrup, and B.T. Christensen. 2003. Linking soil microbial activity to water- and air-phase contents and diffusivities. Soil Sci. Soc. Am. J. 67:156–165.
Schmugge, T.J., and B.J. Choudhury. 1981. A comparison of radiative transfer models for predicting the microwave emission from soils. Radio Sci. 16:927–938.
Schmugge, T.J., P. Gloersen, T. Wilheit, and F. Geiger. 1974. Remote sensing of soil moisture with microwave radiometers. J. Geophys. Res. 79:317–323.
Schneeberger, K., M. Schwank, Ch. Stamm, P. de Rosnay, Ch. Matzler, and H. Fluhler. 2004. Topsoil structure influencing soil water retrieval by microwave radiometry. Vadose Zone J. 3:1169–1179.
Schwinning, S., and O.E. Sala. 2004. Hierarchy of responses to resource pulses in and semi-arid ecosystems. Oecologia 141:211–220.
Schwinning, S., O.E. Sala, M.E. Loik, and J.R. Ehleringer. 2004. Thresholds, memory, and seasonality: Understanding pulse dynamics in arid/semi-arid ecosystems. Oecologia 141:191–193.
Seguis, L., and J.-C. Bader. 1997. Surface runoff modelling related to seasonal vegetation cycles (millet, groundnut, and fallow) in central Senegal. Rev. Sci. EAU/J. Water Sci. 10(4):419–438.
Selker, J., N. van de Giessen, M. Westhoff, W. Luxemburg, and M.B. Parlange. 2005. Fiber optics opens window on stream dynamics. Geophys. Res. Lett. 33:L24401, doi:10.1029/2006GL027979.
Serbin, G., and D. Or. 2004. Ground-penetrating radar measurement of soil water content dynamics using a suspended horn antenna. IEEE Trans. Geosci. Remote Sens. 42:1695–1705.
Seyfried, M.S., and M.D. Murdock. 2004. Measurement of soil water content with a 50-MHz soil dielectric sensor. Soil Sci. Soc. Am. J. 68:394–403.
Seyfried, M.S., and B.P. Wilcox. 1995. Scale and the nature of spatial variability: Field examples having implications for hydrologic modeling. Water Resour. Res. 31:173–184.
Seyfried, M.S., and P. Rao. 1987. Solute transport in undisturbed columns of an aggregated tropical soil: Preferential flow effects. Soil Sci. Soc. Am. J. 51:1434–1444.
Seyfried, M.S., L.E. Grant, E. Du, and K. Humes. 2005. Dielectric loss and calibration of the hydra probe soil water sensor. Vadose Zone J. 4:1070–1079.
Sheets, K.R., and J.M.H. Hendrickx. 1995. Noninvasive soil-water content measurement using electromagnetic induction. Water Resour. Res. 31:2401–2409.
Sherlock, M.D., and J.J. McDonnell. 2003. A new tool for hillslope hydrologists: Spatially distributed groundwater level and soil water content measured using electromagnetic induction. Hydrol. Proc. 17:1965–1977.
Sierra, J. 1997. Temperature and soil moisture dependence of N mineralization in intact soil cores. Soil Biol. Biochem. 29:1557–1563.
Sihvola, A.H. 1999. Electromagnetic mixing formulas and applications. Inst. of Electrical Engineers, London.
Šimůnek, J., D. Jacques, J.W. Hopmans, M. Inoue, M. Flury, and M.Th. van Genuchten. 2002. Solute transport during variably-saturated flow- inverse methods. p. 1435–1449. *In* J.H. Dane and G.C. Topp (ed.) Methods of soil analysis: Part 1. Physical methods. SSSA, Madison, WI.
Singha, K., and S.M. Gorelick. 2005. Saline tracer visualized with three-dimensional electrical resistivity tomography: Field-scale spatial moment analysis. Water Resour. Res. 41:W03019.
Sivapalan, M. 2003. Prediction in ungauged basins: A grand challenge for theoretical hydrology. Hydrol. Proc. 17:3163–3170.
Skoop, J., M.D. Jawson, and J.W. Doran. 1990. Steady-state aerobic microbial activity as a function of soil-water content. Soil Sci. Soc. Am. J. 54:1619–1625.
Smith, R.E., and J.-Y. Parlange. 1978. A parameter-efficient hydrologic infiltration model. Water Resour. Res. 14:533–538.
Smith, R.E., C. Corradini, and F. Melone. 1993. Modeling infiltration for multistorm runoff events. Water Resour. Res. 29:133–144.
Stanford, G., and E. Epstein. 1974. Nitrogen mineralization-water relations in soils. Soil Sci. Soc. Am. J. 38:103–107.
Su, J.G., and E.W. Bork. 2007. Characterization of diverse plant communities in Aspen Parkland rangeland using LIDAR data. Appl. Veg. Sci. 10:407–416.
Sun, Y., D. Ma, P. Schulze Lammers, O. Schmittmann, and M. Rose. 2006. On-the-go measurement of soil water content and mechanical resistance by a combined horizontal penetrometer. Soil Tillage Res. 86:209–217.
Talbot, C.A., F.L. Ogden, and S.E. Howington. 2006. A moisture content-discretized infiltration method. *In* XVI Int. Conf. on Computational Methods in Water Resources, Copenhagen, Denmark, 19–22 June.
Tapley, B.D., S. Bettadpur, J.C. Ries, P.F. Thompson, and M.M. Watkins. 2004. GRACE measurements of mass variability in the earth system. Science 305:503–505.
Tarara, J.M., and J.M. Ham. 1997. Measuring soil water content in the laboratory and field with dual-probe heat-capacity sensors. Agron. J. 89:535–542.
Telford, W.M., L.P. Geldart, and R.E. Sheriff. 1990. Applied Geophysics. 2nd ed. Cambridge Univ. Press, New York.
Texier, S., and S. Pamukcu. 2003. Fiber optic sensor for distributed liquid content quantification in subsurface. *In* FMGM 2003, 6th Int. Symp. on Field Measurements in Geomechanics, NGI, Oslo, Norway. September 2003.
Thomas, A.M. 1966. In situ measurement of moisture in soil and similar substances by fringe capacitance. J. Sci. Instrum. 43:21–27.
Thomsen, A., P. Drosher, and F. Steffensen. 2005. Mobile TDR for geo-referenced measurement of soil water content and electrical conductivity. p. 481–494. *In* J.V. Stafford (ed.) Precision agriculture '05. Wageningen Academic Publishers, Wageningen, The Netherlands.
Thierfelder, T.K., R.B. Grayson, D. von Rosen, and A.W. Western. 2003. Inferring the location of catchment characteristic soil moisture monitoring sites. Covariance structures in the temporal domain. J. Hydrol. 280:13–32.
Tidwell, V.C., and R.J. Glass. 1994. X-ray and visible-light transmission for laboratory measurement of 2-dimensional saturation fields in thin-slab systems. Water Resour. Res. 30:2873–2882.
Topp, G.C., J.L. Davis, and A.P. Annan. 1980. Electromagnetic determination of soil-water content- measurements in coaxial transmission-lines. Water Resour. Res. 16:574–582.
Topp, G.C., and P.A. Ferré. 2002. Thermogravimetric method using convective oven-drying. p. 422–424. *In* J.H. Dane and G.C. Topp (ed.) Methods of Soil Analysis: Part 4. Physical methods. SSSA, Madison, WI.
Topp, G.C., and W.D. Reynolds. 1998. Time domain reflectometry: A seminal technique for measuring mass and energy in soil. Soil Tillage Res. 47:125–132.
Trenberth, K.E., and C.J. Guillemot. 1996. Physical processes involved in the 1988 drought and 1993 floods in North America. J. Clim. 9:1288–1298.
Triantafilis, J., and S.M. Lesch. 2005. Mapping clay content variation using electromagnetic induction techniques. Comput. Electron. Agric. 46:203–237.
Turcu, V.E., S.B. Jones, and D. Or. 2005. Continuous soil carbon dioxide and oxygen measurements and estimation of gradient-based gaseous flux. Vadose Zone J. 4:1161–1169.
Tyndale-Biscoe, J.P., G.A. Moore, and A.W. Western. 1998. A system for collecting spatially variable terrain data. Comput. Electron. Agric. 19:113–128.
Uchida, T., K. Kosugi, and T. Mizuyama. 1999. Runoff characteristics of pipeflow and effects of pipeflow on rainfall-runoff phenomena in a mountainous watershed. J. Hydrol. 222:18–36.
Ulaby, F.T., P.C. Dubois, and J. van Zyl. 1996. Radar mapping of surface soil moisture. J. Hydrol. 184:57–84.
Ulaby, F.T., R.K. Moore, and A.K. Fung. 1981. Microwave remote sensing: Active and passive. Vol. 1. Artech House, Norwood, MA.
Ulaby, F.T., R.K. Moore, and A.K. Fung. 1986. Microwave remote sensing: Active and passive. Vol. 3. Artech House, Norwood, MA.

Underwood, N., C.H.M. van Bavel, and R.W. Swanson. 1954. A portable slow neutron flux meter for measuring soil moisture. Soil Sci. 77:339–340.

Ungar, S.G., R. Layman, J.E. Campbell, J. Walsh, and H.J. McKim. 1992. Determination of soil-moisture distribution from impedance and gravimetric measurements. J. Geophys. Res. Atmospheres 97:18969–18977.

Vachaud, G., A. Passerat de Silans, P. Balabanis, and M. Vauclin. 1985. Temporal stability of spatially measured soil water probability density function. Soil Sci. Soc. Am. J. 49:822–828.

van der Schrier, G., and J. Barkmeijer. 2007. North American 1818–1824 drought and 1825–1840 pluvial and their possible relation to the atmospheric circulation. J. Geophys. Res. 112:D13102.

Wagener, T., M. Sivapalan, J.J. McDonnell, R. Hooper, V. Lakshmi, X. Liang, and P. Kumar. 2004. Predictions in ungauged basis as a catalyst for multidisciplinary hydrology. Trans. Am. Geophys. Union 85(44):451–453.

Wagener, T., M. Sivapalan, P. Troch, and R. Woods. 2007. Catchment classification and hydrologic similarity. Geogr. Compass 1(4):901, doi:10.1111/j.1749-8189.2007.00039.x.

Wait, J.R. 1955. Mutual electromagnetic coupling of loops over a homogeneous ground. Geophysics 20:630–637.

Walker, J.P., G.R. Willgoose, and J.D. Kalma. 2002. Three-dimensional soil moisture profile retrieval by assimilation of near-surface measurements: Simplified Kalman filter covariance forecasting and field application. Water Resour. Res. 38:1301, doi:10.1029/2002WR001545.

Weihermuller, L., J.A. Huisman, S. Lambot, M. Herbst, and H. Vereecken. 2007. Mapping the spatial variation of soil water content at the field scale with different ground penetrating radar techniques. J. Hydrol. 340:202–216.

Wendroth, O., S. Koszinski, and E. Pena-Yewtukhiv. 2006. Spatial association between soil hydraulic properties, soil texture, and geoelectric resistivity. Vadose Zone J. 5:341–355.

Wendroth, O., G. Kühn, P. Jürschik, and D.R. Nielsen. 1997. State-space approach for site specific management decisions. p. 835–842. *In* J.V. Stafford (ed.) Precision Agriculture: Proc. First European Conf., Warwick, UK. BIOS Scientific Publishers, Oxford.

Wendroth, O., W. Pohl, S. Koszinski, H. Rogasik, C.J. Ritsema, and D.R. Nielsen. 1999. Spatio-temporal patterns and covariance structures of soil water status in two northeast-German field sites. J. Hydrol. 215:38–58.

Wenner, F. 1915. A method of measuring earth resistivity. U.S. Bureau Standards Bull. 12:469–478.

Western, A.W., G. Blöschl, and R.B. Grayson. 2001. Toward capturing hydrologically significant connectivity in spatial patterns. Water Resour. Res. 37:83–97.

Western, A.W., and R.B. Grayson. 1998. The Tarrawarra data set: Soil moisture patterns, soil characteristics, and hydrological flux measurements. Water Resour. Res. 34:2765–2768.

Western, A.W., R.B. Grayson, and G. Blöschl. 2002. Scaling of soil moisture: A hydrologic perspective. Annu. Rev. Earth Planet. Sci. 30:149–180.

Western, A.W., R.B. Grayson, G. Blöschl, G.R. Willgoose, and T.A. McMahon. 1999. Observed spatial organization of soil moisture and its relation to terrain indices. Water Resour. Res. 35:797–810.

Whalley, W.R., T.J. Dean, and P. Izzard. 1992. Evaluation of the capacitance technique as a method for dynamically measuring soil-water content. J. Agric. Eng. Res. 52:147–155.

Whitaker, M.P.L., T.P.A. Ferré, B. Nijssen, and J. Washburne. 2006. Design and testing of a low-cost soil-drying oven. Vadose Zone J. 5:856–859.

Wigneron, J.P., Y. Kerr, P. Waldteufel, K. Saleh, M.-J. Escorihuela, P. Richaume, P. Ferrazzoli, P. de Rosnay, R. Gurney, J.-C. Calvet, J.P. Grantg, M. Guglielmettih, B. Hornbuckle, C. Mätzlerj, T. Pellarink, and M. Schwank. 2007. L-band microwave emission of the biosphere (L-MEB) model: Description and calibration against experimental data sets over crop fields. Remote Sens. Environ. 107:639–655.

Wigneron, J.-P., A. Olioso, J.-C. Calvet, and P. Bertuzzi. 1999. Estimating root zone soil moisture from surface soil moisture data and soil-vegetation-atmosphere transfer modeling. Water Resour. Res. 35:3735–3745.

Wildung, R.E., T.R. Garland, and R.L. Buschbom. 1975. Interdependent effects of soil temperature and water-content on soil respiration rate and plant root decomposition in arid grassland soils. Soil Biol. Biochem. 7:373–378.

Wilson, D.J., A.W. Western, and R.B. Grayson. 2004. Identifying and quantifying sources of variability in temporal and spatial soil moisture observations. Water Resour. Res. 40:W02507, doi:10.1029/2003WR002306.

Wilson, D.J., A.W. Western, and R.B. Grayson. 2005. A terrain and data-based method for generating the spatial distribution of soil moisture. Adv. Water Resour. 28:43–54.

Wobschall, D. 1978. Frequency-shift dielectric soil-moisture sensor. IEEE Trans. Geosci. Remote Sens. 16:112–118.

Wolter, B., and M. Krus. 2005. Moisture measuring with nuclear magnetic resonance (NMR). p. 491–504. *In* K. Kupfer (ed.) Electromagnetic aquametry: Electromagentic wave interaction with water and moist substances. Springer, New York.

World Bank. 2006. Reengaging in agriculture water management: Challenges and options. The World Bank, Washington, DC.

Wraith, J.A., D.A. Robinson, S.B. Jones, and D.S. Long. 2005. Spatially characterizing apparent electrical conductivity and water content of surface soils with time domain reflectometry. Comput. Electron. Agric. 46:239–261.

Wraith, J.M., S.D. Comfort, B.L. Woodbury, and W.P. Inskeep. 1993. A simplified waveform analysis approach for monitoring solute transport using time-domain reflectometry. Soil Sci. Soc. Am. J. 57:637–642.

Wrolstad, R.E., E.A. Decker, S.J. Schwartz, and P. Sporns. 2004. Handbook of food analytical chemistry: Water, proteins, enzymes, lipids, and carbohydrates. John Wiley & Sons, Hoboken, NJ.

Yao, T., P.J.Wierenga, A.R. Graham, and S.P. Neuman. 2004. Neutron probe calibration in a vertically stratified vadose zone. Vadose Zone J. 3:1400–1406.

Yen, A.S., B.M. Murray, and G. Rossman. 1998. Water content of the Martian soil: Laboratory simulations of reflectance spectra. J. Geophys. Res. 103:125–133.

Yuan, J., M.A. El-Sherif, A.G. MacDiarmid, and W.E. Jones, Jr. 2001. Fiber optical chemical sensors using a modified conducting polymer cladding. Adv. Environ. Chem. Sensing Tech. Proc. SPIE 4205:170–179.

Zehe, E., H. Elsenbeer, F. Lindenmaier, K. Schulz, and G. Blöschl. 2007. Patterns of predictability in hydrological threshold systems. Water Resour. Res. 43(7):W07434, doi:10.1029/2006WR005589.

Zhou, Q.Y., J. Shimada, and A. Sato. 2001. Three-dimensional spatial and temporal monitoring of soil water content using electrical resistivity tomography. Water Resour. Res. 37:273–285.

Zielinski, J. 2002. Watershed vulnerability analysis. Available at www.cwp.org/vulnerability_analysis.pdf (verified 22 Jan. 2008). Center for Watershed Protection, Ellicot City, MD 21043.

Zreda, M., D. Desilets, and T.P. Ferré. 2005. Cosmic-ray neutron probe: Non-invasive measurement of soil water content. 2005, AGU Fall Meeting Abstracts, 810.